Metal Supported Catalysts for PLA

Ana Filipa Gonçalves Madeira Alves

Thesis to obtain the Master of Science Degree in

Chemical Engineering

Supervisors: Prof. Dr. Ana Margarida Sousa Dias Martins

Prof. Dr. Maria do Rosário Gomes Ribeiro

Dr. Samuel Dagorne

Examination Committee

Chairperson: Prof. Dr. Maria Filipa Gomes Ribeiro

Supervisor: Prof. Dr. Ana Margarida Sousa Dias Martins

Members of the Committee: Dr. Luís Gonçalo Andrade Rodrigues Alves

December 2014

Acknowledgements

I would like to express my deepest gratitude to my supervisors Professor Ana Margarida Martins and Professor Maria do Rosário Ribeiro for all the excellent guidance and support and particularly for the enthusiastic encouragement since the beginning of this master thesis.

I would like to thank most sincerely to my co-supervisor Dr. Samuel Dagorne for the opportunity to finish this research in the CLAC research group at the University of Strasbourg and for his help and stimulating ideas.

I also would like to thank Luís Alves and Ana Elisa Ferreira for their crucial assistance and all the valuable teachings and constructive suggestions given throughout the development of this thesis.

To Christophe, David and Jean-Charles thank you very much for the amazing atmosphere at the laboratory and for the excellent time that I had in Strasbourg. Thank you for making me feel welcome, for teaching and helping me every time I needed.

A special thanks to Karolina Porada for her collaboration and commitment to the work but also her friendship.

To my other colleagues working in the laboratory of Organometallic Chemistry and Homogeneous Catalysis at IST, thank you for your indispensable help during these months.

Last but definitely not least, I would like to express my warmest and heartfelt thanks to my family and friends. Especially to my parents whose loving and unconditional support was essential to allow me becoming a chemical engineer.

Abstract

The search for biodegradable polymers derived from renewable resources aims overcoming sustainability and environment problems caused by petroleum-based polymers. Due to its properties, polylactide is foreseen to be one of the most promising substitutes of this type of polymers.

This thesis reports the study of homogeneous and metal-supported heterogeneous catalysts for the ring-opening polymerization of lactide.

Titanium(IV) tetraisopropoxido and titanium(IV) chloride triisopropoxido supported in SBA-15 were tested for the ring-opening polymerization of lactide. Different reaction conditions were applied and selected polymers samples were characterized by TGA, GPC and DSC. Preliminary polymerization reactions using the titanium compounds as homogeneous catalyst were performed. Both homogeneous and supported systems achieved the same monomer conversion (higher than 90%), being the homogeneous catalyst faster.

Innovative studies in ROP of LA initiated by VO(O^iPr)[ONNO], VO(O^iPr)$_3$ and V(NAda)(O^iPr)$_3$ were also performed. The results obtained showed that while VO(O^iPr)[ONNO] prove not to being active in the ROP of lactide, VO(O^iPr)$_3$ revealed the most active of the three complexes, achieving high yields in 15 minutes with narrow molecular weight distribution, in bulk conditions. The molar ratio between the monomer and the vanadium catalyst influences the reaction outcome, with low ratios giving rise to the formation of *meso*-lactide.

Keywords: Polylactide, Ring-opening polymerization, Mesopourous silica support, Titanium alkoxido catalyst, Vanadium complexes catalysts.

Resumo

O estudo e interesse crescente por polímeros biodegradáveis derivados de fontes renováveis tem como objectivo ultrapassar os problemas ambientais e de sustentabilidade causados pelo uso de polímeros baseados em fontes não renováveis. O polímero do ácido láctico, polilactida, é um dos mais promissores substitutos para os polímeros obtidos a partir de monómeros extraídos do petróleo.

A presente tese consiste no estudo do uso de catalisadores metálicos homogéneos e heterógeneos suportados na polimerização por abertura de anel da lactida.

Tetraisopropóxido de titânio e cloro-triisopropóxido de titânio suportados em SBA-15 foram testados nas reacções de polimerização. Foram aplicadas diferentes condições reaccionais e as amostras de polímeros foram caracterizadas por TGA, GPC e DSC. Foram também realizadas reacções de polimerização com os catalisadores homogéneos de titânio. Com a comparação dos dois sistemas, conclui-se que ambos atingiram a mesma conversão (maior que 90%), sendo o sistema catalítico homogéneo mais rápido.

Estudos inovadores sobre a performance de compostos de vanádio na polimerização por abertura de anel da lactida foram realizados. Os complexos usados foram VO(O^iPr)[ONNO], VO(O^iPr)$_3$ and V(NAda)(O^iPr)$_3$. Os resultados obtidos permitem concluir que enquanto VO(O^iPr)[ONNO] provou não ser activo na produção de PLA, VO(O^iPr)$_3$ mostrou-se o mais activo dos três compostos de vanádio, atingindo 90% de conversão, em 15 minutos, em *bulk*, e formação de polímeros com uma distribuição de pesos moleculares estreita (PDI próximo de 1). A razão molar entre o monómero e o catalisador influencia a reacção, tendo-se verificado que baixas razões entre os dois componentes deram origem à formação de *meso*-lactide.

Palavras-Chave: Polilactida, Polimerização por abertura de anel, Catálise Heterogénea, Sílica mesoporosa, Catalisador de alcóxido de titânio, Catalisadores de complexos de vanádio.

Table of Contents

List of Tables

List of Figures

Abbreviations and Symbols

Ada	1-adamantyl
A_{ext}	External area
BET	Brunauer-Emmett-Teller
CPG	Controlled pore glass
D_p	Pore diameter
DCM	Dichloromethane
DSC	Differential Scanning Calorimetry
eq.	Equivalent
GPC/SEC	Gel Permeation Chromatography/Size Exclusion Chromatography
i-Pr = ^{i}Pr	Isopropyl
LA	Lactide
L-lactide	(S,S)-lactide
$[M]_0$	Monomer concentration at t=0
[M]t	Monomer concentration at time t
MCM	Mobil Crystalline Materials
M_n	Number-average molecular weight
$M_{n(SEC)}$	Number-average molecular weight obtained by GPC/SEC
$M_{n(corrected)}$	Corrected number-average molecular weight
$M_{n(theo)}$	Theoretical number-average molecular weight
M_p	Molecular weight of the highest peak
M_w	Weight-average molecular weight
MW	Molecular Weight
n-Bu	Butyl
NMR	Nuclear Magnetic Resonance
PCL	Poly(caprolactone)
PDI=M_w/M_n	Polydispersity Index
PE	Poly(ethylene)
PGA	Poly(glycolic acid)
PHAs	Polyhydroxyalkanoates
PHB	Poly(hydroxybutyrate)
PLA	Polylactide
PLLA	Poly(L-lactide)
PS	Poly(styrene)
ROP	Ring-Opening Polymerization
RT	Room Temperature
S_{BET}	BET surface area
Salen	*N,N'*-bis(salicylaldehydo)ethylenediamine

SBA	Santa Barbara Amorphous
SEM	Scanning Electron Microscopy
T_c	Crystallization temperature
TEM	Transmission Electron Microscopy
T_g	Glass-transition temperature
TGA	Thermogravimetric analysis
THF	Tetrahydrofuran
T_m	Melting temperature
V_p	Pore volume

Scope of the work

Plastics play an extremely important role in modern society. Nowadays, the application of plastics in the world is increasing, so that their production can be recognized as one of the indicators of the development of modern chemical industry. The increasing consumption of these materials, commonly based on petrochemical raw materials (i.e. non-renewable resources), raises concerns on their sustainability. Besides this, the problem of tons of paper and plastic ending up in landfills every year creates a global problem of landfills overflowing with non-biodegradable materials. Both reasons have a tremendous and harmful impact on the environment and the human health.

In order to fight these problems, biodegradable and renewable polymers have attracted much attention over the last decades. One of the most known worldwide examples is poly-lactic acid (PLA), which is a compostable, biodegradable polymer derived from renewable sources. Its physical and mechanical properties can be modified by manipulation of the polymer architecture and by several processing treatments applied after the polymerization reactions. This gives rise to a lot of different final products and, consequently, a broad range of applications. In fact, besides the good mechanical properties that allow PLA to be an alternative in the main applications of commodity plastics, the production and use of this polymer offers a solution to environmental problems, providing significant energy savings and improving agricultural economies [1].

The present thesis comes as a following of the work that has been developed and reported over the last decades and studies homogeneous and heterogeneous metal based catalysts for the ring-opening polymerization of lactide.

Chapter I emphasis the importance and main applications of PLA and a bibliographic study of metal based catalysts used for the ring-opening polymerization of lactide is provided.

Chapter II describes a series of catalytic reactions using titanium alkoxidos catalysts in homogeneous and SBA-15-supported systems for the polymerization of lactide. Preliminary polymerization reactions with the homogeneous catalysts were performed and heterogeneous supported catalysts were prepared and tested in the polymerization of LA. Different reaction conditions were applied and the characterization of the obtained polymers was performed using TGA, GPC and DSC. The comparison between both systems concerning reactions' behaviors and the characteristics of the obtained polymers are discussed in this chapter.

In Chapter III the ROP of LA initiated by vanadium complexes including kinetic studies is presented.

A detailed description of all experimental procedures is provided in Chapter IV.

Chapter I

BIBLIOGRAPHIC STUDY

I.1 Biodegradable Polymers

"Conventional plastics" or "commodity plastics'' play a major role in our everyday life. However, these long-term stability materials are primarily based on petrochemical and non-renewable resources, which raises concerns on their sustainability. The increasing consumption of plastics and the wastes resulting from their utilization have a severe impact on the environment and consequently in the human health. The accumulation and disposal of non-degradable plastic wastes can cause soil and water pollution and climatic change. Biodegradable and renewably derived polymers have attracted much attention as they are an interesting way to overcome the problems associated to petroleum-based polymers [2].

Besides these concerns, biodegradable polymers have become the focus of increasing interest in recent decades also for biomedical applications. Biodegradable polymers have gained widespread application in biomedical technology, for use in sutures, drug delivery devices and tissue engineering [3].

A biodegradable polymer is a polymer in which the degradation of the organic material is caused by biological processes resulting from the action of naturally-occurring microorganisms (such as bacteria, fungi and algae) to yield CO_2, water and biomass. Two key steps occur in the biodegradation of polymers. First, a depolymerization step where there is the cleavage of the macromolecular chain into smaller molecules, e.g., oligomers, dimers and monomers. These molecules are small enough to pass the semi-permeable outer bacterial membranes and then to be used as carbon and energy sources. In a second step, known as mineralization, these oligomeric fragments are converted into biomass, water and gases such as CO_2 and CH_4 [4].

Biodegradable polymers can be classified according to their synthesis process [5] as follows: (i) those from biomass such as agro-polymers from agro-resources (e.g., starch or cellulose), (ii) those obtained by microbial production such as polyhydroxyalkanoates (PHAs), (iii) those conventionally and chemically synthesized from bio-derived monomers, e.g., polylactic acid (PLA), (iv) those obtained from fossil resources. They can further be classified into two main categories: the agro-polymers and the biodegradable polyesters as it is shown in Figure 1.

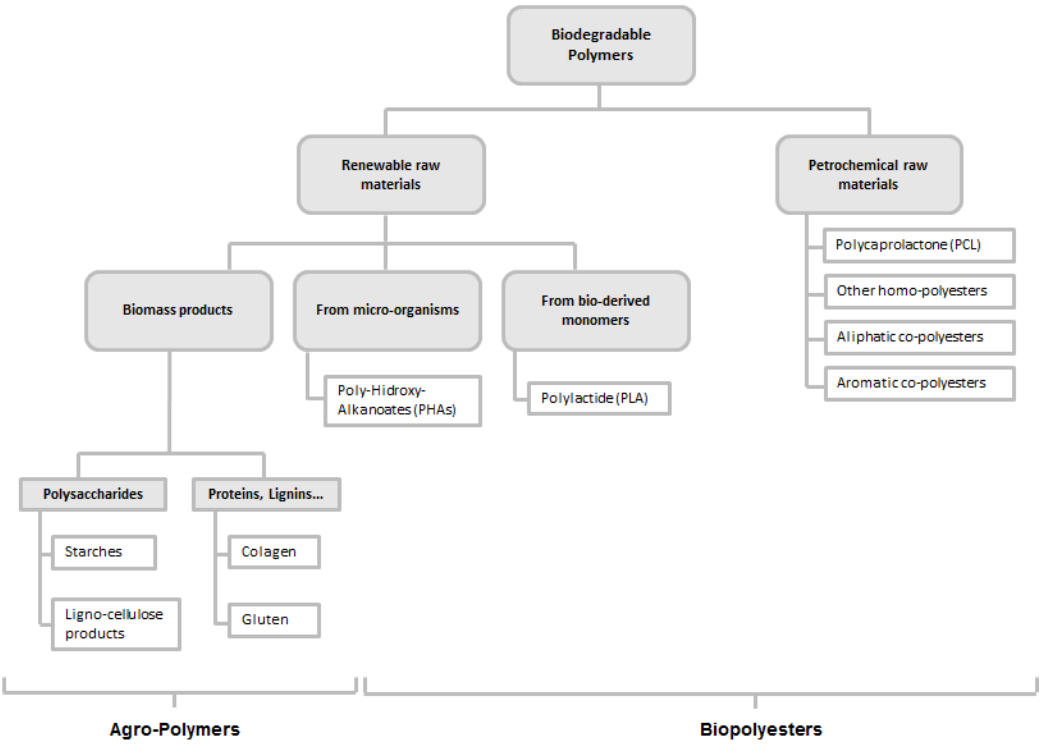

Figure 1 - Classification of the main biodegradable polymers.

I.2 Polyesters as biopolymers

Aliphatic polyesters constitute an important class of biopolymers and are among the most used biodegradable polymers in biomedical applications. In particular, homo- and copolymers derived from hydroxyacids and their dimers i.e. polymers derived from glycolic acid or glycolide, lactic acid or lactide, ε-caprolactone, and 3-hydroxybutyrate, which structures are shown in Figure 2.

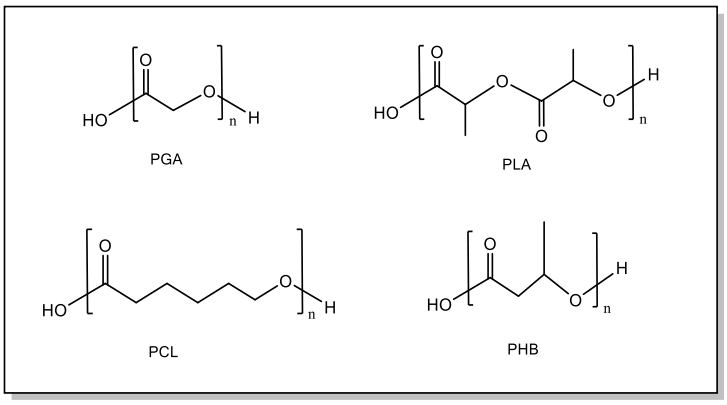

Figure 2 - Examples of biodegradable polyesters: poly(glycolic acid) (PGA); polylactide (PLA); poly(ε-caprolactone) (PCL); poly(3-hydroxybutyrate) (PHB).

These polymers can be obtained from various chemical routes: polycondensation [6], enzymatic processes [7] or ring-opening polymerization (ROP) of cyclic esters [8] such as glycolide, lactide and ε-caprolactone.

I.3 Polylactide

Polylactic acid (PLA) is a highly versatile, biodegradable, aliphatic polyester derived from renewable resources.

PLA was for first time recognized in 1932 when Carothers et al. first mentioned Ring-Opening Polymerization (ROP) of lactide to PLA [8a]. Nearly 40 years passed until the advantages and possible applications for biodegradable polymers were recognized in the 1970s. [5b]. PLA was first used in 1974 in combination with polyglycolic acid (PGA) as a suture material in the USA and it started being produced on a large-scale in the 1990s. [5c]

Over the last decades, the increasing interest in biodegradable polymers especially in the physical, chemical and processing characteristics of PLA and its broad spectrum of applications have been reported. Nowadays, thanks to the efforts in research and to technological improvements, PLA is one of the leading bio-based plastics with an annual production capacity of 180000 tons. The largest producer is NatureWorks® LLC and has a capacity of 140000 tons/year. A growth in PLA production capacity reaching 800000 tons/year is expected by 2020 [9].

I.3.1 Production

PLA is produced via polymerization of lactic acid that is produced by fermentation of glucose using a bacteria of the genus *lactobacillus*. Glucose can be obtained from various sources such as starch, corn or sugar feedstock. Lactic acid can be directly polycondensed into PLA or can react by condensation leading to its dimer lactide (LA) which is polymerized by ROP using metal complexes, organic compounds or enzymes as initiators. Since it is a biodegradable polymer, PLA suffers decomposition into CO_2 and H_2O closing the lifecycle of PLA represented in Figure 3 [5c].

Industrially, PLA is prepared so far by direct polycondensation of lactic acid (Mitsui Toatsu Chemicals process) or by the ring-opening polymerization of the dimer initiated by $Sn(Oct)_2$ (Cargill Dow LLC). The polycondensation route consists in an equilibrium reaction and it is difficult to remove all the traces of water, which present a limitation in what concerns the control over molecular weight and, in consequence, the mechanical properties of the polymer [10]. Concerning this, most work has been focused in the process that follows a ring-opening polymerization strategy of lactide developed by Cargill Dow LLC which yields to high molecular weight PLA in excellent conversion and purity. [1]

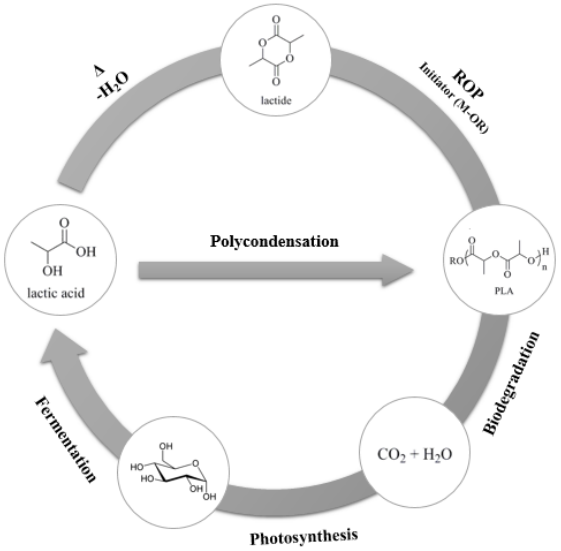

Figure 3 - Lifecycle of lactic acid: Synthesis of lactide monomer from natural resources, lactide polymerization in the presence of a metal catalyst and biodegradation of PLA.

I.3.2 Structure and properties

PLA is an aliphatic ester with lactide (lactic acid dimer) as monomeric unit.

Lactide has two asymmetric carbons and thus it exists in three stereoisomeric forms: *L*-lactide, *D*-lactide and *meso*-lactide – Figure 4.

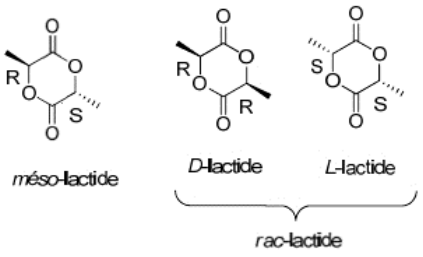

Figure 4 - Lactide stereoisomers.

Since the L-lactic acid is the naturally occurring form, PLA is commercialized as the pure enantiomeric poly(L-lactic acid), PLLA. The racemic mixture, *rac*-lactide, is also commercialized.

Due to these stereocenters, and depending on the initial stereochemistry of the LA monomer and the ROP stereoselectivity, it is possible to obtain polymers with different stereoregularity and thus different microstructures, which determine their thermal and mechanical properties. This allows the production of materials that can be used over a broader range of applications.

The ROP of either pure enantiomers L- and D-lactide yields isotactic PLA featuring all stereocenters along the polymer chain having the same configuration – Figure 5.

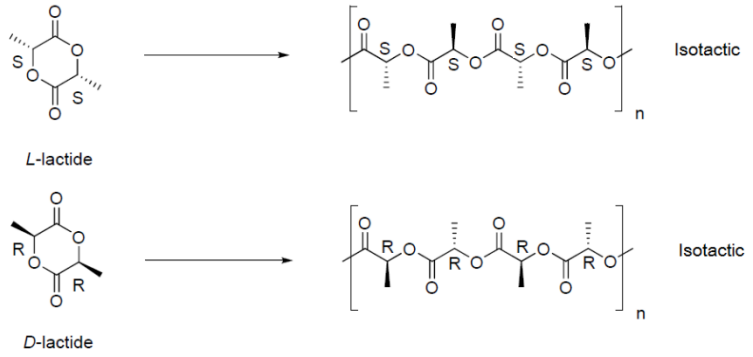

Figure 5 - Production of isotactic PLA from enantiomeric pure LA monomers.

On the other hand, the ROP of *rac*-lactide may give several PLA microstructures: atactic PLA resulting from a ROP proceeding with no tacticity control, the resultant structure being a random distribution of configurations of the stereocenters; isotactic stereoblock PLA featuring two isotactic blocks; and heterotactic PLA obtained by the alternating insertion of RR and SS lactide enantiomers, as illustrated in Figure 6.

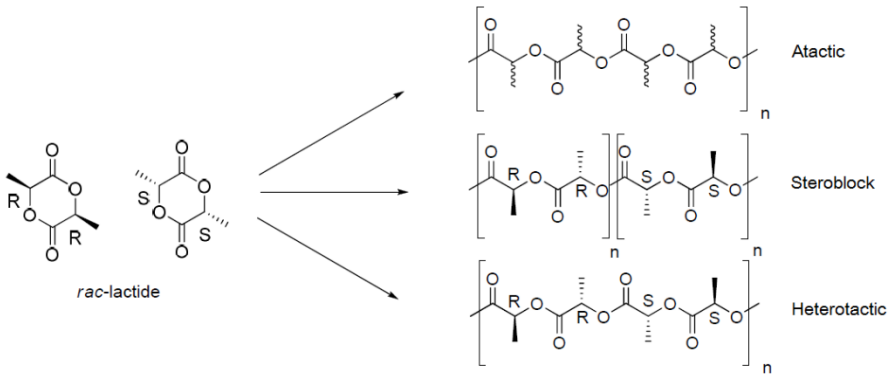

Figure 6 - The different tacticities of PLAs obtained from *rac*-LA.

Finally, the ROP of *meso*-lactide yields atactic PLA and also syndiotactic PLA which has alternating configurations of the sequential stereocenters. These structures are shown in Figure 7. However, side reactions like transesterification, chain termination or insertion errors influence the final microstructure.

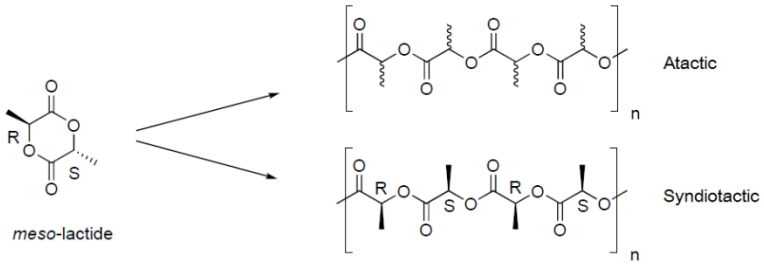

Figure 7 - The different tacticities of PLAs obtained from meso-LA.

As previously mentioned the stereoregularity influences the final structural and thermal properties of the polymer. The ability to control the stereochemical architecture permits precise control over the speed of crystallization and the final degree of crystallinity, the mechanical properties and the processing temperatures of the material [1]. The higher the stereoregularity, the stronger the intermolecular forces, so the greater the mechanical and thermal properties of the polymer [11a].

Due to its stereoregularity, PLLA is semicrystalline and it has a melting temperature in the range of 170-180ºC, depending on the molecular weight and the size of the crystallites, and presents a glass transition temperature ranging from 55ºC and 65ºC [11b]. Atactic PLA and heterotactic PLA are amorphous polymers with T_g in the region of 50-60ºC [11c], depending on the molecular mass. Higly syndiotactic PLA is a semycristalline material with T_g around 35ºC and Tm about 152ºC [11c]. Stereocomplexes of PLA (a racemic mixture of PLLA and PDLA) feature a higher melting temperatures, around 230ºC [11d], than the corresponding homopolymers, and T_g values vary between 65-72ºC [11b].

I.3.3 Applications

PLA offers unique advantages concerning biodegradability, accessibility, thermoplastic processibility and ecofriendliness being an outstanding competitor for the same applications as commodity plastics i.e. packaging, agricultural products and disposable materials. The polymer has been highlighted for applications in medicine, surgery and pharmaceuticals as well [1].

The modification of PLA can happen via different methods like by variation of molecular weight, stereochemistry, degree of crystallinity, or by blending or copolymerization or several processing procedures such as extrusion, injection molding, blow molding or fiber spinning [5c]. These modifications allow to achieve different final products and, consequently, a broad diversity of applications.

Polylactide has excellent mechanical properties comparable to conventional polymers such as PS and PE and can be used as packaging materials (cups, bottles, films and container).

It is generally recognized as safe (GRAS) by the United State Food and Drug Administration (FDA) and it is appropriate for all food packaging applications [1], [5c].

It can also be applied in textiles (shirts, furniture textiles) and non-wovens (diapers) and for the production of adhesives [1].

Good mechanical properties, absorbability and the degradation into non-toxic products explain the popularity of PLA in biomedical applications and make it ideal for tissue engineering, resorbable sutures and sustained-release drug delivery systems [1], [3].

The biodegradability and compostability that characterize PLA make it useful to disposable ware (containers, disposable dishes, utensils and compostable waste bags). The PLA wastes could be recycled via melting and re-manufacturing, but they are mainly removed by degradation in soil and humus, which enhance the soil quality and support plants growth [1].

I.4 Ring-opening polymerization of lactide

I.4.1 ROP of cyclic esters

Polyesters were originally synthesized via step-growth polymerization based on homo polycondensation of hydroxycarboxylic acids derivatives or hetero polycondensation of a diol with a dicarboxylic acid. But in order to obtain high-molar-mass polymers based on these processes, a sufficiently high equilibrium constant is required and, in the case of heteropolycondensation, 1:1 stoichiometric ratio must be strictly preserved.

Ring–opening polymerization has become a simpler and popular alternative method for the polymerization of lactones and related cyclic monomers. ROP allows the synthesis of 'tailor–made' polymers with a high molecular weight and a nearly monodisperse weight distribution that make these polymers valuable for medicinal and pharmaceutical applications [8c]. There are many factors affecting the course of the polymerization of lactones: (i) the size of the monomer ring, (ii) the position, number and nature of the ring substituents, (iii) the reaction conditions, such as the type of initiator, catalyst, solvent, concentration of the monomer and temperature, (iv) undesired side reactions based on transesterification [8c].

The ring-opening polymerization of cyclic esters may proceed according to several pathways which are determined by the nature of the initiator used. These have been recently reviewed and include: anionic polymerization [12], cationic polymerization [13] metal-free or nucleophilic polymerization [14], activated monomer mechanism [15] and coordination/insertion polymerization [16].

I.4.2 Mechanisms of the ROP of lactide

ROP remains by far the most widely used method for the synthesis of polylactide. This polymerization process allows to reach high molecular weights and a much higher control of the polymer final properties by adjusting the proportions and the sequence of L- and D-lactic acid units, and also the polymer chain ends. [12a]

Since the pioneering work of Kleine et al. in the 1950s [17] metal-based catalytic systems have attracted considerable attention for the polymerization of cyclic esters and numerous studies have been carried out to explain the coordination polymerization mechanism. By changing the nature of metal center and the ligands, a broad range of initiators have been prepared and evaluated. Alternative pathways based on anionic, cationic or nucleophilic initiators have also been evaluated. [12a]. All the mechanisms are represented in the Figures 8 to 13, with emphasis in the coordination/insertion approach.

❖ **Anionic polymerization**

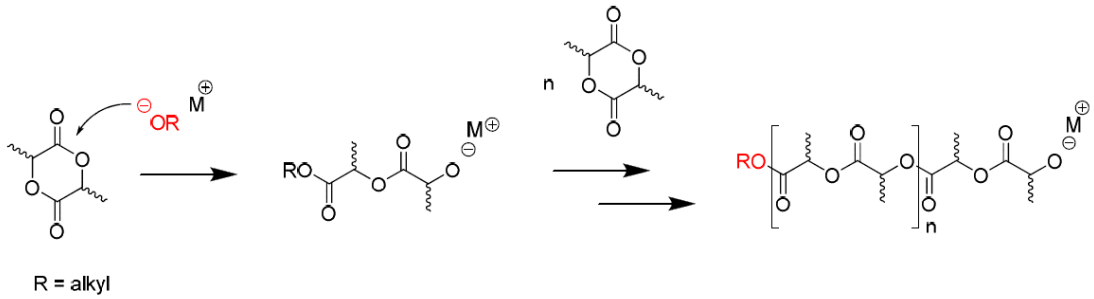

Figure 8 - Anionic ROP of lactide.

❖ **Cationic polymerization**

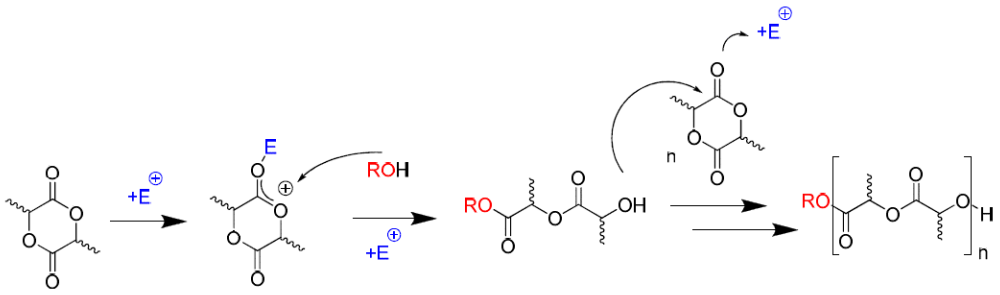

Figure 9 - Cationic ROP of lactide through electrophilic monomer activation.

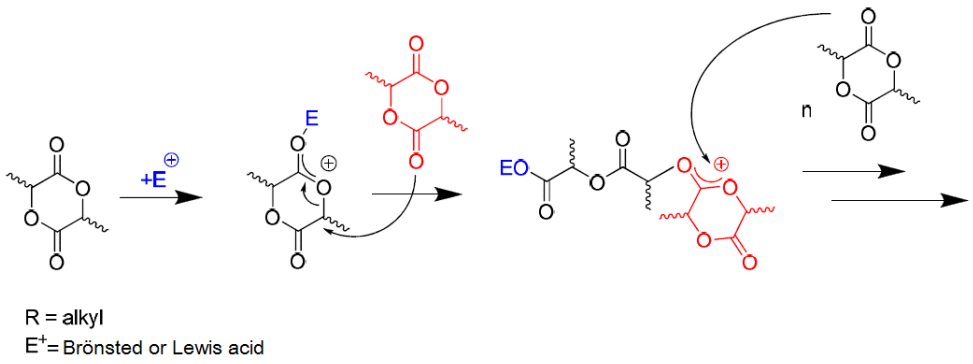

Figure 10 - Cationic ROP of lactide through a chain-end activation mechanism.

❖ **Nucleophilic polymerization**

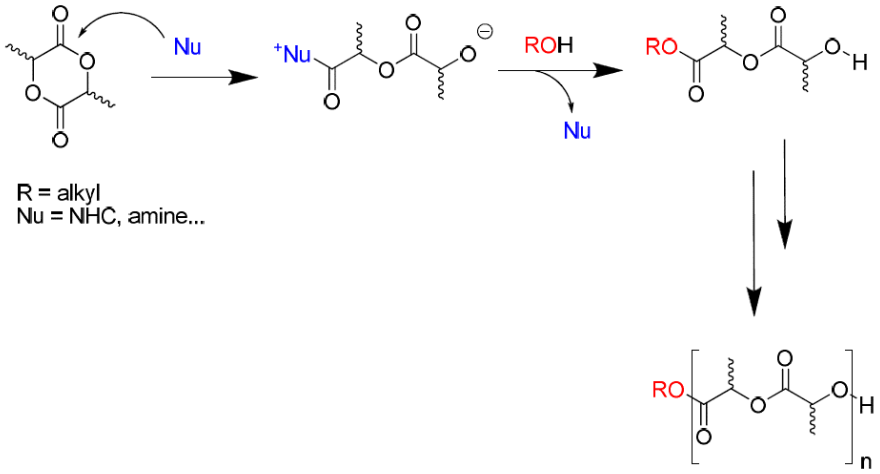

Figure 11 - Nucleophilic ROP of lactide.

❖ **Polymerization via activated monomer mechanism**

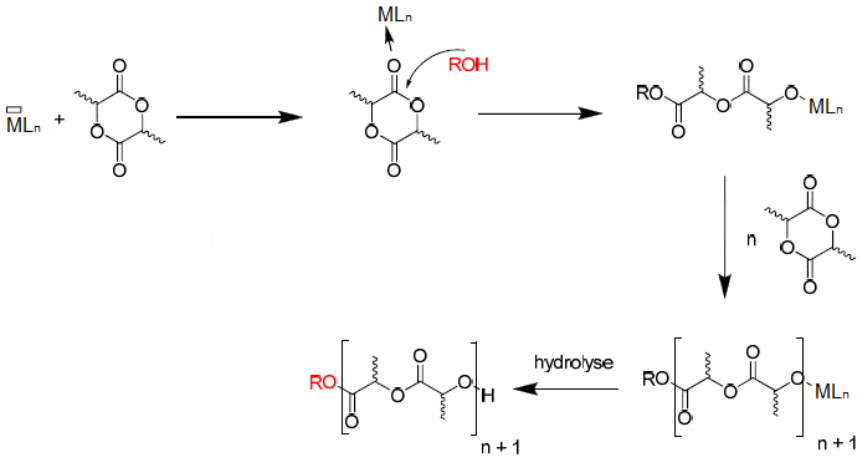

Figure 12 - ROP of lactide via activated monomer mechanism.

❖ **Coordination-insertion polymerization**

Metallic complexes of M-X type (X= alkoxido, amido) have received a great attention as initiators for the polymerization of cyclic esters. [18]. In general, the ROP of cyclic esters, including lactide, initiated by these type of complexes follows a coordination/insertion mechanism.

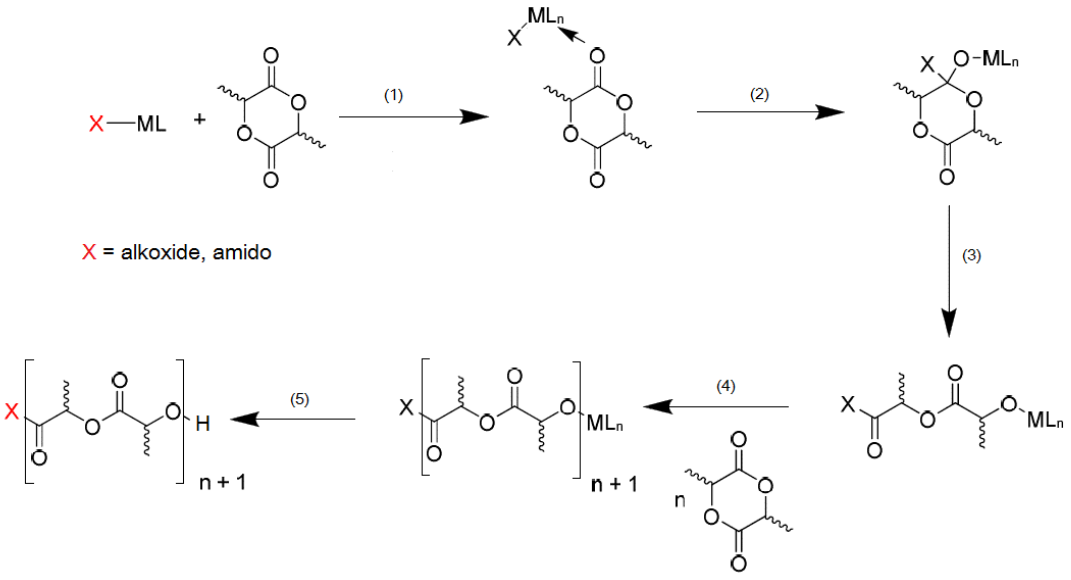

Figure 13 - Coordination-insertion ROP of lactide.

This mechanism was formulated for the first time in 1971 by Dittrich, Schultz et al. [19] and in the end of the 1980s the mechanism of polymerization of lactide using $Al(Oi\text{-}Pr)_3$ as initiator was experimentally proved by Kricheldorf et al. [20] and Teyssié et al. [21], independently.

The mechanism proceeds through an initial coordination of the monomer onto a Lewis acid metal center (1) followed by a nucleophilic attack by the metal-bonded alkoxido/amido group at the carbonyl group of the lactide (2). Subsequently there is a ring-opening reaction by the cleavage of the acyl-oxygen bond (3), creating a new metal alkoxido species that attacks a new lactide monomer as a nucheophile leading to the chain-propagation (4). Termination by hydrolysis of the metal-alkoxido active bond (5) yields hydroxyl end capped polymer chain, while the other end is occupied by the alkoxido/amido group - Figure 13.

The benefits of ROP in conjunction with a “living” method leads to a present consensus that this approach is a powerful and versatile addition-polymerization method.

This type of polymerization allows to consider a control of the chain length of polymer by the initial monomer stoichiometry. In fact, the use of suitable well-defined initiators for example ligand-supported metal alkoxido complexes may produce predictable molecular-weight [17] and/or functionalized polymers [22]. Ideally in this type of polymerization, i.e. in the absence of side reactions, the polymer mass formed increases linearly with the consumption of the monomer, with a growing polymer chain per metal center. [23] However a slow initiation step and secondary reactions can occur, leading to variations in molecular weights and, as a consequence, in high PDI values [24]. The main side reaction is transesterification [25] which can occur intra- or intermolecularly as shown in the Figure 14 [21].

For a good polymerization control, the initiator must combine a high activity, higher initiating rate compared to the propagation step and limit transesterification reactions during the polymerization. Alkoxido and amido complexes of Lewis acidic and oxophilic metals are usually excellent candidates to obtain narrowly-disperse polymers in a controlled (and possibly stereocontrolled) manner.

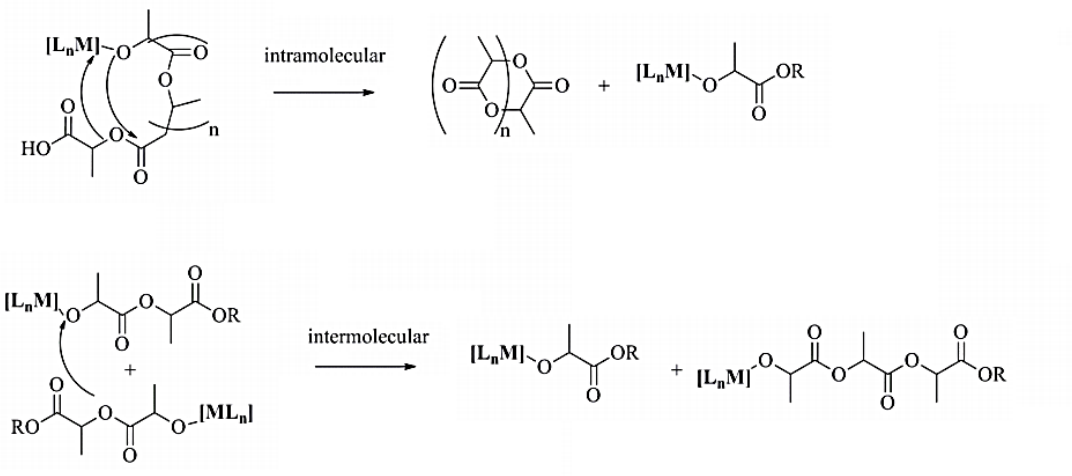

Figure 14 - Intra- and intermolecular transesterification reactions during the polymerization of lactide.

I.4.3 Metal-based initiators for ROP of lactide

Concerning the aim of this thesis, the bibliographic study of the catalysts used in the ROP of lactide will focus mainly on metal-based initiators.

Over the last decades, numerous efforts to develop efficient metal catalytic systems to promote the ROP of lactide under mild conditions and combining it with catalytic efficiency and polymerization control have been made [12c].

Among the most widely used complexes for the ROP of lactide are tin(II) octonoato, ($Sn(Oct)_2$), aluminum alkoxidos, namely, $Al(O\text{-}i\text{-}Pr)_3$, and zinc(II) lactato ($Zn(Lact)_2$), represented in Figure 15 [12a].

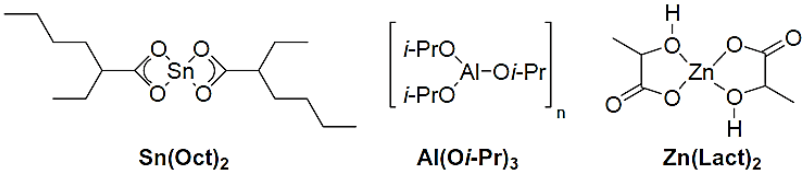

$Sn(Oct)_2$ **$Al(Oi\text{-}Pr)_3$** **$Zn(Lact)_2$**

Figure 15 - Structure of tin octonoato, aluminium isopropoxido and zin lactato.

$Sn(Oct)_2$ is the most used complex for the industrial preparation of PLA. It is highly active presenting typical reaction times in bulk at 140-180°C range from minutes to a few hours and leading to high-molecular-weight polymers (up to 10^5 or even 10^6 Da in the presence of an alcohol) [26]. The mechanism is shown in Figure 16. However, applications of tin initiators stays controversial because of their toxicity, especially in the case of biomedical applications.

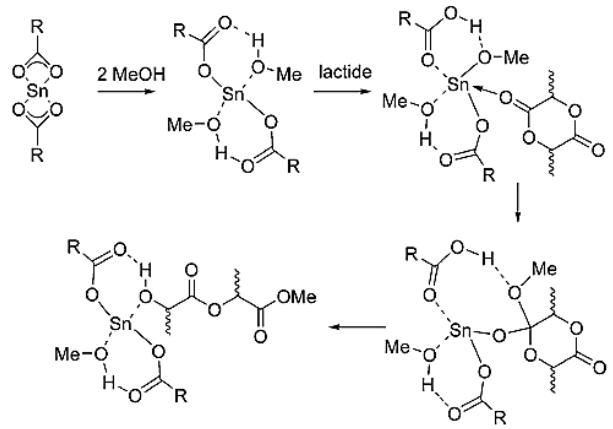

Figure 16 - Predicted mechanism for ROP of lactide catalyzed by $Sn(Oct)_2$ in presence of methanol.

Aluminum alkoxidos have also proved to be efficient catalysts for the ROP of cyclic esters [12a]. However, the main example $Al(O\text{-}i\text{-}Pr)_3$ revealed to be less active than $Sn(Oct)_2$ (in bulk at 125-180°C, reaction times of several days are usually required and molecular weights are generally lower than 10^5 Da) [26].

Zinc derivatives as potential nontoxic catalysts have attracted much interest. In fact, the combination of $Zn(Lact)_2$ with a primary alcohol is demonstrated to increase its activity and allows for a better control of the polymerization, as in the case of $Sn(Oct)_2$ [27].

According to experimental and theoretical data [28], polymerization of LA with these catalysts proceeds via coordination-insertion mechanism. In this type of approach, the efficiency of the molecular-weight control depends on the ratio $k_{propagation}/k_{initiation}$ and on the extent of transesterification reactions which depends on the metallic initiator [29]. Side reactions occur within polymerization with $Sn(Oct)_2$, leading to broad molecular-weight distributions (PDI value around 2), but only at high or even complete conversion with $Al(O\text{-}i\text{-}Pr)_3$, yielding lower PDI indexes (less than 1.5) [26],[30]. Also the ROP with $Al(O\text{-}i\text{-}Pr)_3$ proceeds via coordination-insertion mechanism with three active chains growing per metallic center and it was found that an aggregation phenomena is associated to the practical use of these simple alkoxidos [31].

The relatively low activity of aluminium alkoxidos stimulated the study of other metals featuring alkoxido ligands. Some examples are trivalent yttrium and lanthanum alkoxidos $L_n(OR)_3$ (L_n=La, Y and R=*i*-Pr, *n*-Bu) have proved to be much more active than the related aluminum alkoxidos, and they efficiently promote the ROP of lactide in dichloromethane solution at room temperature [32]. Other metal alkoxidos such as oxoalkoxido clusters of general formula $[L_{n_5}(\mu\text{-}O)\text{-}(O\text{-}i\text{-}Pr)_{13}]$ (L_n= Y, La) and the iron cluster $Fe_5(\mu\text{-}O)(OEt)_{13}$] were found to efficiently initiate ROP of lactide. But still gave rise to a non-controlled process resulting in broad PDI values [33].

All these conclusions motivated the investigation of well-defined single-sites catalysts of this type to enhance their catalytic activity toward the ROP of lactide and limit the transesterification side reactions. Generally, these catalysts consist of complexes of the type L_nMR where M is Lewis acidic-metal center, L_n an ancillary ligands and R an initiating group, mostly, as mentioned before, alkoxidos or amidos.

Several complexes featuring different ancillary ligands (principally *O* - donors, *N* - donors and *N,O* - donors) have been reported to promote lactide ROP of LA in a controlled manner via a coordination – insertion mechanism [12a].

Biphenolatos and methylenebiphenolatos have been evaluated as examples of *O*-Donor Ligands for aluminum, zinc and lithium [34] – Figure 17. Al and Zn complexes show much lower activity than Li aggregates. In fact, the latter shows a good activity in the ROP of lactide (complete conversion after only a few hours in dichloromethane at 0ºC) and polymers with molecular weights up to 14000g/mol and narrow distributions are obtained.

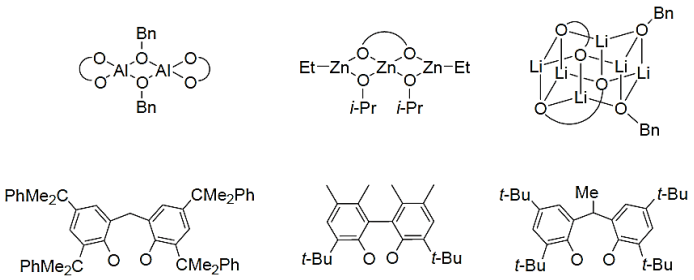

Figure 17 - Representative Al, Zn and Li complexes featuring (methylene)biphenolato ligands.

Nitrogen-based ligands were tested aiming to achieve better control of the aggregation phenomenon observed with *O*-Donor Ligands.

It was discovered that tripodal trispyrazolyl–hydroborate ligands create adequate steric hindrance around the metallic center to prevent aggregation. The metals tested included magnesium, zinc and calcium and revealed to be highly active for the ROP of lactide with the following reactivity order Ca>Mg>Zn, based on the difference in polarity of the initiating M–O bonds. However, the inverse trend was observed for the molecular weight distributions of the resulting polymers, calcium derivatives leading to higher polydispersity indexes (ca. 1.6–1.7) than magnesium and zinc initiators (ca. 1.1–1.25) [35].

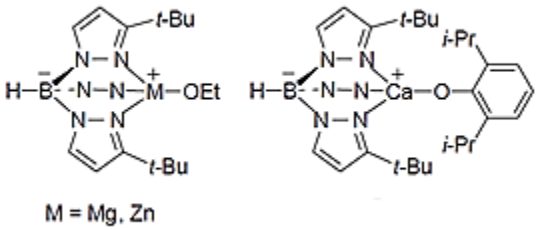

Figure 18 - Representative Mg, Ca and Zn comples featuring trispyrazolyl-hydroborate ligands.

β-Diiminate complexes of divalent metals, mainly zinc and magnesium, but also calcium, tin and iron(II), have also been considered for the ROP of lactide. All the complexes were shown to catalyze lactide ROP efficiently in dichloromethane at room temperature. For complexes bearing an alkoxido initiating group, comparative studies have suggested the reactivity order Mg>Zn≈Fe>Sn, which parallels the electropositivity of the metal [36].

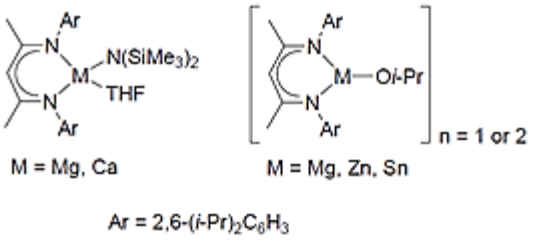

Figure 19 - Representative Mg, Ca, Zn and Sn complexes featuring β-diiminate ligands.

Chelating ligands combining N- and O-donors have also been studied in the design of well-defined complexes for the ROP of lactide.

Studies dedicated to aluminum complexes featuring Salen ligands have been reported [12a]. All the complexes proved to be moderately active in well controlled polymerizations. Modifications of steric and/or electronic properties of the aryl and imino substituents as well as the flexibility of the spacer leads to the versatility and accessibility of the Salen ligands [37]. These studies have been further expanded to the related saturated Salan complexes [38] – Figure 20.

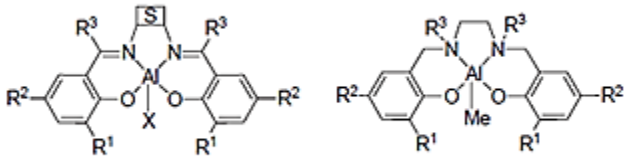

Figure 20 - General structure of Al complexes featuring Salen and Salan ligands (S=spacer).

Chisholm and coworkers initiated the study of complexes derived from bulky Schiff bases (i.e. half-SALEN ligands) to compare with β-Diiminates [39]. The bulky phenoxido coligand (Figure 21-1b) presents a lower activity towards ROP of lactide when compared with the amido complex (Figure 21-1a). Higher activities could be achieved with the introduction of an amino side-arm at the Schiff base ligand (Figure 21-2) [40]. A related phenolato-based ligand bearing a single ethylene-diamine arm has also been studied by Hillmyer and Tolman as the zinc complex represent in Figure 21-3. This complex was tested in polymerization of lactide in DCM at room temperature and the rate constant for ROP was found to be higher than the rate constant obtained for β-diiminate derivative and even higher than with the trispyrazolyl–hydroborate. The polymers obtained present high molecular weights (130000g/mol) and relatively low polydispersity indexes (around 1.4) [41].

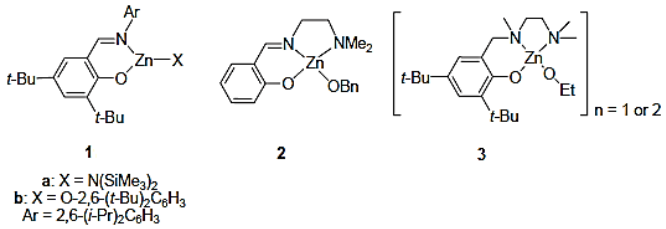

Figure 21 - Zn complexes featuring half-Salen and diamino-phenolate ligands.

Aminobiphenolato ligands featuring a pendant amino or ether group coordinated to Group III metals and lanthanides have also been tested in ROP of lactide (Figure 22). These complexes revealed to be very active proceeding within a few minutes at room temperature in toluene or THF. The polymerization is well controlled and polymers with predictable M_n and low polydispersity indexes (lower than 1.2) were obtained. In this case, ROP is based on fast exchange reactions between alcohol and alkoxido at the metal and allows the production of large quantities of polymers with only small amounts of metal complexes (Figure 22) [42].

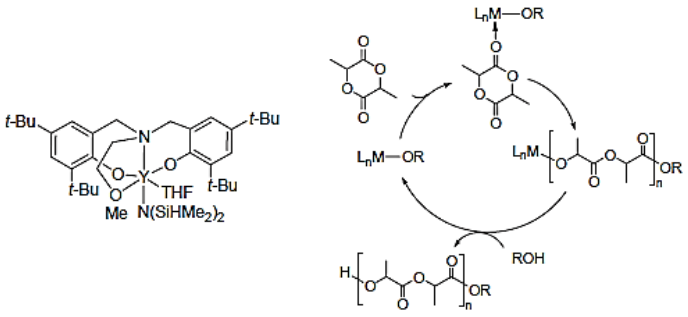

Figure 22 - Selected Y complex featuring a methoxy-amino-biphenolate ligand and schematic representation of catalytic ROP based on alcohol exchange reactions (RO refers to the exogeneous alkoxy group or to the growing polymer chain).

I.5 Heterogeneous catalytic systems

Despite the significant progress in polymerization of lactide and the proficiency of many of such systems based on Lewis acidic metals, the major drawback of homogeneous catalyst lays on their removal and recycling.

Actually, supported catalytic system are a promising approach to accomplish potential enhancements in selectivity and conversion in polymerization processes and the recovery or recycle of the catalyst which may result in reducing costs and certainly in a significant progress from the industrial point of view. For example, the application of metal alkoxido catalysts grafted onto solid supports is a good way to achieve polyesters free from metallic residues. Such residues can be toxic constraining polymer applications as a biomaterial.

The heterogenization of homogeneous catalysts is well developed for catalytic processes that lead to small molecules. It makes separation of the product easier, improves selectivity and

conversion. However, for polymerization processes, the technology is far less advanced in what concerns heterogeneous catalysts.

The polymerization process is carried out in confined channels of the support material, e.g. zeolites or mesoporous silica – Figure 23. When compared to microporous materials, mesoporous materials can be adapted to accommodate larger molecules. Therefore, they are considered as an attractive option for polymerization reactions, because mass transport and diffusion problems are reduced. [43]

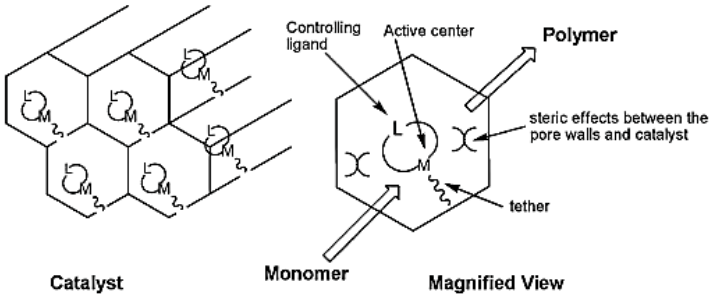

Figure 23 - Confinement effect in heterogeneous polymerization catalysis.

I.5.1 Supports – mesoporous silica

The control of the surface chemistry as well as the strict control of the surface geometry has to be taken into consideration while designing a heterogeneous catalyst because high surface areas and fast mass transfer of the reactants and products to and from the catalytic sites are required.

Mesoporous materials have pores in the range of 2-50 nm, according to the IUPAC classification [44]. These materials are of great interest due to their large surface area which makes them suitable as catalysts. Moreover their characteristics and properties are easy to tune. In fact, small changes in the synthesis procedure can result in large changes in morphology, pore structure and size of the mesopores, which offers great opportunities in the design of the heterogeneous catalysts [45]. The range of compositions of such materials is wide, but main components are oxides such as SiO_2, TiO_2, ZnO_2, Fe_2O_3 or combination of other metal oxides.

M41S are mesopourous silicas, usually referred to MCM materials, which stands for Mobil Crystalline Materials. They were reported for the first time in 1992 [46] and synthesized by the Mobil group. Various types of mesoporous silicas with different pore structures were synthesized, e.g. MCM-48 with a cubic pore structure or MCM-41 with hexagonally ordered cylindrical pores and lamellar MCM-50 phases [45].

Mesoporous materials based on MCM-41 have high surface areas of about 1000 m^2/g, and their pores have well-defined sizes and uniform shapes that are ordered in hexagonal channels [48], as shown in Figures 24 and 25.

It was found that the diameter of the pores could be controlled by changing the length of the template molecule. By changing the silica sources, surfactants, auxiliary compounds or reaction conditions, there is also a possibility to produce new mesoporous systems. The change in synthesis conditions results in the change of the thermal, hydrothermal and mechanical properties of the materials. Othman reported that thermal, hydrothermal and hydrolytic stabilities for MCM-41-based silicates are excellent [47].

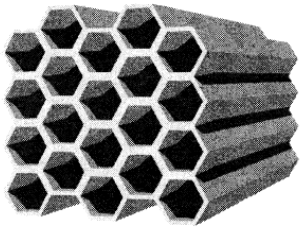

Figure 24 - MCM-41 structure [47].

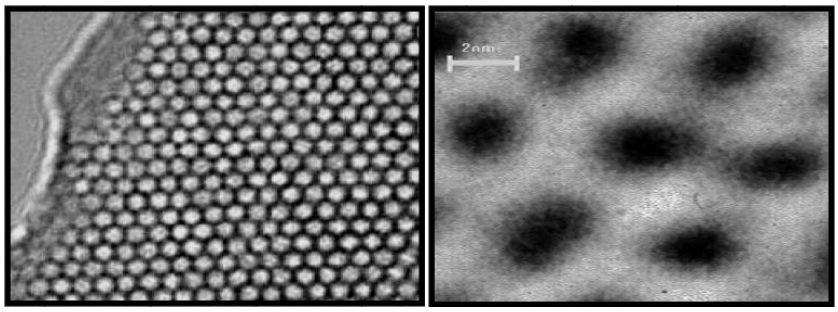

Figure 25 - High resolution transmission electron microscopy (HRTEM) images of MCM-41 with hexagonal channels [47].

Another family is the so-called SBA-X materials (Santa Barbara Amorphous) which were first reported in 1998 [48]. The X is a number corresponding to a specific pore structure and surfactant. SBA-15, the most extensively studied, has hexagonally ordered cylindrical pores and is synthesized with P123 as surfactant [49].

In SBA-15, shown schematically in Figure 26, the mesopores are cylindrical and organized in a hexagonal lattice, as proven in the TEM image presented in Figure 27. The size of the mesopores varies between 6.5-15 nm and the thickness of the pore walls range from 3.1 to 4.8 nm. Between the cylindrical pores, micropores connecting the cylinders to each other are present. Such micropores are called corona and they create a network which is responsible for the high surface area of SBA-15 [50].

Figure 26 - SBA-15 structure [50].

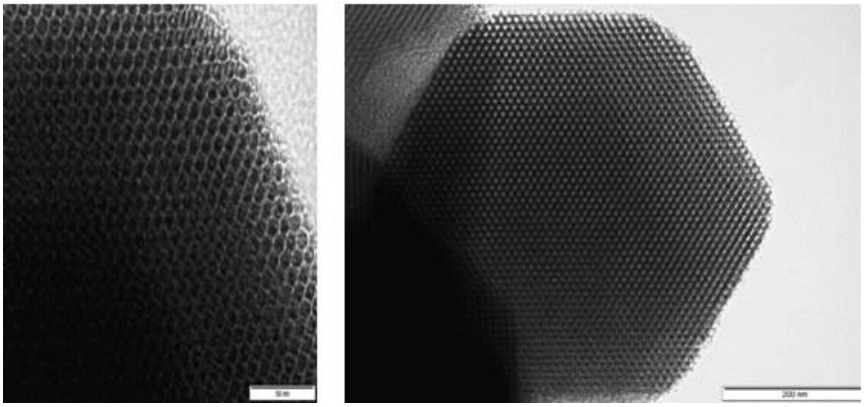

Figure 27 - TEM images of SBA-15 [50].

Due to the possibility of controlling the pores size of these materials, they have found a lot of applications, such as e.g. in separation of hydrocarbons, as a molecular sieves for biomolecules, as template for growing nanoparticles or in catalysis for the anchoring of metal compounds into the silica [49].

During the preparation of these materials each step (synthesis, hydrothermal treatment, drying and washing and calcination) can affect the final product of SBA-15, being crucial for the final properties.

There are also other types of mesoporous silicas such as MSU, KIT, FDU and AMS where the materials are synthesized with variation in e.g. synthesis conditions and surfactants [49].

I.5.2 Supported catalysts for ROP of lactide

Only few examples of supported catalytic systems for cyclic esters polymerization were described in the literature, and only a small group of heterogeneous initiators have been reported. However, the heterogeneous systems in polymerization reactions with the silica-supported catalysts showed numerous advantages, such as high monomer conversion, possibility of recycling of the initiator and sometimes high molecular weights, as well as narrow polydispersities of obtained polymers. Examples of such heterogeneous systems used in ROP of lactide have been described and they will be here summarized.

One of the earliest heterogenization of tin homogeneous initiator was reported by Pinnavia and co-workers in 1996 [51]. The tin-substituted hexagonal mesoporous silica (Sn-HMS) was synthesized with neutral amine surfactant assembly on silicon and tin(IV) alkoxido precursors at room temperature. The catalyst containing 1.0 mol% of Sn was prepared by mixing tetraethylorthosilicate with tin(IV) isopropoxido. The resulting solution was added under vigorous stirring to a solution of dodecylamine ethanol and deionized water for 18 h. The product was filtered, washed with ethanol and calcinated in air at 550ºC for 6 h. The specific surface area of the calcinated product registered was S_{BET}=886m^2/g. When tested in lactide polymerization, the catalyst enabled to achieve 82% conversion in 72h at 130°C. Obtained polymers presented high molecular mass (36000g/mol) and narrow PDI (1.1). When tried with pure tin oxide as catalyst, the conversion was lower (73%) and the polymerization product had a much lower molecular mass (17800g/mol) and a higher polydispersity (1.7). Thus the authors concluded that the ordered pore structure improves the average molecular weights and polydispersity in comparison homogeneous catalysts. This was explained by the imposed steric restrictions on the propagating PLA chains and intermolecular transesterification reactions.

Another attempt on the synthesis of heterogeneous catalyst based in tin was recently reported. Lee et. al. [52] synthesized supported $Sn(OMe)_2$ catalysts on pretreated silica. The initiators contained various tin contents from 2.14 to 5.09 (wt.%) and a series of bulk polymerization reactions of lactide were carried out with homogeneous methoxido catalyst and silica-supported tin alkoxido catalyst in order to compare the characteristics of the produced polylactide. The specific surface area was S_{BET}=268 m^2/g for the support, while for the prepared catalyst were varying between 261–237 m^2/g depending of the tin content (the higher the tin content the lower the specific surface area of the supported catalyst). In the same reaction conditions, the supported catalysts showed higher conversion than homogeneous catalysts. For 5.09% of tin content, in homogeneous catalysis, 38% conversion after 1h reaction and 92% conversion after 5h reaction were observed and, 58% after 1h reaction and 94% after 5h reaction for supported system. Although the PDIs of obtained PLAs were nearly similar, the M_w values of PLA obtained by supported catalysts were lower: after 1h reaction, 40000 g/mol for homogeneous and 31600-56100 g/mol for heterogeneous (depending on the tin content); after 5h reaction, 95500 g/mol for homogeneous and 59200-68300 g/mol for heterogeneous (depending of the tin content). The authors claimed that the immobilization of $Sn(OMe)_2$ over SiO_2 should not affect the chemical nature of the active sites. Other possible explanation of molecular weight decrease given by the authors was that it could have been connected with the acidic nature of SiO_2, resulting in a faster chain transfer rate. One of the most important conclusions of this work was the successful recover up to 85% of the spent supported catalyst by simple filtration – Figure 28. Thus it was proven, that metal-free grade of PLA could be produced with the heterogeneous catalyst system, and recycling of the catalyst was possible.

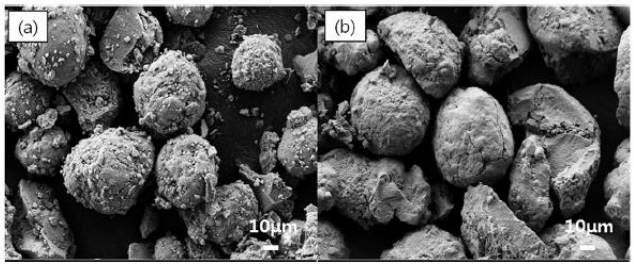

Figure 28 - SEM images of the (a) fresh catalyst and (b) separated catalyst after the polymerization [52].

Supported catalysts were also prepared using zinc β-diiminate complexes by C.W. Jones et al. [53]. The catalyst was immobilized on mesoporous silica SBA-15 and also on glass with controlled porosity (CPG-246). The complexes used as homogeneous initiators were able to effectively polymerize lactide. The registered conversion of monomer was 96% for 30 min reaction at 25°C. It was produced a high molecular weight (15630 g/mol) polymer with a narrow polydispersity (1.09). Despite the high conversion, only oligomeric products were obtained. SBA-15-immobilized catalyst successfully polymerized lactide at 80°C in toluene. 65% monomer conversion was achieved for 24h reaction and the polymer with a low molecular weight (1285 g/mol) but a narrow PDI (1.12) was formed. Similarly, CPG-immobilized catalyst gave a PLA with molecular weight of 1395 g/mol and PDI of 1.09. The researchers concluded the supports structure have a strong influence on the ability to produce high molecular weight PLAs and that this kind of zinc complexes as initiators could produce high molecular weight polymers when immobilized on nonporous support. The surface silanols can contribute to premature chain transfer processes resulting in lower molecular weight, oligomeric products. In order to avoid such terminating processes, attempts were undertaken via capping the unreacted silanol moieties.

In 2009, Kim et al. reported two titanium-supported systems: $TiCl(O\text{-}i\text{-}Pr)_3/SiO_2$ and $Ti(O\text{-}i\text{-}Pr)_4/SiO_2$ [54]. The catalysts were prepared by immobilizing titanium(IV) chloride triisopropoxido and titanium(IV) tetraisopropoxido on pretreated silica. The specific surface area of silica was 260 m^2/g for pure, calcinated silica, and 246 and 229 m^2/g for $TiCl(O\text{-}i\text{-}Pr)_3/SiO_2$ and $Ti(O\text{-}i\text{-}Pr)_4/SiO_2$, respectively. Morphologies of treated silica, $TiCl(O\text{-}i\text{-}Pr)_3/SiO_2$ and $Ti(O\text{-}i\text{-}Pr)_4/SiO_2$ are shown in Figure 29. Measurements indicate that the immobilization did not affect the morphology of the support.

A series of LA polymerization reactions were conducted with homogeneous alkoxido catalyst and with silica-supported titanium alkoxido catalyst in order to compare their catalytic activity and the characteristics of obtained PLA. The characteristics of polymers obtained in 12h polymerization reactions at 70°C are presented in the Table 1.

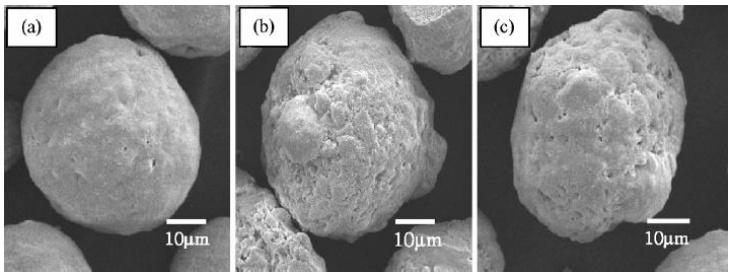

Figure 29 - SEM photographs of (a) calcined silica, (b) $TiCl(O^iPr)_3/SiO_2$, and (c) $Ti(O^iPr)_4/SiO_2$ [54].

Table 1 - Characteristics of PLA produced with homogeneous and heterogeneous titanium(IV) alkoxido catalyst [54].

Catalyst	Conversion (%)	Mn (g/mol)	Mw (g/mol)	PDI	Tm (ºC)
$TiCl(O\text{-}i\text{-}Pr)_3$	72	9650	13600	1,41	161,5
$TiCl(O\text{-}i\text{-}Pr)_3/SiO_2$	70	29500	36200	1,23	166,2
$Ti(O\text{-}i\text{-}Pr)_4$	66	9590	15100	1,57	154,3
$Ti(O\text{-}i\text{-}Pr)_4/SiO_2$	74	30300	36300	1,20	165,6

In conclusion, the activity of heterogeneous catalyst was lower than the homogeneous, however, the conversion was higher for heterogeneous system. Polylactide with similar molecular weights and PDIs were produced using both initiators, $TiCl(O\text{-}i\text{-}Pr)_3/SiO_2$ and $Ti(O\text{-}i\text{-}Pr)_4/SiO_2$, but the molecular weight of PLA obtained with the silica-supported catalyst was 2.5 times higher than that produced with the homogeneous catalyst. In comparison with homogeneous catalysts, the PDI of the produced PLA with both supported catalysts is lower. The authors suggested that an unclear restriction of transesterification reactions might be associated to a changes of the environment of the active sites during the immobilization. Concerning the results of melting temperatures, the authors thought that the differences in molecular weights of the polymers made using supported catalyst results in variations of the melting temperatures.

Wanna and coworkers [55] also immobilized titanium(IV) isopropoxido on aluminum- and calcium-incorporated MCM-41-type silica as a support. The specific surface area for the MCM-41 was 1502 m^2/g and not much lower for the incorporated silica. Scanning electron microscope photographs showed that neither titanium grafting nor polymerization processes influences the material morphology (Figure 30).

Catalysts were used in ring-opening polymerization of lactide, as well as reactions with homogeneous alkoxido catalyst were also conducted. Characteristics of obtained PLA using all of the catalysts are presented in Table 2.

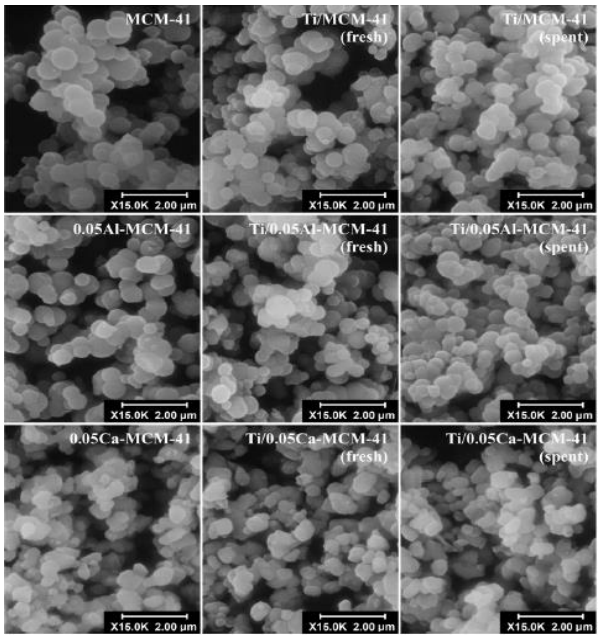

Figure 30 - SEM photographs of the supports, the fresh catalysts, and the spent catalysts [55].

Table 2 - Characteristics of PLA produced with various catalyst [55].

Catalyst	Reaction time (h)	Conversion (%)	M_n (g/mol)	M_w (g/mol)	PDI	T_m (ºC)
Ti(O-*i*-Pr)$_4$	1	100	4400	55000	1,24	141,5
Ti/MCM-41	1	100	8900	10300	1,16	160,8
Ti/0,01Al-MCM-41	1,5	100	12700	15300	1,20	161,7
Ti/0,05Al-MCM-41	2,5	100	10700	12200	1,14	152,7
Ti/0,1Al-MCM-41	2	100	11100	12700	1,14	156,6
Ti/0,01Ca-MCM-41	5	100	11500	13200	1,15	154,0
Ti/0,05Ca-MCM-41	5	70	7200	8200	1,14	150,9
Ti/0,1Ca-MCM-41	5	7,9	-	-	-	-

In ring-opening polymerization of lactide all the catalysts were able to self-initiate the reaction. Ti/MCM-41 led to 100% conversion in the shortest time, followed by Ti/Al-MCM-41. However, a higher amount of aluminum reduced reaction rate. Ti/Ca-MCM-41 exhibited much lower polymerization rate of lactide than other titanium supported catalysts. Only with a small amount of calcium incorporated into the support, it was possible to achieve 100% conversion of lactide in 5h reaction. Thus, the incorporation of calcium in MCM-41 negatively affected the polymerization rate, but increased the molecular weight. One more time, a better polydispersity and higher molar mass of the polylactide were attained using the synthesized heterogeneous catalyst instead of the homogeneous analog $Ti(OiPr)_4$.

I.6 References

[1] Ren J., *Biodegradable Poly(Lactic Acid): Synthesis, Modification, Processing and Applications*, Tsinghua University Press Beijing and Springer-Verlag Berlin Heidelberg, 2010.

[2] Scott G., *Degradable Polymers: Principles and Applications*, Springer, B.V., 2002.

[3] A. A. El-Fattah, E.-R. Kenawy, S. Kandil, *International Journal of Chemical and Applied Biological Sciences*, **2014**, *1*, 2.

[4] (a) Robertson, G.L.; *Food Packaging: principals and pratice*, CRC Press Taylor & Francis Group, 3rded., 2013; (b) A. A. Shah, F. Hasan, A. Hameed, S. Ahmed, *Biotechnology Advances*, **2008**, *26*, 246.

[5] (a) Avérous, L.; Pollet, E.; *Environmental Silicate Nani-Biocomposites*, Springer, 2012; (b) Dutta S., Hung W., Huang B., Lin Ch*., Advances in polymer Science*, **2012**, *245*, 219; (c) M. Jamshidian, E. A. Thrrany, M. Imran, M. Jacquot, S.Desorby, *Comprehensive Reviews in Food Acience and Food Safety*, **2010**, *9*, 552.

[6] (a) W.H. Carothers, *Chem. Rev.*, **1931**, *8*, 353; (b) K.W.Kim, S.I. Woo, Macromol. *Chem. Phys.*, **2002**, *203*, 2245.

[7] (a) R.A. Gross, A.Kumar, - Kalra, *Chem. Rev.*, **2001**, 101, 2097; (b) S. Matsumura, *Adv. Polym. Sci*., **2006**, *194*, 95; (c) A.-C. Albertsson, R. K. Srivastava, *Advanced Drug Delivery Reviews*, **2008**, *60*, 1077.

[8] (a) W.H. Carothers, C.L. Dorough, F.J. Van Natta, *J. Am. Chem. Soc*., **1932**, *54*, 761; (b) K. M. Stridsberg, M. Ryner, A.-C. Albertsson, *Adv. Polym. Sci*., **2002**, 157, 41; (c) P. Dubois, O. Coulembier, J.-M. Raquez, *Handbook of Ring-Opening Polymerization*, Wiley-VCH, Weinheim, 2009.

[9] *Growth in PLA bioplastics: a production capacity of over 800,000 tonnes expected by 2020*, nova-Institute, **2012**, Germany.

[10] R. E. Drumright, P. R. Gruber, D. E. Henton, *Adv. Mater.*, **2000,** *12*, 1841.

[11] (a) Du, Y. D.; Lemstra, P. J.; Nijenhuis, A. J.; Van Aert, H. A. M.; Bastiaansen, C., M*acromolecules*, 1995, *28*, 2124; (b) A. K. Mohanty, M. Misra, L. T. Drzal, *Natural Fibers, Biopolymers, and Biocomposites*, Taylor & Francis Group, 2005; (c) T. M. Ovitt; G. W. Coates, *Journal of the American Chemical Society,* **1999***, 121,* 4072; (d) T. M. Ovitt; G. W. Coates, *J. Polym. Sci., Part A: Polym. Chem*., **2000**, *38*, 4686.

[12] (a) O. Dechy-Cabaret, B. Martin. Vaca, D. Bourissou, *Chem. Rev.,* **2004**, *104*, 6147; (b) C. Jerome, P. Lecomte, *Advanced Drug Delivery Reviews*, **2008**, *60*, 1056; (c) P. Dubois, O. Coulembier, J.-M. Raquez, *Handbook of Ring-Opening Polymerization*, Wiley-VCH, Weinheim, 2009.

[13] (a) D. Bourissou, B. Martin-Vaca, A. Dumitrescu, M. Graulier, F. Lacombe, *Macromolecules*, **2005**, *38*, 9993; (b) Penczek, S., Kubisa, S., Matyjaszewski, K.; *Cationic Ring-Opening Polymerization***,** Spinger, 1985; (c) Y. Okamoto, *Makromol. Chem.*, Macromol. Symp. 42/43, **1991**, 117-133

[14] (a) N. E. Kamber, W. Jeong, R. M. Waymouth, *Chem. Rev.*, **2007**, *107*, 5813; (b) M. K. Kiesewetter, E. J. Shin, J. L. Hedrick, R. M. Waymouth, *Macromolecules,* **2010**, *43*, 2093.

[15] D. Bourissou, B. Martin-Vaca, A. Dumitrescu, M. Graullier, F. Lacombe, *Macromolecules,* **2005**, *38*, 9993.

[16] (a) J. Wu, T.-L. Yu, C.-T. Chen, C-C. Lin, *Coord. Chem. Rev*., **2006**, *250*, 602; (b) B. J. O'Keefe, M. A. Hillmyer, W. B. Tolman, *J. Chem. Soc., Dalton Trans.*, **2001**, 2215; (c) O. Dechy-Cabaret, B. Martin. Vaca, D. Bourissou, *Chem. Rev.,* **2004**, *104*, 6147; (d) P. Dubois, O. Coulembier, J.-M. Raquez, *Handbook of Ring-Opening Polymerization*, Wiley-VCH, Weinheim, 2009;

[17] J. Kleine, H.-H Kleine, *Makromol. Chem*, **1959**, *30*, 23

[18] (a) A. Löfgren, A.-C. Albertsson, P. Dubois, R. Jerôme, Rev. Macromol. Chem. Phys., **1995**, *C35*, 379; (b) W. Kuran, Prog. Polym. Sci., **1998**, *23*, 919; (c) A. Duda, S. Penczek, In Polymers from Renewable Resources: Biopolyesters and Biocatalysis, ACS Symposium Series 764, American Chemical Society: Washington, D.C., **2000**,160.

[19] W. Dittrich, R. C. Schulz, *Angew. Makromol. Chem.,* **1971,** *15*, 109.

[20] H. R. Kricheldorf, M. Berl, M. Scharnagl, *Macromolecules***, 1988,** *21*, 286.

[21] P. Dubois, C. Jacobs, R. Jerôme, P. Teyssié, *Macromolecules*, **1991**, *24*, 2266.

[22] (a) C. K. Williams, *Chem. Soc. Rev.,* **2007**, *36*, 1573; (b) R. O. MacRae, C. M. Pask, L. K. Burdsall, R. S. Blackburn, C. M. Rayner, P. C. McGowan, *Angew. Chem. Int. Ed.*, **2011**, *50*, 291.

[23] R. P. Quirk, B. Lee, *Polym. Int.* **1992**, *27*, 359.

[24] S. Penczek, A. Duda, R. Szymanski, *Macromol. Symp*., **1998**, *132*, 441.

[25] (a) H. R. Kricheldorf, I. Kreiser-Saunders, *Makromol. Chem*., **1990**, *191*, 1057; (b) Labet M., Thielemans W., *Chem. Soc. Rev*., **2009**, *38*, 3484.

[26] P. Degée, P. Dubois, R. Jerôme, S. Jacobsen, H.-G. Fritz, *Macromol. Symp.*, **1999**, *144*, 289.

[27] H.R. Kricheldorf, I. Kreiser-Saunders, D. O. Damrau, *Macromol. Symp.*, **2000**, *159*, 247.

[28] M. Ryner, K. Stridsberg, A.-C. Albertsson, H. von Schenk, M. Svensson, *Macromolecules,* **2001**, *34*, 3877.

[29] (a) H. R. Kricheldorf, M. Berl, N. Scharnagl, *Macromolecules,* **1988**, *21*, 286; (b) J. Baran, A. Duda, A. Kowalski, R. Szymanski, S. Penczek, *Macromol. Symp.* **1997**, *123*, 93. (c) S. Penczek, A. Duda, R. Szymanski, *Macromol. Symp.,* **1998**, *132*, 441.

[30] (a) P. Degée, P. Dubois, R. Jerôme, *Macromol. Symp.* **1997**, *123*, 67. (b) P. Degée, P. Dubois, R. Jerôme, *Macromol. Chem. Phys.* **1997**, *198*, 1973.

[31] A. Kowalski, A. Duda, S. Penczek, *Macromolecules,* **1998**, *31*, 2114.

[32] (a) W. M. Stevels, M.J.K. Ankone, P.J. Dijkstra, J. Feijen, *Macromolecules*, **1996**, *29*, 3332; (b) W. M. Stevels, M.J.K. Ankone, P.J. Dijkstra, J. Feijen, *Macromolecules*, **1996**, *29*, 6132; (c) A. Amgoune, C. M. Thomas, J.-F. Carpentier, *Pure Appl. Chem.*, **2007**, 79, 2013.

[33] (a) H. Ma, J. Okuda, *Macromolecules,* **2005**, *38*, 2665; (b) M. Solt, A.Södergard, Macromolecules, **1999**, *32*, 6412.

[34] (a) B.-T. Ko, C.-C. Woo, C.-C. Lin, *Organometallics*, **2000**, *19*, 1864; (b) M. H. Chisholm, D. Navarro-Llobet, W. J. Simonsick, *Macromolecules,* **2001**, *34*, 8851; (c) Y.-C. Liu, B.-T. Ko, and C.-C. Lin, *Macromolecules,* **2001**, *34*, 6196; (d) M. H. Chisholm, C.-C. Lin, J. C. Gallucci, and B.-T. Ko, *Dalton Transactions*, **2003**, 406; (e) B.-T. Ko, C.-C. Lin, *Journal of the American Chemical Society*, **2001**, *123*, 7973; (f) M.-L. Hsueh, B.-H. Huang, J. Wu, C.-C. Lin, *Macromolecules*, **2005**, *38*, 9482.

[35] (a) M. H. Chisholm, J. Gallucci, K. Phomphrai, *Chemical Communications*, **2003**, 48; (b) M. H. Chisholm, J. C. Gallucci, K. Phomphrai, *Inorg. Chem.*, **2004**, *43*, 6717.

[36] (a) B. M. Chamberlain, M. Cheng, D.R. Moore, T.M. Ovitt, E.B Lobkovsky, G.W. Coates, *Journal of the American Chemical Society*, **2001**, *123* , 3229 ; (b) J.M. Smith, R.J. Lachicotte, P.L. Holland, *Chemical Communications,* **2001**, 1542 ; (c) A.P. Dove, V.C. Gibson, E.L. Marshall, M.H.S. Rzepa, A.J.P. White, D.J. Williams, *Journal of the American Chemical Society* , **2006**, *128*, 9834.

[37] (a) M. Wisniewski, A. Le Borgne, N. Spassky, *Macromolecular Chemistry and Physics*, **1997**, *198* , 1227 ; (b) Z. Tang, X. Chen, X. Pang, Y. Yang, X. Zhang, X. Jing, *Biomacromolecules*, **2004**, *5*, 965; (c) T. M. Ovitt, G. W. Coates, Journal of Polymer Science Part A – Polymer Chemistry, **2000**, *38*, 4686.

[38] P. Hormnirun, E. Marshall, V.C. Gibson, A.J.P. White, D.J. Williams, *Journal of the American Chemical Society*, **2004**, *126*, 2688

[39] M. H. Chisholm, J.C. Gallucci, H. Zhen, *Inorganic Chemistry*, **2001**, *40*, 5051

[40] H.-Y. Chen, H.-Y. Tang, C.-C. Lin, *Macromolecules*, **2006**, *39*, 3745

[41] C.K. Williams, L. E. Breyfogle , S. K. Choi , W. Nam , V. G. Young , M. A. Hillmyer and W. B. Tolman, *Journal of the American Chemical Society*, **2003**, *125* ,11350.

[42] (a) C.X. Cai , A. Amgoune, C.W. Lehmann, J.C. Carpentier, *Chemical Communications*, **2004** 330; (b) A. Amgoune, C. M. Thomas, T. Roisnel, J.C. Carpentier, *Chemistry – A European Journal*, **2006**, *12*, 169; (c) A. Amgoune, C.M. Thomas, J.C. Carpentier, *Macromolecular Rapid Communications*, **2007**, *28*, 693.

[43] Barbaro P., Ligouri F., *Heterogenized homogeneous catalysts for fine chemicals production-Materials and Processes*, Springer, 2010.

[44] IUPAC Manual of Symbols and Terminology, *Pure appl. Chem.*, **1972**, *31*, 579

[45] D. Trong On, D. Desplantier-Giscard, C. Danumah, S. Kaliaguine, *Applied Catalysis A: General*, **2003**, 253, 545.

[46] C. T. Kresge, M. E. Leonowicz, W. J. Roth, J. C. Vartuli, J. S. Beck, *Nature*, **1992**, 359.

[47] Z. A. ALOthman, *Materials*, **2012**, *5*, 2874.

[48] D. Zhao D., J. Feng, Q. Huo, N. Melosh, G.H. Fredrickson, B. F. Chmelka, G. D. Stucky, *Science*, **1998**, *279*.

[49] Johansson, E., *Controlling the pore size and morphology of mesoporous silica*, Licentiate Thesis No. 1451, Department of Physics, Chemistry and Biology, Linköping University, 2010.

[50] Johansson, E., *Desing of mesoporous silica templates for nanoparticle growth*, Thesis for the degree of Master of Science, Department of Physis, Göteborg University, 2008.

[51] T. M. Abdel-Fattah T., T. J. Pinnavia, *Chem. Commun.*, **1996**, 665.

[52] E. Lee, K. Lee, J. Jang, E. Kim, J. S. Chung, Y. Do, S.C. Yoon, S. Y. Park, *Journal of Molecular Catalysis A: Chemical,* **2014**, 385, 68.

[53] C. W. Jones, K. Yu, *Journal of Catalysis*, **2004**, *222*, 558.

[54] E. Kim, E. W. Shin, I.-K. Yoo, J. S. Chung, *Journal of Molecular Catalysis A: Chemical*, **2009**, *298*, 36.

[55] N. Wanna, T. Kraithong, T. Khamnaen, P. Phiriyawirut, S. Charoenchaidet, J. Tantirungrotechai, *Catalysis Communications*, **2014**, *45*, 118.

Chapter II

TITANIUM SUPPORTED CATALYSTS FOR ROP OF L-LACTIDE

Based on the literature background highlighted in the previous chapter, titanium supported catalysts appear as potentially suitable initiators for the ROP of LA. In this work, this type of catalysts was investigated and an evaluation of the influence of impregnation and polymerization conditions was performed. A comparison between the heterogeneous catalytic systems and their homogeneous analogues was performed.

II.1 Results and Discussion

II.1.1 Preparation of the support

SBA-15 was synthesized following a procedure described by the Catalysis and Reaction Engineering Research Group of Instituto Superior Técnico, Lisboa [1]. SBA-15 was dried under the following conditions: heat rate 5°C/min until 400°C under an air stream of 80 ml/min, kept at 400°C for 2 hours in air and 1 hour under nitrogen.

II.1.2 Characterization of the support

The support and pore structures were characterized by Nitrogen Adsorption, using BET adsorption isotherms, Scanning Electron Microscopy (SEM) and Transmisson Electron Microscopy (TEM).

The results of Nitrogen Adsorption analysis are shown in Table 3, where S_{BET} is BET surface area, V_p is pore volume, A_{ext} is external area and D_p is pore diameter.

Table 3 - Parameters of the mesoporous material used as support.

S_{BET} (m^2/g)	V_p (cm^3/g)	A_{ext} (m^2/g)	D_p (Å)
743	1.12	87	70

SEM and TEM images of SBA-15 are shown in Figure 31 and Figure 32. SEM's picture shows the characteristic microstructure of SBA-15 with well-defined channels. The picture obtained by TEM confirms the expected and typical pore structure of SBA-15, being clear that the samples have cylindrical pores arranged in a hexagonal pattern.

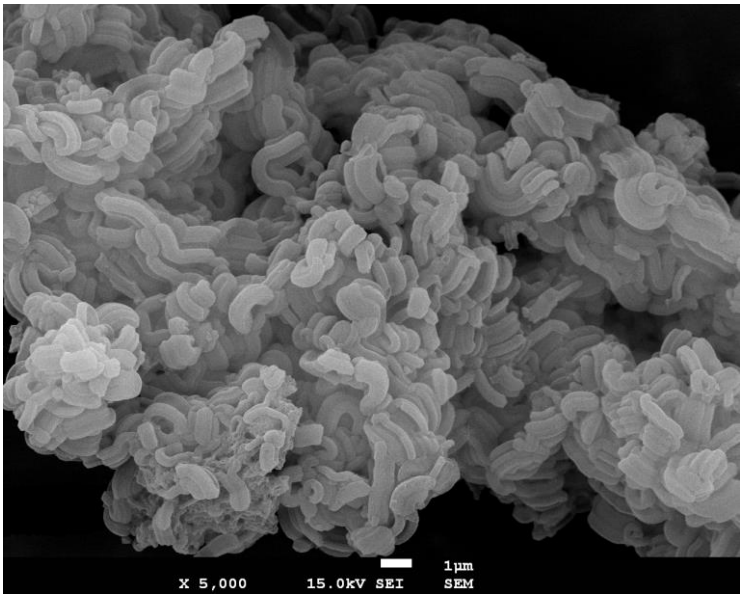

Figure 31 - SEM picture of SBA-15.

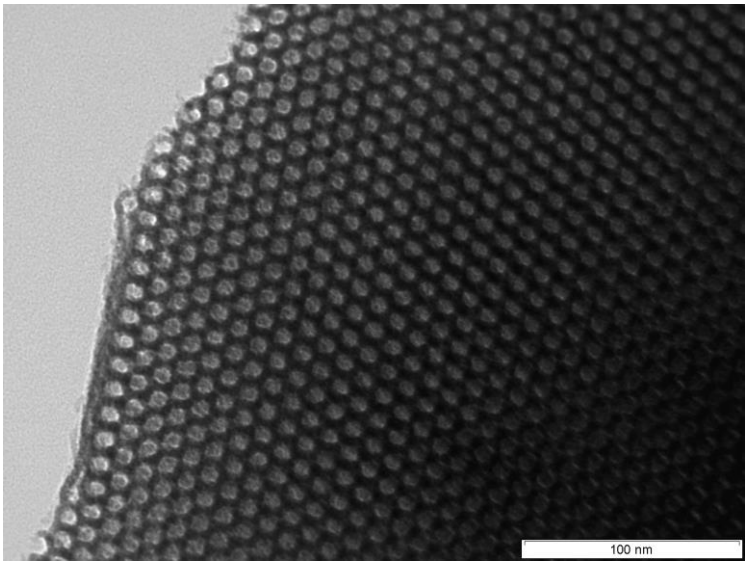

Figure 32 - TEM picture of SBA-15.

II.1.3 Preparation of the catalysts

Two different titanium complexes were used in this work: titanium(IV) tetraisopropoxido ($Ti(O\text{-}i\text{-}Pr)_4$) and titanium(IV) chloride triisopropoxido ($TiCl(O\text{-}i\text{-}Pr)_3$). The heterogeneous catalysts were prepared by immobilization of $Ti(O\text{-}i\text{-}Pr)_4$ or $TiCl(O\text{-}i\text{-}Pr)_3$ on SBA-15 under nitrogen. Predetermined amounts of mesoporous silica, titanium complex and toluene were charged in a schlenk tube and the reactions were carried out in different conditions concerning the impregnation time (1.5 hours and 3 hours) and the impregnation temperature (50ºC and room temperature, *ca.* 21°C). Different amounts of titanium were immobilized in order to obtain different

Ti(mmol)/SBA-15(g) ratios. After impregnation, the catalysts were used right away in the polymerization reactions.

In order to determine the amount of titanium compounds that were effectively grafted, the content of the toluene supernatant solutions was analyzed by ^{1}H NMR after separation of the catalyst by filtration. The solvent was evaporated to dryness and the residue was dissolved in d_8-toluene and analyzed by ^{1}H NMR. This analysis allowed concluding about the amount of isopropoxido groups that might have remained in solution. All the titanium was impregnated if no proton resonances of isopropoxido groups were observed in the NMR spectra. The results are shown along the next section.

II.1.4 Polymerization reactions

Polymerization of L-lactide was carried out using a schlenk tube with a magnetic stirring bar. Predetermined amounts of the supported catalyst suspension in toluene and purified L-lactide were charged into a schlenk under nitrogen. The reactions were carried out under different conditions of temperature, time and L-lactide/Ti molar ratio and were terminated by addition of 2 ml of water. The polymers were fully precipitated out of solution by addition of an excess of methanol. The suspension was filtered under vacuum and the composite obtained was dried at 40°C under vacuum overnight.

The yields of the reactions were calculated based on the weight of the dried polymer and the mass of lactide charged into the schlenk tube.

The content of SBA-15 in selected samples of the composites was obtained by Thermogravimetric Analysis and the melting temperature of selected samples was determined by Differential Scanning Calorimetry.

Soxhlet extraction in THF was used to separate the polymer from the supported catalyst and the number-average and weight-average molar masses and PDI of some of the polylactide samples was determined by Gel Permeation Chromatography.

II.1.4.1 Polymerization reactions catalyzed by Ti(O-*i*-Pr)$_4$/SBA-15

Different impregnation times and temperatures were applied to check the influence of these parameters on the reaction yields, molecular weights and polymer properties. The results obtained for the polymerization reactions of L-lactide are shown in Table 4.

Table 4 - Polymerization of L-LA using Ti(O-i-Pr)$_4$/SBA-15.

Run	Impregnation conditions		Ti/SBA-15 (mmol/g)		Reaction conditions[a]		Yield[b] (%)	SBA-15 content[c] (%)
	t (h)	T(ºC)	Initial	Final	T (ºC)	t (h)		
1	3	50	0.54	0.54	70	24	79	14.3
2	3	50	0.76	0.76	70	24	87	11.5
3	3	50	0.76	0.76	70	24	85	-
4	3	RT	0.76	0.76	70	24	67	-
5	3	RT	0.76	0.76	70	24	75	7.8
6	3	RT	0.76	0.76	70	24	79	-
7	1.5	50	0.76	0.76	50	4	0	-
8	1.5	50	0.76	0.76	70	4	51	-
9	1.5	50	0.76	0.76	70	4	59	11.1
10	1.5	50	0.76	0.76	90	4	75	-
11	1.5	50	0.76	0.76	110	4	72	11.2
12	1.5	50	0.76	0.76	70	24	77	12.3
13	1.5	50	0.76	0.76	70	24	78	-

[a]Polymerization conditions: LA/Ti=100:1, solvent: toluene.

[b]$(mass\ of\ polymer\ /mass\ of\ lactide) \times 100\%$

[c]Determined by TGA

The initial and final Ti/SBA-15 ratios presented in Table 4 show that under the impregnation conditions used, all the titanium is effectively grafted on the support. The molar amounts of 0.54 and 0.76 mmol of titanium per gram of SBA-15 correspond to 2.5 (wt.%) and 3.5 (wt.%) of titanium in the catalyst, respectively.

Polymerization reactions performed with the catalysts that were prepared by impregnation of Ti(O-*i*-Pr)$_4$ on SBA-15 during 3 hours, at 50°C resulted in high yields of PLA. The catalysts having a higher amount of titanium led to a higher reaction yields (entries **1** to **3**). Under these conditions, the use of 0.76 mmol of titanium /1 g of SBA-15 led to 87% yield.

The impregnation temperature does not have an influence in the amount of titanium that was grafted on SBA-15. However, it influences the polymerization reaction. In fact, for 3 hours reaction time and RT, the catalysts led to an average PLA yield of 74%, lower than the one obtained using the catalyst prepared during 3 hours, at 50ºC (entries **4** to **6** *versus* entries **1** to **3**).

When the impregnation reactions were carried out for 1.5 hours at 50ºC there was no evidence of Ti(O-*i*-Pr)$_4$ in the supernatant toluene solution and, in accordance, the increasing of impregnation time did not lead to significant differences in PLA yields (entries **2,3** and **12,13**). These results show that there is no advantage in using longer times than 1.5 hours for impregnation reactions of Ti(O-*i*-Pr)$_4$.

The influence of the temperature and time on the polymerization reactions using Ti(O-*i*-Pr)$_4$/SBA-15 was also studied. The results are shown in Figures 33 and 34. The temperatures

reactions were studied at 50ºC, 70ºC, 90ºC and 110ºC. Run **7** showed that at 50ºC no polymer was obtained. However, from temperatures above 70ºC, the rate of the reactions increase with the temperature, until 90ºC, but there is no significant increase above that temperature (runs **8**, **9**, **10** and **11**). The yields obtained for reactions **12** and **13**, which are carried out during 24h at 70ºC, are similar to the yield obtained for reaction **10** that was performed at 90ºC during 4h.

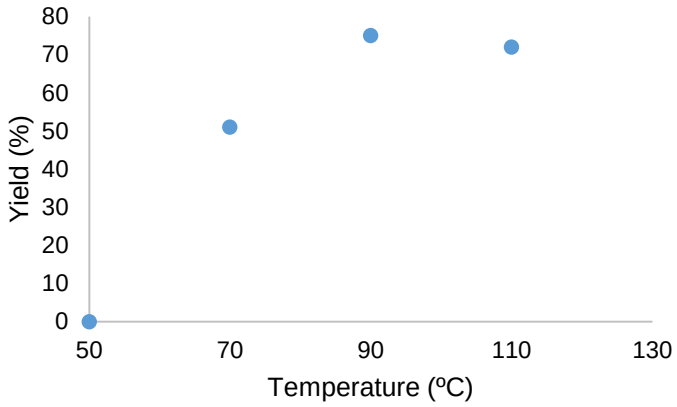

Figure 33 - Effect of the polymerization temperature on the PLA yield after 4h – runs 7, 8, 10, 11.

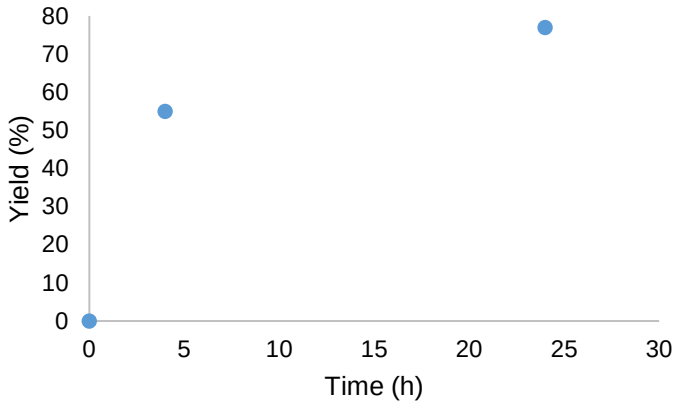

Figure 34 - Effect of the polymerization time on the PLA yield at 70ºC – runs 8 and 12.

Aliquots taken from the reaction solution after 2 and 4 hours for reaction **8** were analyzed by ^{1}H NMR. The results are presented in Figure 35 that represents LA conversion along the time.

The analysis revealed that the monomer conversion was 31% after 2 hours and 61% after 4 hours. These results indicate that the monomer conversion is directly proportional to the reaction time, which means that during this period of time the rate of the reaction is constant. The difference between PLA yield (51%) and monomer conversion may be associated to experimental errors.

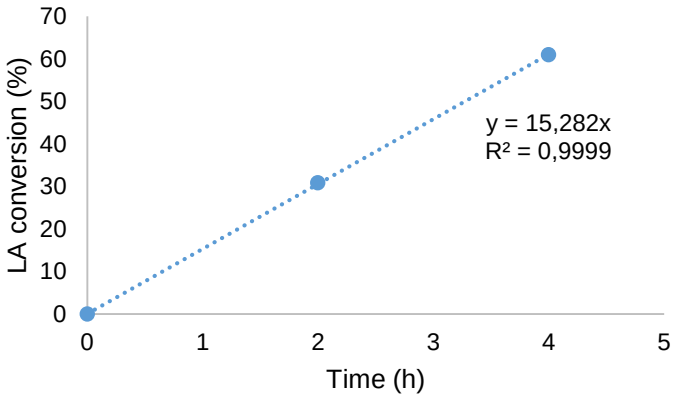

Figure 35 - Monomer conversion versus time – run 8.

The influence of LA/Ti ratio was also evaluated and the results are shown in Table 5. Run **14** was performed with the double amount of LA used for runs **12** and **13**. A comparison between entries **12**, **13** and **14** shows that lactide is polymerized and the overall yields obtained are very similar.

Table 5 – Polymerization of L-LA using Ti(O-*i*-Pr)$_4$/SBA-15.

Run	Impregnation conditions		Ti/SBA-15 (mmol/g)		Reaction conditions[a]		Yield[b] (%)	SBA-15 content[c] (%)
	t (h)	T(ºC)	Initial	Final	T (ºC)	t (h)		
14	1.5	50	0.76	0.76	70	24	75	5.8
15	1.5	50	0.76	0.76	70	24+24	75	4.6

[a]Polymerization conditions: LA/Ti=200:1, solvent: toluene.

[b]$(mass\ of\ polymer\ /mass\ of\ lactide) \times 100\%$

[c]Determined by TGA

Experiment **15** was performed to check if the polymerization reactions display "living" behavior. A polymerization reaction with LA/Ti=100:1 using Ti(O-*i*-Pr)4/SBA-15 catalysts was performed and after 6 hours, the monomer conversion was determined by NMR analysis as 96%. The reaction was continued until 24 hours and then the same amount of lactide was added and the reaction was continued for further 24 hours. The final PLA yield after 48 hours was 75%, which confirms that the second portion of lactide was also polymerized. Determination of molecular weights of samples 12, 14 and 15 did not confirm that the system was "living", because the molecular weight of the polymer did not increase to the double, but this experiment showed that the system could be reused, which means that the catalyst did not deactivate (see section II.6.1.2).

For reaction **15**, aliquots of the reaction mixture were taken after 2, 4 and 6 hours to check the monomer conversion by ^{1}H NMR. The results are presented in Figure 36. It shows that half of the monomer was already converted after 2 hours and after 4 hours the conversion reached

80% being complete after 6 hours with a monomer conversion of 96%. After the second addition of LA, aliquots were taken at 2 and 24 hours for NMR analysis. The polymerization rate of lactide after the second addition was lower than before, maybe due to diffusional problems caused by the presence of PLA. The decomposition of the catalyst is not likely to have occurred because in this LA conversion would be much lower.

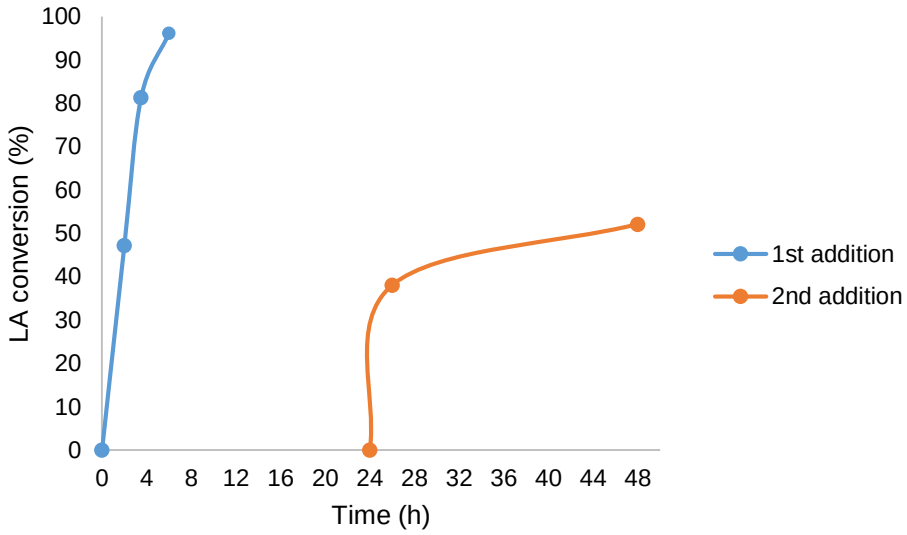

Figure 36 - Monomer conversion versus time during the first and second additions – run 15.

Attempts to isolate the supported catalysts after impregnation reaction were not well succeeded. Filtration of the solvent and drying under vacuum overnight allowed isolating of a solid that did not reproduce the activity obtained in the experiments described above. The results of the polymerization reactions performed with the isolated solids are displayed in Table 6.

Table 6 – Polymerization of L-LA using Ti(O-*i*-Pr)$_4$/SBA-15 after filtration, washing and drying.

Run	Impregnation conditions		Ti/SBA-15 (mmol/g)		Reaction conditions[a]		Yield[b] (%)	SBA-15 content[c] (%)
	t(h)	T(ºC)	Initial	Final	T (ºC)	t (h)		
16	3	50	0.54	0.54	70	24	11	36.2
17	3	50	0.76	0.76	70	24	3	43.1
18	3	50	10	6.50	70	24	-	-

[a]Polymerization conditions: LA/Ti=100:1, solvent: toluene.

[b]$(mass\ of\ polymer\ /mass\ of\ lactide) \times 100\%$

[c]Determined by TGA

The results show that the isolation of the supported catalysts led to a significant decrease in activity probably caused by decomposition. In the experiments carried out the amounts of titanium and SBA-15 were very small and the filtration led to the loss of product because SBA-15

stayed stacked on the filter. These difficulties might have contributed to the controversial results obtained. This procedure (impregnation followed by isolation of the supported catalyst) was reported by other authors and there is no reason to believe that it could not be applied in this case [2], [3].

Kim et al. reported heterogeneous lactide polymerization systems using Ti(O-*i*-Pr)$_4$ supported on silica (sylopol 948, Grace Davison) [2] and used impregnation conditions similar to those used in this work – 3 hours at 50°C in toluene –followed by filtration of the solvent, washing with toluene and drying under vacuum. The titanium content in the catalyst was determined as 3.22 wt% and the lactide polymerizations were performed under the conditions used in this work – L-lactide/Ti = 100:1, 70°C, in toluene – reaching 74% conversion of the monomer in 12 hours.

Wanna et al. reported a similar heterogeneous catalytic system based on titanium(IV) tetraisopropoxido supported catalyst on MCM-41 [3]. The catalyst was prepared and isolated and the polymerization of lactide was conducted in bulk at 110ºC using 7.74 (wt.%) of titanium. The authors obtained 100% monomer conversion after 2 hours. Aluminum- and calcium-incorporated MCM-41 silicas were also used as a supporting materials to prepare heterogeneous catalyst based on titanium tetraisopropoxido. Its application in lactide polymerization also resulted in high monomer conversion in the same reaction conditions (results in Table 2).

II.1.4.1 Polymerization reactions catalyzed by TiCl(O-*i*-Pr)$_3$/SBA-15

Different impregnation times and temperatures were applied to check the influence of these variables on the reaction yield, molecular weights and polymer properties. The results obtained for the polymerization reactions of L-lactide using TiCl(O-*i*-Pr)$_3$/SBA-15 are shown in Table 7.

Initial and final Ti/SBA-15 ratios show that, under the impregnation conditions used, all the titanium is effectively bonded to the support with exception of run **21** where the Ti/SBA-15 ratio was much higher (5mmol/g). In this case, only 60% of metal was retained.

Comparing runs **19/20** with **22/23** it may be concluded that the preparation of the catalyst at room temperature resulted in lower yields than obtained with catalysts prepared at 50ºC. While, the polymerization reactions led to an average yield of 87%, for entries **19** and **20**, 67% average polymerization yield was achieved in runs **22** and **23**.

Table 7 – Polymerization of L-LA using TiCl(O-*i*-Pr)$_3$/SBA-15.

Run	Impregnation conditions		Ti/SBA-15 (mmol/g)		Reaction conditions[a]		Yield[b] (%)	SBA-15 content[c] (%)
	t (h)	T(ºC)	Initial	Final	T (ºC)	t (h)		
19	3	50	0.76	0.76	70	24	90	9.3
20	3	50	0.76	0.76	70	24	85	9.2
21	3	50	5	3.05	70	24	90	-
22	3	RT	0.76	0.76	70	24	70	10.5
23	3	RT	0.76	0.76	70	24	67	-
24	1.5	50	0.76	0.76	70	24	78	-
25	1.5	50	0.76	0.76	70	24	55	-
26	1.5	50	0.76	0.76	70	24	47	-

[a]Polymerization conditions: LA/Ti=100:1, solvent: toluene.

[b]$(mass\ of\ polymer\ /mass\ of\ lactide) \times 100\%$

[c]Determined by TGA

The results obtained for the polymerizations reactions that used TiCl(O-*i*-Pr)$_3$/SBA-15 catalyst prepared during 1.5 hour and 50°C were not reproducible (entries **24** to **26**). Also, as it is shown section II.1.6.2, the polylactides obtained with the TiCl(O-*i*-Pr)$_3$ catalyst had much lower molecular weights then the ones obtained with Ti(O-*i*-Pr)$_4$. Due to these problems and considering the short time available for the experimental part of the work, further and extended studies using TiCl(O-*i*-Pr)$_3$ supported in SBA-15 have not been conducted.

II.1.4.3 Homogeneous Catalysis

In order to compare the performance with supported catalyst with that of the correspondin homogeneous systems, Ti(O-*i*-Pr)$_4$ and TiCl(O-*i*-Pr)$_3$ were tested for L-lactide polymerization. All reactions were performed in toluene, using a molar ratio of LA/Ti=100:1. The yields in isolated PLA obtained for different reaction times are shown in Tables 8 and 9, respectively.

Despite both complexes catalyze the polymerization of lactide to PLA, Ti(O-*i*-Pr)$_4$ revealed to be a better catalyst than TiCl(O-*i*-Pr)$_3$. Ti(O-*i*-Pr)$_4$ revealed to be inactive at room temperature as precipitation of polymer was not observed upon addition of H_2O after 2 h of reactions. However, at 70ºC, polymerization reactions using Ti(O-*i*-Pr)$_4$ as catalyst attain very high PLA yields after 2 hours. On the other hand, the reactions using TiCl(O-*i*-Pr)$_3$ as catalyst are slower affording 30% yield after 2 hours, but the amount of PLA obtained after 24 hours corresponds to 89% yield.

Table 8 - Polymerization of L-LA using Ti(O-*i*-Pr)$_4$.

Run	Reaction conditions[a]		Yield (%)
	T (ºC)	t (h)	
27	RT	2	-
28	70	2	81
29	70	2	80
30	70	4	70
31	70	6	76
32	70	6	82
33	70	24	79
34	70	24	74
35	70	24	80

[a]Polymerization conditions: LA/Ti=100:1, solvent: toluene.

Table 9 - Polymerization of L-LA using TiCl(O-*i*-Pr)$_3$.

Run	Reaction conditions[a]		Yield (%)
	T (ºC)	t (h)	
36	70	2	31
37	70	24	89

[a]Polymerization conditions: LA/Ti=100:1, solvent: toluene.

Figure 37 shows a graphical representation of LA conversion over time for experiment **30**. The monitoring of the reaction was made by ^{1}H NMR analysis of aliquots taken after 2 and 4 hours reaction.

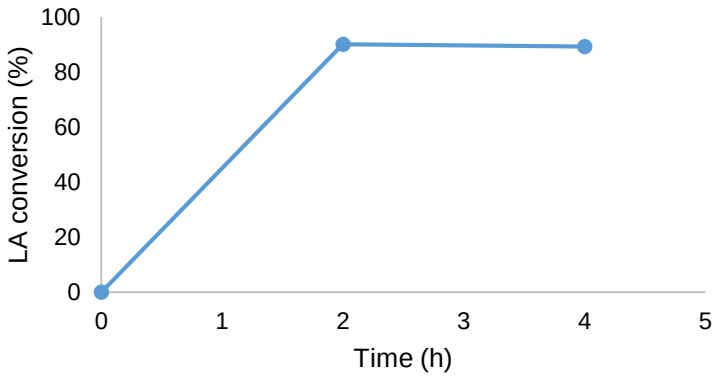

Figure 37 - LA conversion versus reaction time using Ti(O-*i*-Pr)$_4$ - reaction 30.

The analysis revealed that the monomer was fully converted after 2 hours (around 90%). However, the PLA isolated yields were slightly lower, close to 80%. This may be associated with experimental errors related to the recovering of the polymers from solutions or with the formation of a small amount of oligomers that do not precipitate out of solution and give rise to lactide consumption.

Kim and coworkers [2] have described the polymerization of lactide with the same two catalysts in the same experimental conditions. After 24 hours of reaction they reported a monomer conversion of 70% for Ti(O-*i*-Pr)$_4$ and 73% for TiCl(O-*i*-Pr)$_3$. The comparison of the latter values with those reported in Tables 12 and 13 confirms the reproducibility of the catalysts behavior, although the values reported in this work are slightly higher. The differences observed may result from the extremely high sensitivity of the catalysts to fortuitous experimental errors.

In Figure 38, the comparison of homogeneous and heterogeneous systems is presented. The polymerization conditions for both reactions are the same.

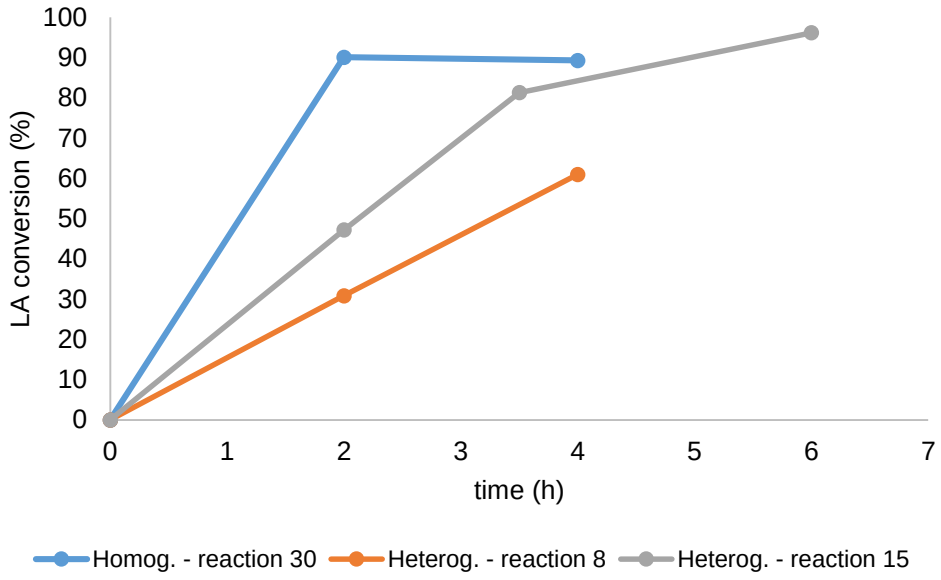

Figure 38 - LA conversion versus time - comparison between homogeneous (reaction 30) and heterogeneous systems (reactions 8 and 15).

Both systems achieved the same monomer conversion, but the heterogeneous reactions required longer times. The homogeneous reaction is fast and full conversion is reached after 2 hours, while for the heterogeneous catalyst, full conversion is reached after 6 hours.

II.1.5 Polymerization Kinetics

In order to study the kinetics of the polymerization reactions, two experiments were performed in a NMR tube and the reactions were followed by the ^{1}H-NMR spectroscopy. The spectra were recorded every 12 minutes until the total monomer conversion. The amounts of lactide and PLA were obtained by integration of characteristic peaks at around 4 ppm for L-lactide and at around 5 ppm for PLA. Plots of the experimental results are shown in Figures 39 and 40 for Ti(O-*i*-Pr)$_4$ and TiCl(O-*i*-Pr)$_3$ catalysts, respectively.

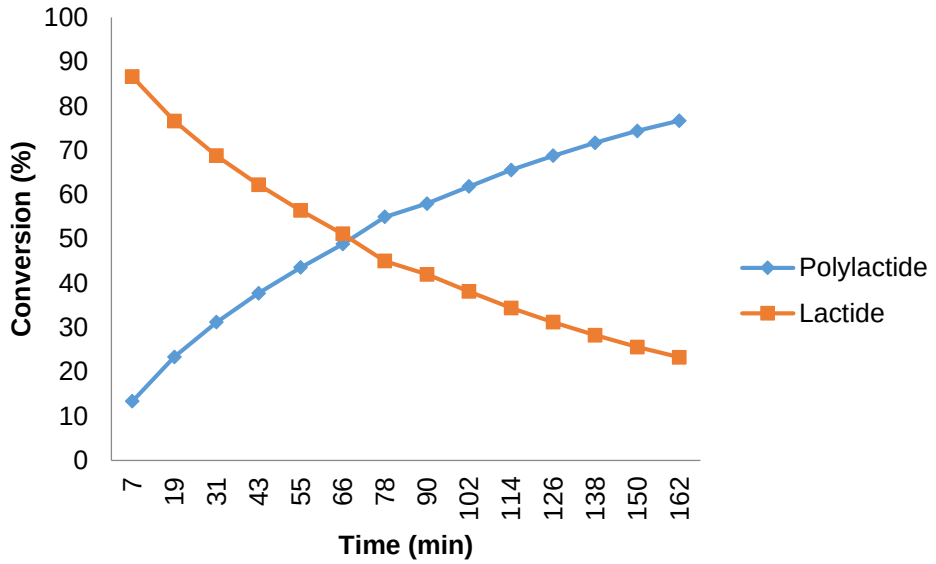

Figure 39 - Plot of percentages of LA and PLA along the time for Ti(O-i-Pr)$_4$ (LA/Ti=50:1, 50ºC, 162 min, solvent: toluene).

The points of intersection of the curves shown in Figures 39 and 40 corresponds to a monomer-to-polymer ratio of 1:1 and it is achieved after approximately 1 hour in both reactions.

For Ti(O-*i*-Pr)$_4$ the formation of polymer reaches almost 80% after 3 hours, and this is also the percentage that corresponds to the monomer conversion.

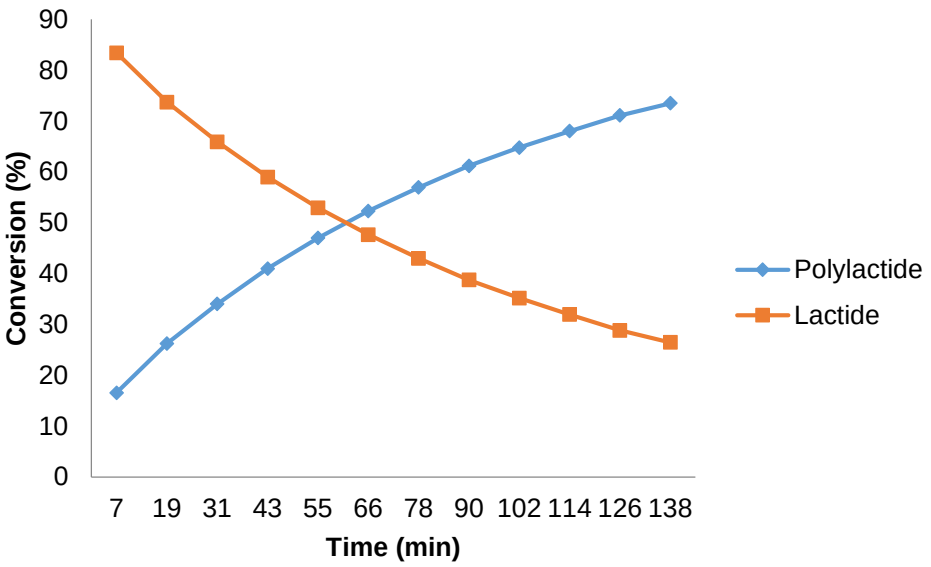

Figure 40 - Plot of percentages of LA and PLA along the time for $TiCl(O\text{-}i\text{-}Pr)_3$ (LA/Ti=50:1, 50ºC, 138 min, solvent: toluene).

Using $TiCl(O\text{-}i\text{-}Pr)_3$ as catalyst, the formation of polymer reaches 70% after 2 hours and at the end of the experiment, after 2.5 hours, the conversion of lactide is 74%.

The graphics of Figures 39 and 40 show that the rate of the reaction, corresponding to the slope of the lines, decreases very slowly along the time. Furthermore, the rates of both reactions are very similar and the same monomer conversions were achieved using both catalysts.

Figure 41 presents the NMR spectra of an experiment performed with $TiCl(O\text{-}i\text{-}Pr)_3$ and it shows the consumption of lactide and the formation of the polymer along the time.

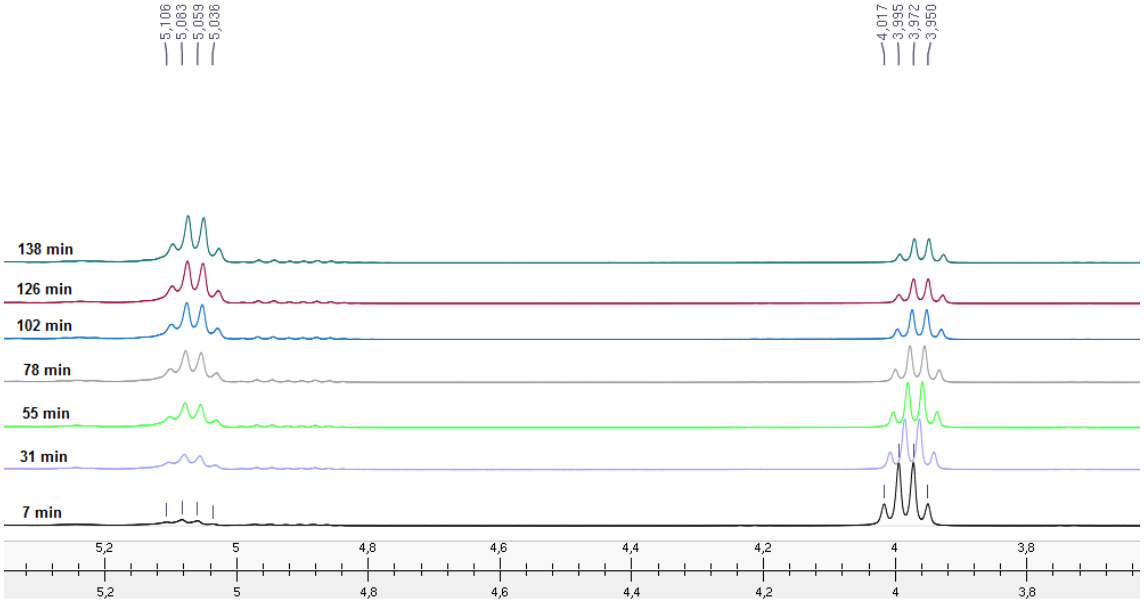

Figure 41 - NMR spectrum of experiment using $TiCl(O\text{-}i\text{-}Pr)_3$ for 7, 31, 55, 78, 102, 126 and 138 minutes.

II.1.6 Characterization of the polymers

II.1.6.1 Thermogravimetric Analysis

TGA is a thermal analysis technique that measures the amount and rate of weight variation of a material as a function of temperature and time in a controlled atmosphere. TGA measurements are used primarily to determine the composition of materials and their thermal stability.

Thermogravimetric Analysis was performed on selected samples in order to determine the content of SBA-15 in the final polymerization product. The values obtained were presented while the presentation of the polymerization results (see section II.1.4).

TGA curves represents the mass loss of polymer in function of temperature. The mass that remains corresponds to the SBA-15, since it does not degrade during the analysis. Examples of TGA curves are shown in Figures 42 and 43 for two samples obtained from reactions **2** and **22**, respectively.

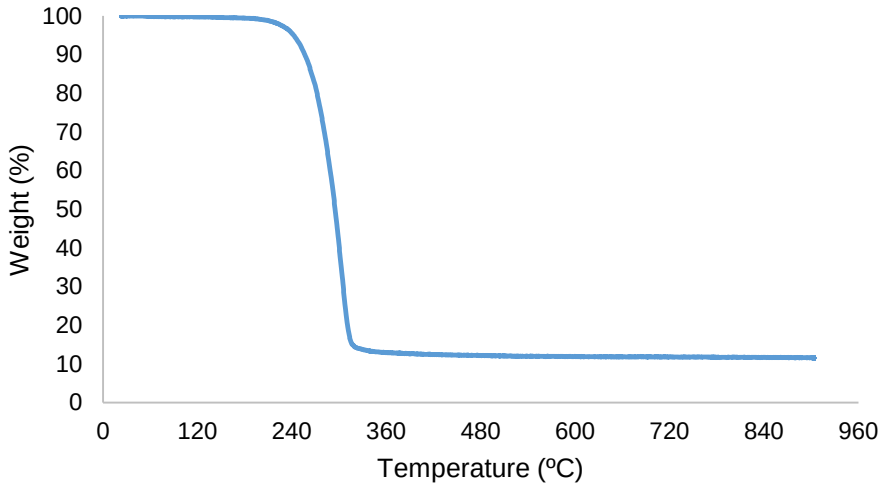

Figure 42 - TGA weight loss curve for PLA obtained in reaction 2.

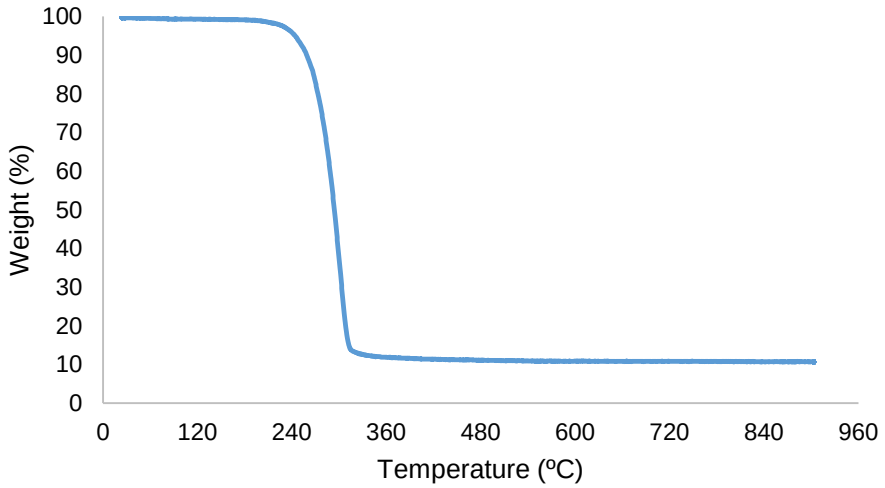

Figure 43 - TGA weight loss curve for PLA obtained in reaction 22.

Reactions **2** and **22** were performed in the same conditions with Ti(O-*i*-Pr)$_4$ and TiCl(O-*i*-Pr)$_3$ prepared under different impregnation temperatures. TGA analysis revealed that weight loss in sample **2** was 88.6%, which corresponds to 11.4% content of SBA-15 in the final reaction product. For sample **22**, weight loss was 89.5%, which corresponds to 10.5% content of SBA-15 in the final reaction product.

Table 10 shows the values of content of SBA-15 obtained by TGA and the expected values based on the amount of SBA-15 charged into the schlenk and the amount of composite obtained. The values are very similar, with exception of runs **16** and **17** that correspond to experiments including the isolation of the catalyst. These results confirm the loss of SBA-15 during the experiments, explaining the low activity of the catalyst in reactions **16** and **17**.

Table 10 - Values of SBA-15 content determined by TGA and SBA-15 content expected.

Run	SBA-15$_{TGA}$ content[a] (%)	SBA-15$_w$ content[b] (%)
1	14.3	14
2	11.5	10
5	7.8	11
9	11.1	14
11	11.2	11
12	12.3	12
14	5.8	6
15	4.6	6
16	36.2	52
17	43.1	76
19	9.3	9
20	9.2	10
22	10.5	12

[a]Determined by TGA

[b]$(mass\ of\ SBA-15/mass\ of\ composite) \times 100\%$

II.1.6.2 Gel Permeation Chromatography

The values of M_n (number-average molecular weight), M_w (weight-average molecular weight), M_p (molecular weight of the longest polymer chain) and PDI were determined by GPC analysis in THF with a polystyrene standard for calibration. A correcting factor of 0.58 was applied for M_n, M_w and M_p values [4].

As example, the chromatogram of GPC for sample **14** is shown in Figure 44 and the results of GPC analyses are shown in Tables 11 to 13.

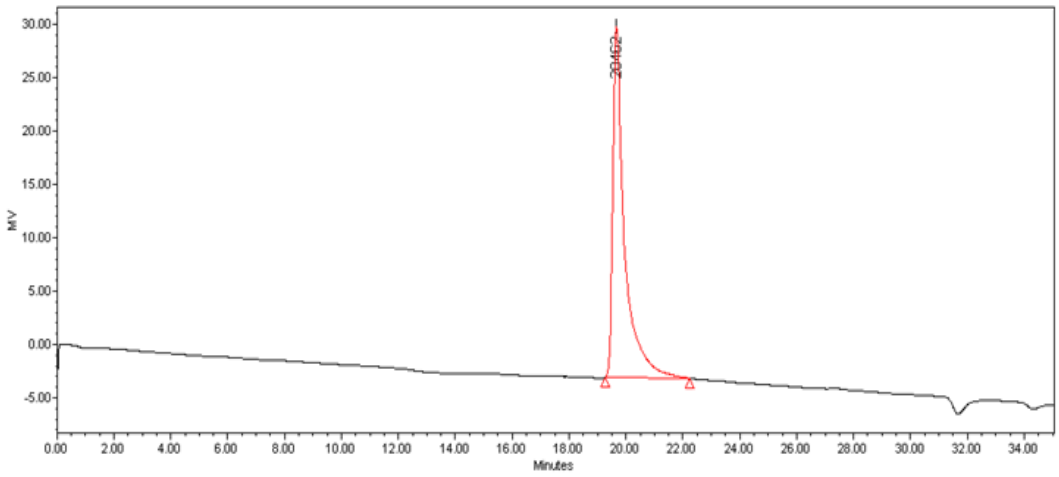

Figure 44 - GPC chromatogram for sample 14.

Table 11 - GPC analysis results.

Run[a]	Impregnation conditions		Reaction conditions		Yield (%)	Mn (g/mol)	Mw (g/mol)	Mp (g/mol)	PDI
	T (ºC)	t (h)	T (ºC)	t (h)					
2	50	3	70	24	87	5545	9684	12153	1.75
5	RT	3	70	24	75	6841	10446	12446	1.53
9	50	1.5	70	4	59	3485	5420	6117	1.56
11	50	1.5	110	4	72	4589	8595	12278	1.87
12	50	1.5	70	24	77	3007	5708	9335	1.90

[a]Polymerization conditions: Ti(O-i-Pr)$_4$/SBA-15, LA/Ti=100:1, solvent: toluene.

Table 12 - GPC analysis results.

Run[a]	Impregnation conditions		Reaction conditions		Conversion (%)	Mn (g/mol)	Mw (g/mol)	Mp (g/mol)	PDI
	T (ºC)	t (h)	T (ºC)	t (h)					
14	50	1.5	70	24	75	5335	9196	11868	1.72
15	50	1.5	70	24+24	75	3480	5995	7919	1.72

[a]Polymerization conditions: Ti(O-i-Pr)$_4$/SBA-15, LA/Ti=200:1, solvent: toluene.

Table 13 - GPC analysis results.

Run[a]	Impregnation conditions		Reaction conditions		Conversion (%)	Mn (g/mol)	Mw (g/mol)	Mp (g/mol)	PDI
	T (ºC)	t (h)	T (ºC)	t (h)					
20	RT	3	70	24	85	5431	8949	11476	1.65
22	50	3	70	24	70	4060	6414	8216	1.58

[a]Polymerization conditions: $TiCl(O\text{-}i\text{-}Pr)_3$/SBA-15, LA/Ti=100:1, solvent: toluene.

Since the monomer conversion was different for each sample, a theoretical value of M_n should be calculated for an appropriate comparison of the results and an understanding of the influence of impregnation and reaction conditions in the molecular weight and polydispersity index values. But, in this case, the calculation is difficult because not all the amount of titanium grafted on the catalyst works as active species in polymerization and even the ones that work like that are different, having different reactivity.

M_w values of the analyzed samples ranged from 5000 to 11000 g/mol. Polidispersity index values were between 1.5 and 1.9, which does not indicate a narrow molecular weight distribution.

The polymer samples obtained using supported $Ti(O\text{-}i\text{-}Pr)_4$ present different molecular weights and PDIs, depending on the impregnation or reaction conditions (Table 11). The highest molecular weight polymer was obtained with catalyst prepared during 3 hours at RT and it presented the lowest PDI value (reaction **5**). For samples **2** and **5**, the molecular weight does not follow the increasing of yield, indicating an influence of the impregnation temperature. In this case, the molecular weight slightly decreased and a higher PDI was obtained with a higher impregnation temperature – entry **5** versus **2**. Comparing samples **2** and **12**, shows that shorter impregnation times led to polymers with lower molecular weights and higher PDIs, suggesting that different active species are formed.

Keeping the impregnation reactions and comparing reactions **9** and **11** obtained in shorter reaction time (4 hours) and at two different temperatures, 70 °C and 110 °C, higher molecular weight was achieved for the polymer formed at higher temperature. However, it presents a higher PDI value. Concerning the polymerization time influence, samples **9** and **12**, show that M_n values do not follow the increasing of yield and the highest PDI value was obtained for 24 hours reaction. Having in mind that for polymers obtained with supported $Ti(O\text{-}i\text{-}Pr)_4$ full conversion is reached after 6 hours, a higher PDI value suggests that during the polymerization time in which monomer concentration is very low, secondary reactions (transesterification) may occur. This could explain the variations in molecular weight and the highly broad molecular weight distribution, however further GPC tests of samples along 24 hours of experiment should be performed.

The polymers **12** and **14** were obtained with the catalyst prepared in the same conditions, but the molar ratio between the monomer and titanium for sample **14** was twice bigger. The molecular weight of sample **14** is almost the double of polymer **12** and the PDI is lower. If

controlled polymerization operates, and if conversion is kept constant, the observed molecular weights between sample **14** and **12** should exhibit a ratio of 2.

The experiment **15** can be compared with experiment **14** – Table 12. The impregnation and reaction conditions were the same, but in run **15** half of the monomer was added after the first amount was already converted. The results show that the molecular weights of sample **15** are similar to those achieved with LA/Ti=100:1. It can be concluded that when the first portion of lactide was converted the polymer chains were terminated and after addition of a second crop of lactide new chains were initiated. So, the result did not confirm that the polymerization was "living", but revealed that the catalyst may be reused.

Finally, for the polymers obtained using supported TiCl(O-*i*-Pr)$_3$, samples **20** and **22** were obtained under different impregnation conditions – Table 13. The GPC results are similar to those obtained with supported Ti(O-*i*-Pr)$_4$ – higher molecular weights were achieved when the catalyst impregnation conditions were 3 hours and RT.

Comparing both supported catalysts, polymers obtained with Ti(O-*i*-Pr)$_4$ presented higher molecular weights than polymers obtained using TiCl(O-*i*-Pr)$_3$.

Kim et al. reported Mw and PDI values for polymerization of L-lactide using silica supported Ti(O-*i*-Pr)$_4$ and TiCl(O-*i*-Pr)$_3$ (shown in Table 1) [2]. Much higher molecular weights, around 36000 g/mol, and narrower molecular weights distribution (PDI around 1.2) were achieved for both systems.

II.1.6.3 Differential Scanning Calorimetry

Differential scanning calorimetry (DSC) monitors heat effects associated with phase transitions as a function of temperature. In a DSC analysis, the difference in the amount of heat required to increase the temperature of a sample and a reference (an inert material such as alumina), which are maintained at the same temperature, is measured as a function of temperature.

DSC measurements were carried out to determine the melting temperature (T_m), crystallization temperature (T_c) and degree of crystallinity (χ_c) and all measurements were made at a heating rate of 10 ºC/min over a temperature range of 25-210ºC.

The samples were first heated to 210ºC at a rate of 10ºC/min which results in the melting of the polymer sample. This first cycle is done to eliminate any thermal history of the samples. In a second cycle, the samples are cooled until 25ºC at a rate of 10ºC. Crystallization of the melted polymer occurs. The third cycle consists in a second heating of the crystallized sample.

Sample weights were corrected for the SBA-15 content obtained by TGA. T_m and T_c corresponds to the peaks from the first and second cycles. The fusion and crystallization enthalpies correspond to the areas of the peaks of the DSC curves obtained in the interval of temperatures of 90ºC to 190ºC. To calculate the degree of crystallinity the values of the melting enthalpy were divided by the theoretical melting heat of 100% crystalline polylactide (ΔH_f^o) which value is 93 J/g [5].

The thermal properties of the samples determined by DSC are shown in Table 14.

For some samples, there is more than one melting point, which may result from different melting processes that occurred due to different microstructures in the polymer. T_m values and degree of crystallization change between the 1st and 3rd cycles. The initial properties of the polymer sample were changed after first melting and crystallization. So, in the third cycle, the melting points of the polymers range from 155 to 164ºC and the degree of crystallization from 51% to 68%. Tc values range from 105ºC to113ºC.

Table 14 - DSC results – melting temperature, crystallization temperature and degree of crystallization.

Sample number	1st cycle				2nd cycle	3rd cycle			
	T_m (°C)			$\chi_{c,1}$ [a] (%)	T_c (°C)	T_m (°C)			$\chi_{c,3}$ [a] (%)
2	143.6	165.6		79.3	110.0	162.3			60.9
5	165.6			75.0	110.4	161.6			59.2
9	143.7	147.3	159.5	47.5	105.1	157.1			51.0
11	146.8	153.2	161.8	54.5	108.6	138.7	158.8		54.4
12	144.1	150.4	165.1	72.0	113.0	159.4			61.2
14	165.4			72.3	109.4	160.7			64.8
15	169.1			74.3	109.6	163.5			66.9
20	149.6	164.0		77.3	110.1	135.1	157.9	160.8	65.6
22	134.0	154.3	158.6	60.8	111.3	136.7	155.5	161.9	65.0
35	157.7	162.8		79.0	106.9	159.3			68.3

[a] $\chi_c = \Delta H_t / \Delta H_f^o$

Polymers samples **2** and **5** obtained with $Ti(O^iPr)_4$/SBA-15 presented higher values of T_m, but lower degree of crystallinity in 3rd cycle, than polymers from samples **20** and **22** using $TiCl(O^iPr)_3$/SBA-15, under the same impregnation conditions.

For $Ti(O^iPr)_4$/SBA-15, the impregnation temperature did not seem to have a critical influence in the thermal properties of the polymers obtained – samples **2** and **5**. These samples, which have the highest molecular weights, gave rise to high melting points, high crystallization temperatures, but not very high percentages of crystallinity in 3rd cycle. DSC curves for these samples are shown in Figures 45 to 47.

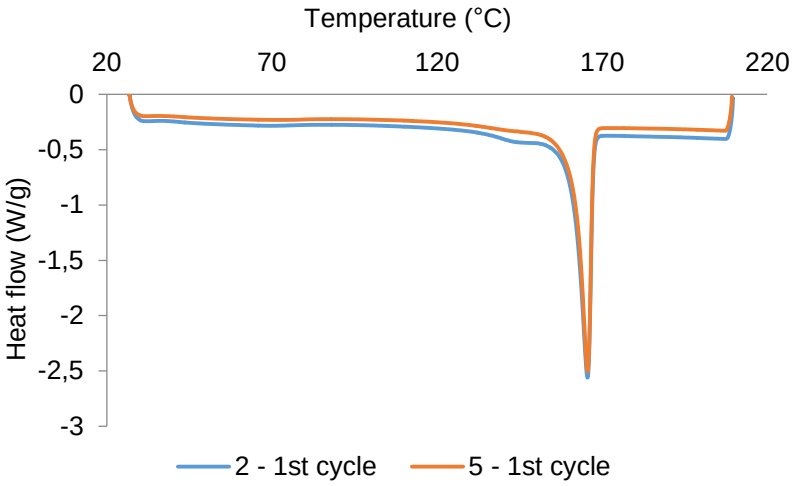

Figure 45 - DSC curve: Plot of 1st cycle for samples 2 and 5.

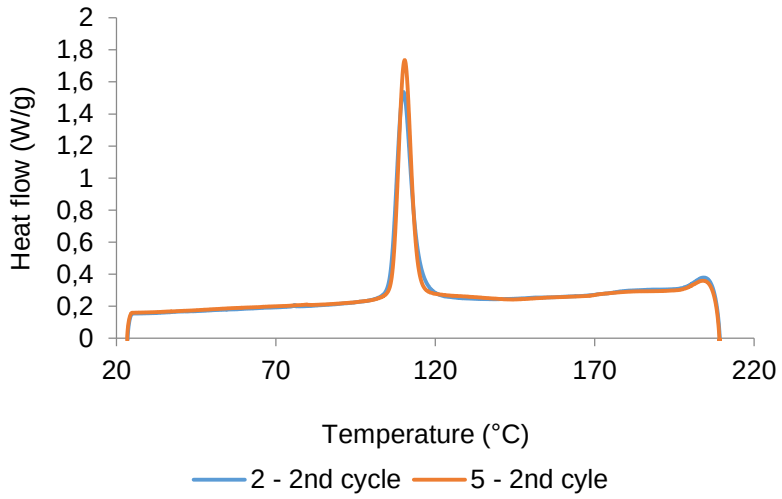

Figure 46 - DSC curve: Plot of 2nd cycle for samples 2 and 5.

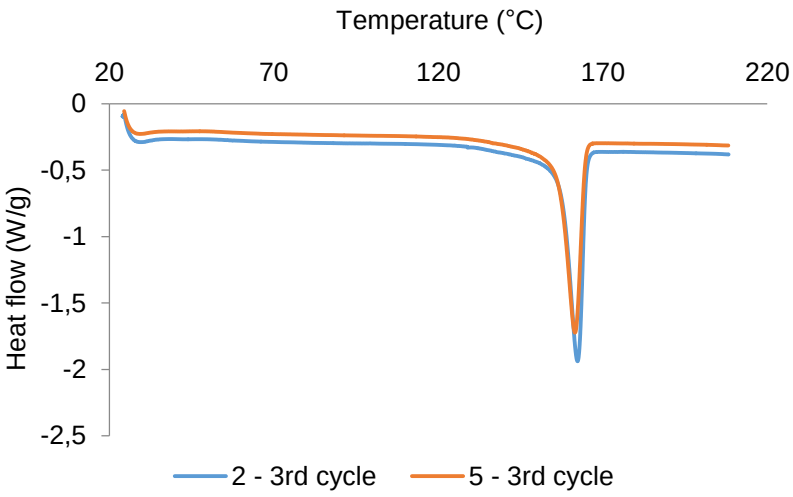

Figure 47 - DSC curve: Plot of 3rd cycle for samples 2 and 5.

However, using $TiCl(O^iPr)_3$/SBA-15 catalyst, supported catalysts obtained at 50ºC yield to higher T_m values than those prepared at RT. Changing impregnation temperature results in the formation of different microstructures in the polymer samples, which are highlighted in the DSC curves obtained for samples **20** and **22** by the peaks asymmetry related to different melting processes and indicative of higher heterogeneity of crystallite sizes – Figures 48 to 50.

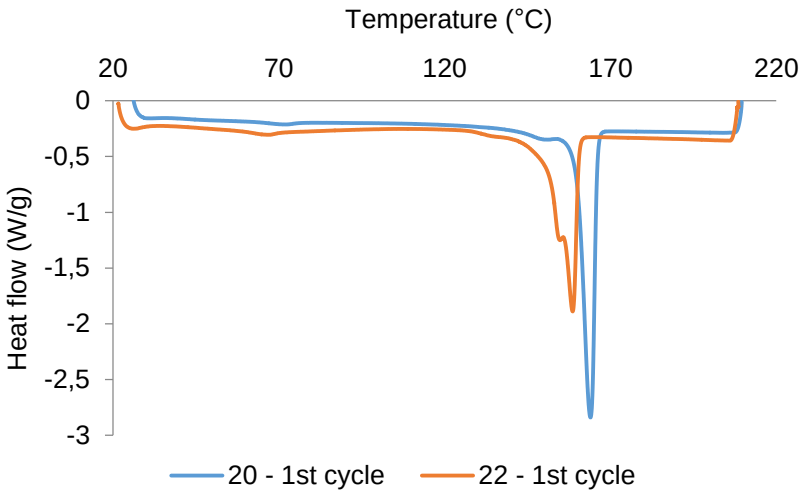

Figure 48 - DSC curve: Plot of 1st cycle for samples 20 and 22.

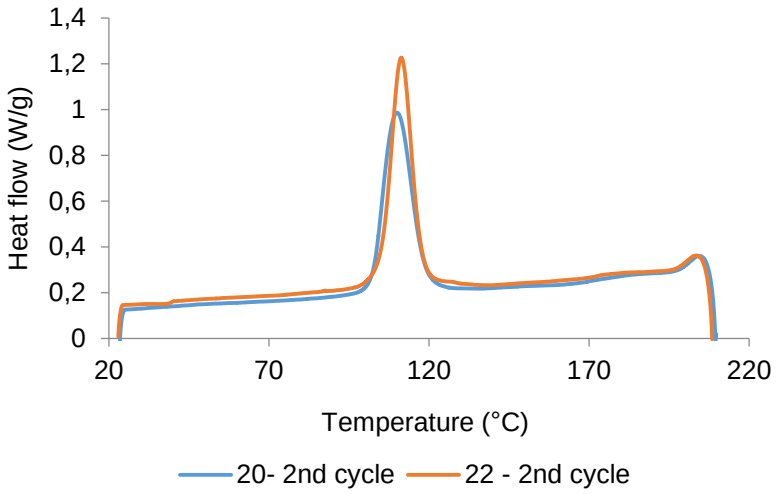

Figure 49 - DSC curve: Plot of 2nd cycle for samples 20 and 22.

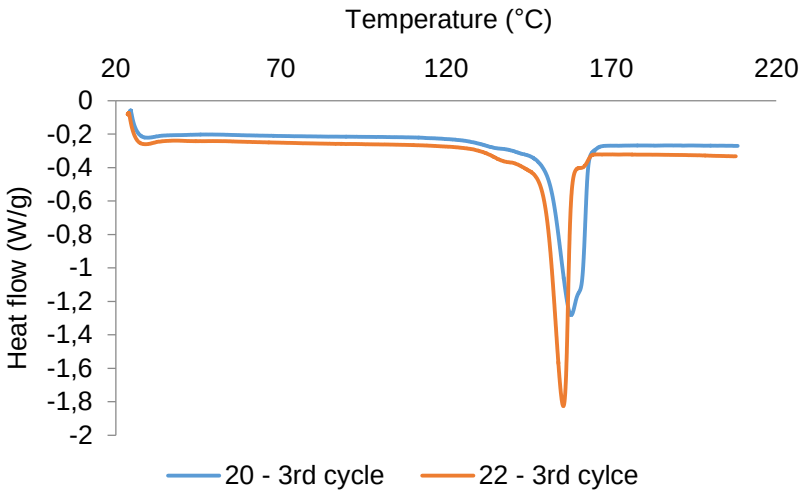

Figure 50 - DSC curve: Plot of 3rd cycle for samples 20 and 22.

For Ti(O*i*Pr)$_4$/SBA-15 catalyst, the influence of impregnation time and polymerization conditions in the thermal properties was checked – samples **5** to **18**. The influence of the impregnation time was evaluated by the comparison between samples **2** and **12**. As seen before, the decreasing of impregnation time results in lower molecular weights. So, as expected, the T_m is lower for sample **12**, obtained with the catalyst prepared for 1.5 hours at 50ºC. DSC curves for these samples are shown in Annex 1 - Figures 61 to 63.

For sample **11** obtained from polymerization reaction at 110ºC, a higher value of T_m, T_c and degree of crystallinity in the 3rd cycle were obtained when compared with sample **9** obtained at 70ºC. So, the temperature of polymerization influenced the microstructure of the polymer, which was expected since the same influence was observed in the molecular weights of these polymers. DSC curves for these samples are shown in Annex 1 - Figures 64 to 66.

Samples **9** and **12** were obtained under the same impregnation conditions but different polymerization times, 4 and 24 hours, respectively. DSC curves highlight the formation of different microstructures resulting in different thermal properties. For sample **12** is observed higher T_m and degree of crystallinity values. The highest T_c value (113ºC) was obtained for sample **12**, which presents also the highest content of SBA-15 (12.3%), suggesting that the presence of SBA-15 contributes for crystallization processes at a higher temperature. DSC curves are shown in Annex 1 - Figures 67 to 69.

Doubling up the LA/Ti molar ratio, higher T_m and degree of crystallinity values were achieved, as expected by the higher molecular weights. In contrast with sample **12**, the peaks in the DSC curves for sample **14** presents a symmetric behavior. DSC curves for these samples are shown in Annex 1 - Figures 70 to 72.

Sample **15** was performed to check the living behavior of the ROP of lactide using Ti(O*i*Pr)$_4$/SBA-15 catalyst. In terms of thermal properties, the experiment led to higher melting

points and degree of crystallinity in the 3rd cycle than for sample **14** (which lactide addition was made all at once). This result is controversial with the higher molecular weight obtained for sample **14**. DSC curves are shown in Annex 1 - Figures 73 to 75.

Polymer sample **35** was obtained using homogeneous catalyst. Samples **2**, **5** and **12** were obtained from reactions using supported $Ti(O^iPr)_4$ (independently of the impregnation conditions) in the same polymerization conditions (70ºC, 24 hours, LA/Ti=100:1) that sample **35**, Higher melting temperature, lower T_c and the highest degree of crystallinity in 3rd cycle were observed for sample **35**. DSC curves for sample **35** is shown in Annex 1 - Figures 76 to 78.

T_m values obtained were in accordance with results reported by Kim et al. (shown in Table 1) [2]. T_m values were around 165ºC for polymers produced by supported $Ti(O^iPr)_4$ or $TiCl(O^iPr)_3$ catalysts and 5-10ºC lower for samples produced by the same homogeneous systems. However, T_m value for heterogeneous $TiCl(O^iPr)_3$ catalysts was higher than for the supported $Ti(O^iPr)_4$.

II.2 Conclusions and Perspectives

Polymerization of L-lactide was performed using two different titanium compounds: titanium(IV) tetraisopropoxido and titanium(IV) chloride triisopropoxido. Both were tested in heterogeneous catalysis using SBA-15 as support.

The preparation of the catalysts included a study of the impregnation conditions in order to achieve a good compromise between the amount of titanium effectively grafted onto the support and the performance of the catalyst in the ROP of lactide in terms of PLA isolated yield. Concerning the results obtained, a Ti/SBA-15 ratio of 3.5% was chosen for both catalysts. Two sets of time and temperature impregnation conditions (3 or 1.5 hours at 50ºC or RT) were tested in order to see their influence on polymer yield and properties. Despite the impregnation conditions, both catalysts proved efficient when tested in the ROP of lactide.

For Ti(O-*i*-Pr)$_4$, independently of impregnation conditions, reactions performed during 24 hours at 70°C gave rise to high PLA yields close to 80%. However, GPC analysis shows that the highest molecular weights and the narrowest molecular weight distribution were achieved with the catalyst prepared during 3 hours of impregnation time, at room temperature. Shorter impregnation times led to polymers with lower molecular weights and higher PDIs, suggesting that different active species are formed. The effect of impregnation temperature did not seem to have a critical influence over the molecular weight results.

The effect of reaction time and temperature on the polymerization reactions was also evaluated. Ti(O-*i*-Pr)$_4$/SBA-15 catalysts prepared during 1.5 hours of reaction at 50°C were selected. Higher reaction temperature originate higher molecular weights polymers but also higher PDI values. Concerning the influence of the polymerization time, the molecular weights of the polymers obtained are very similar and a higher PDI value was observed for higher polymerization times, suggesting the occurrence of secondary reactions like transesterification, but further GPC tests along polymerization time should be performed. In terms of PLA yield, it is noteworthy that the yields achieved during 24 hours reaction at 70°C were very similar to those achieved at higher temperature with shorter reaction time (4 hours, 90°C). However, the molecular weights were higher for the polymers obtained under the latter conditions.

TiCl(O^{i}Pr)$_3$/SBA-15 was also prepared under different impregnation conditions and tested in polymerization of lactide. The reactions performed with the catalyst prepared during 3 hours at 50°C resulted in high yields (more than 85%) but the highest molecular weight polymers were obtained in reactions with the catalyst prepared during 3 hours at RT, similarly to Ti(O^{i}Pr)$_4$/SBA-15. In the case of this catalyst, the impregnation temperature seemed to influence the PLA yield, such that the lower the temperature, the lower the yield. Changing the impregnation conditions to 1.5 hours and 50ºC, a problem in reproducibility of the results showed up.

In order to achieve higher molecular-weight polymers, higher lactide/titanium ratio was applied. The GPC results showed that almost two times higher molecular weights of polymer were obtained with LA/Ti=200:1 in comparison to the polymer obtained with LA/Ti=100:1.

Experiment with two sequential additions of monomer did not confirm that the system had a “living” behavior. However, after converting the first portion of L-lactide, the reaction continued and the monomer that was added after 24h of reaction was consumed. Yet, the molecular weight of the polymer obtained was lower than that of the polymer obtained from a single addition of 200:1 ratio of LA/Ti, confirming that the heterogeneous catalyst may be reused.

A comparison between homogeneous and heterogeneous catalytic systems using $Ti(O\textit{i}Pr)_4$ was performed. The homogenous system proved to be efficient in lactide polymerization and faster than supported catalyst, that need longer times to convert all the monomer. Both systems achieved the same PLA isolated yield (around 80%) and monomer conversion (more than 90%).

Polymers were characterized by Thermogravimetric Analysis and Differential Scanning Calorimetry. TGA was used to determine the SBA-15 content for selected samples. The values obtained were in accordance with the expected ones. Melting and crystallization temperatures and the degree of crystallinity were determined by DSC for selected samples. The melting points of the polymers formed range from 155 to 164ºC and and the degree of crystallization from 51% to 68%. Under the same impregnation conditions, the polymers samples obtained with $Ti(O^{i}Pr)_4$/SBA-15 presented higher values of T_m, but lower degree of crystallinity, than the polymers obtained with $TiCl(O^{i}Pr)_3$/SBA-15. For $Ti(O^{i}Pr)_4$/SBA-15, the impregnation temperature used for the preparation of the catalysts did not seem to have a critical influence in the thermal properties of the polymers obtained. However, for $TiCl(O^{i}Pr)_3$/SBA-15 catalyst, supported catalyst obtained at 50ºC yield to higher T_m values than those prepared at RT. Changing the impregnation temperature results in the formation of different polymer microstructures that originate different fusion processes.

The influence of impregnation time and polymerization conditions in the thermal properties was studied for $Ti(O^{i}Pr)_4$/SBA-15 catalyst. Lower molecular weights polymers and the T_m values were attained for samples obtained from impregnation reactions carried out during 1.5h. On the other hand, an increase of reaction times and temperatures originates higher T_m and T_c values, as well as higher degree of crystallinity of the polymers, and it follows the increase of the molecular weights of the polymers. Higher LA/Ti molar ratio gave rise to higher T_m and degree of crystallinity values. Despite of having lower molecular weight, the experiment with two sequential monomer additions led to the highest melting point, 163.5ºC, and higher degree of crystallinity than the sample prepared with lactide added all at once.

Higher melting temperature, lower T_c and the highest degree of crystallinity (68%) were observed for polymer sample prepared using homogeneous $Ti(O^{i}Pr)_4$ catalyst.

To understand better the distribution of titanium in the support surface and maybe to clarify aspects of the systems behavior, Inductively Coupled Plasma Spectroscopy (ICP) and Energy Dispersive Spectroscopy (EDS) analysis could be performed after impregnation and also after polymerization tests. ICP would be used to measure the titanium content of the heterogeneous catalysts and EDS to measure the titanium content on the surface of the supported catalysts.

Taking in consideration that, besides the changes on polymer structure and molecular weights, an additional advantage of heterogeneous over homogeneous catalysis is catalysts' recover and reuse, further work is still required to assess these properties.

II.3 References

[1] Artur Bento, PhD Thesis, *Development of high performance polyethylene nanocomposites, via in-situ polymerization in mesoporous materials*, Instituto Superior Técnico, Lisboa, 2014.

[2] E. Kim, E. W. Shin, I.-K. Yoo, J. S. Chung, *Journal of Molecular Catalysis A: Chemical*, **2009**, *298*, 36.

[3] N. Wanna, T. Kraithong, T. Khamnaen, P. Phiriyawirut, S. Charoenchaidet, J. Tantirungrotechai, *Catalysis Communications*, **2014**, *45*, 118.

[4] A. Kowalsaki, A.Duda, S. Penczek, *macromolecules,* **1998**, *31*, 2114; M.Save, M. Schappacher, A. Soum, *Macromol. Chem. Phys.,* **2002**, *203*, 889.

[5] W. Zhai, Y. Ko, W. Zhu, A. Wong, C.B. Park, *Int. J. Mol. Sci.*, **2009**, *10*, 5381

Chapter III

VANADIUM COMPLEXES AS CATALYSTS FOR ROP OF LACTIDE

The most commercially important compound is vanadium pentoxide (V_2O_5) that is used for the production of sulfuric acid. The metal is very oxophilic and it forms a high variety of oxides in which the vanadium displays oxidation states IV and V. Vanadium compounds present catalytic activity in many reactions and in biologic medium [1]. So far, studies including vanadium compounds and ROP of lactide have not been reported. In this chapter, innovative studies using vanadium complexes as catalysts for the ring-opening polymerization of lactide are described.

III.1 Results and Discussion

Three different vanadium complexes were used in this work: VO(O^iPr)[ONNO], VO(O^iPr)$_3$ and V(NAda)(O^iPr)$_3$. Their structures V1, V2 and V3 are shown in Figure 51.

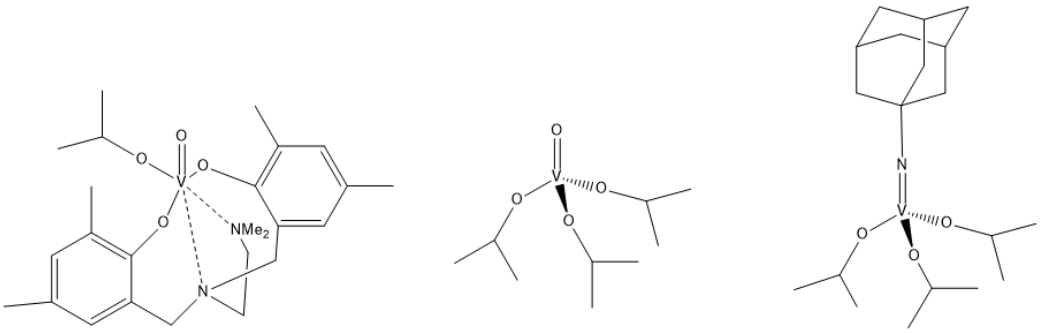

(V1) **(V2)** **(V3)**

Figure 51 - Structures of the vanadium complexes.

Complex V1 is a very dark violet solid, while V2 is a colorless liquid and V3 is a yellow oil at room temperature. All compounds present good solubility in DCM, THF and toluene.

The complexes were assessed as catalysts for the ring-opening polymerization of *rac*-lactide. The polymerization reactions were performed in bulk and in solution using different sets of experimental conditions (solvent, time and temperature).

Concerning bulk polymerizations, predetermined amounts of the desired vanadium compound and *rac*-lactide were charged in a vial equipped with Teflon-tight screw cap, using a LA/catalyst ratio of 100:1 inside a glovebox. The mixtures were heated until 130ºC and stirred during a certain time.

In the case of polymerization reactions performed in solution, predetermined amounts of the desired vanadium compound, *rac*-lactide and solvent were charged in a vial equipped with a Teflon-tight screw cap, inside a glovebox, and the solutions were vigorously stirred during a certain time, at a prefixed temperature.

In both cases the reactions were terminated by exposition to air and quenching with wet dichloromethane. Aliquots were taken and analyzed by ^{1}H NMR sprectroscopy to determine the monomer-to-polymer conversion.

The polymer samples were dried under vacuum and analyzed by SEC. Molecular weight values ($M_{n(corrected)}$) were corrected applying a 0.58 factor to the number-average molecular weights determined by GPC [2]. These values were compared to the theoretical ones ($M_{n(theo)}$) which were calculated using the following equation:

$$M_{n(theo)} = MW(LA) \times conv \times \frac{number\ of\ eq.LA/1\ eq.catalyst}{number\ of\ i\text{–Pr}\ groups} \quad \text{equation (1),}$$

where *MW(LA)* is the molecular weight of lactide (144.13 g/mol) and *conv* stands for conversion.

The results for each catalyst are following presented. It is worth making a previous note about the small reproducibility of the results. It results from experimental errors associated to the weighing of the catalysts, which were used in very small amounts in the catalytic essays, and also with the physical states of the compounds V2 and V3, a liquid and an oil, respectively.

❖ **Catalyst V1**

In Table 15 are presented the results obtained using catalyst V1 in ROP of *rac*-LA.

Table 15 – Polymerization of *rac*-LA using V1 and LA/catalyst=100:1.

Run	Solvent	T (ºC)	t (h)	Conversion[a] (%)	$M_{n(corrected)}$[b] (g/mol)	$M_{n(theo)}$[c] (g/mol)	PDI[d]
38	DCM	RT	18	1	-	-	-
39	DCM	RT	18	1	-	-	-
40	THF	60	4	0	-	-	-
41	toluene	90	4	2	-	-	-
42	toluene	100	18	26	-	-	-
43	bulk	130	2	38	2272	5477	1,13

[a]Determined by ^{1}H NMR analysis

[b]Determined from GPC analysis by using polystyrene standards

[c]Calculated according to the conversion (MW_{LA}=144.13g/mol) using equation (1)

[d]Determined from GPC analysis

V1 did not proved to be an appropriate catalyst for the ring-opening polymerization of lactide. Polymerization reactions carried out in DCM, THF and toluene solutions at RT, 60ºC and

90ºC, display practically null conversion. In toluene, at 100ºC, 26% conversion was achieved. In bulk, at 130ºC, the system reacted faster but only 38% conversion was reached after 2h. Despite this low conversion value, a narrow molecular weights distribution was determined (PDI value near to 1), which indicates a good polymerization control.

❖ **Catalyst V2**

The results obtained for the ROP of lactide in solution and in bulk using catalyst V2 are presented in Tables 16 and 17, respectively.

Table 16 - Polymerization of *rac*-LA obtained in solution with catalyst V2 and LA/catalyst=100:1.

Run	Solvent	T (ºC)	t (h)	Conversion[a] (%)	$M_{n(corrected)}$[b] (g/mol)	$M_{n(theo)}$[c] (g/mol)	PDI[d]
44	DCM	RT	18	1	-	-	-
45	toluene	90	2	0	-	-	-
46	toluene	90	2	1	-	-	-
47	toluene	90	3	3	-	-	-
48	toluene	90	3	6	-	-	-
49	toluene	90	4	47	2024	2258	1,07
50	toluene	90	5	35	2834	1682	1,08
51	toluene	90	6	72	3155	3459	1,09
52	toluene	90	6	77	3803	3699	1,16
53	toluene	90	8	93	6910	4468	1,21
54	toluene	90	8	95	5043	4564	1,17
55	toluene	90	12	92	7726	4420	1,14
56	toluene	90	16	95	-	-	-
57	toluene	90	18	91	5210	4372	1,27
58	toluene	100	18	90	5840	4324	1,32

[a]Determined by ^{1}H NMR analysis

[b]Determined from GPC analysis by using polystyrene standards

[c]Calculated according to the conversion (MW_{LA}=144.13g/mol) using equation (1)

[d]Determined from GPC analysis

V2 is an efficient catalyst for the ROP of lactide in toluene solution. Total conversion is achieved after 8 hours. Figure 52 presents the ^{1}H NMR sprectum obtained for sample **54**, after 8 hours, where *rac*-LA and PLA characteristic peaks appeared at around 5.0 ppm and 5.2-5.3 ppm, respectively.

It is noteworthy that the values of corrected and theoretical molecular weights are very similar indicating that there are three PLA chains initiated by each one of the isopropoxido groups of the catalyst. The higher molecular weight value observed was 7726 g/mol for sample **55**

prepared in toluene, at 90ºC, for 12 hours. PDI values between 1.1 and 1.3 indicate a good polymerization control –Table 16.

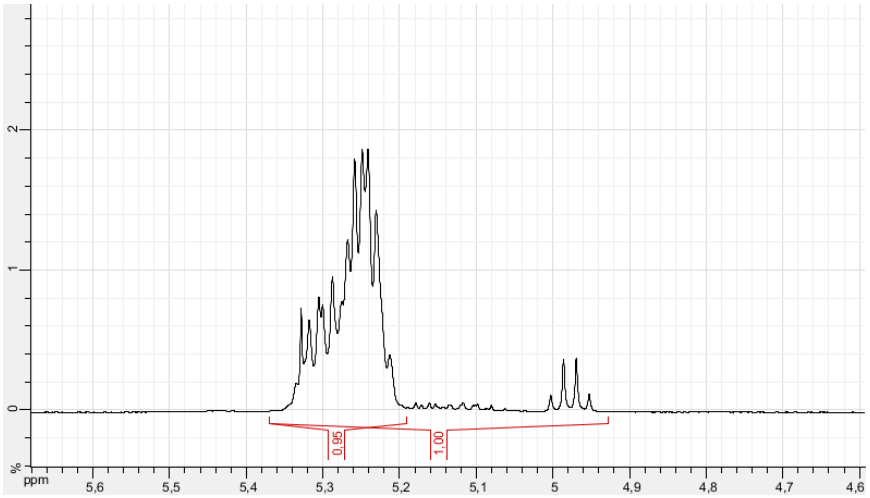

Figure 52 - ^{1}H NMR sprectrum: ROP of *rac*-LA using V2 in solution - run 54.

The results in Table 17, revealed that catalyst V2 is much more active in bulk conditions, presenting low PDI values between 1.1 and 1.3. In fact, the reaction is completed after 15 minutes, which corresponds to 89% conversion. Again, the values of corrected and theoretical molecular weighs are very similar indicating that there are three PLA chains initiated by each of the isopropoxido groups.

Table 17 - Polymerization of *rac*-LA obtained in bulk at 130ºC with catalyst V2 and LA/catalyst=100:1.

Run	t	Conversion[a] (%)	$M_{n(corrected)}$[b] (g/mol)	$M_{n(theo)}$[c] (g/mol)	PDI[d]
59	2 min	2	-	-	-
60	5 min	24	1424	1153	1,09
61	7 min	34	-	-	-
62	7 min	52	3030	2498	1,12
63	10 min	79	3334	3795	1,16
64	15 min	89	4841	4276	1,25
65	30 min	91	8511	4372	1,22
66	30 min	90	4983	4324	1,29
67	1h	93	5558	4420	1,26
68	2h	91	7890	4372	1,28

[a]Determined by ^{1}H NMR analysis

[b]Determined from GPC analysis by using polystyrene standards

[c]Calculated according to the conversion (MW_{LA}=144.13g/mol) using equation (1)

[d]Determined from GPC analysis

Assuming that the polymerization is a first order reaction, there is a linear relation between ln ($[M]_0/[M]_t$) and time expressed by equation (2).

$$-\frac{d[LA]}{dt} = k \cdot [LA] \Leftrightarrow -\int_{[LA]_0}^{[LA]} \frac{d[LA]}{[LA]} = \int_0^t k\, dt \Leftrightarrow -\ln[LA]_t + \ln[LA]_0 = k(t-0) \Leftrightarrow$$

$$\Leftrightarrow \ln\left(\frac{[LA]_0}{[LA]_t}\right) = kt \qquad \text{equation (2),}$$

where *k* is the reaction rate constant in [time^{-1}], *t* is time, $[LA]_0$ is the lactide concentration at t=0, $[LA]_t$ is the lactide concentration at time t.

$[LA]_0/[LA]_t$ was calculated by equation (3), attending the definition of conversion:

$$conv = \frac{[LA]_0 - [LA]_t}{[LA]_0} \Leftrightarrow [LA]_0/[LA]_t = \frac{1}{1-conv} \qquad \text{equation (3)}$$

where *conv* is conversion.

The graphical representation of ln ($[LA]_0/[LA]_t$) versus time in solution and bulk conditions are presented in Figures 53 and 54, respectively.

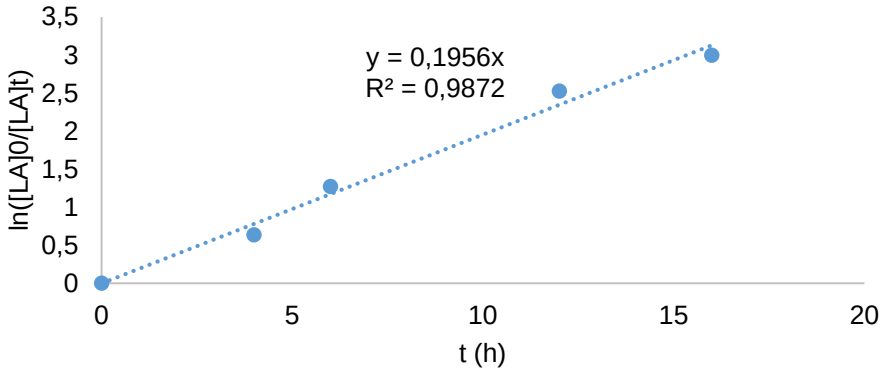

Figure 53 - Plot of ln($[LA]_0/[LA]_t$) versus time using V2 in toluene at 90ºC - runs 49, 51, 55 and 56.

The deviation of the results to the expected linear tendency is probably due to experimental errors. As already mentioned, having in mind that V2 is a liquid and that small amounts of catalyst were used, minimal mistakes in the weighing procedure could generate large deviations that differ from one experiment to the other. The experimental points to build the graphs were chosen in order to optimize the correlation factor (R^2) associated to the linear behavior.

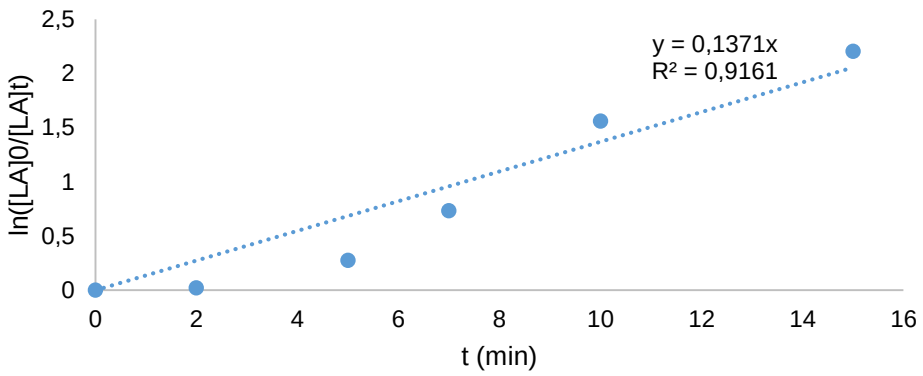

Figure 54 - Plot of $\ln([LA]_0/[LA]_t)$ versus time using V2 in bulk at 130ºC – runs 59, 60, 62, 63 and 64.

An alternative justification for the larger results deviation in bulk conditions (Figure 54) may be related to the fact that in these conditions the reaction rate is larger than in solution and thus it may happen that the monomer is not completely melted.

The graphical representations of $M_{n(corrected)}$ and PDI *versus* monomer-to-polymer conversion for solutions and bulk reactions are presented in Figures 55 and 56. Linear correlation between the molecular weights with the time of reactions were observed. In both conditions, M_n values rise up to 5000 g/mol. As previously noted, the higher PDI values are obtained at higher conversions, but these values remain between 1.0-1.2, which reflects a good polymerization control.

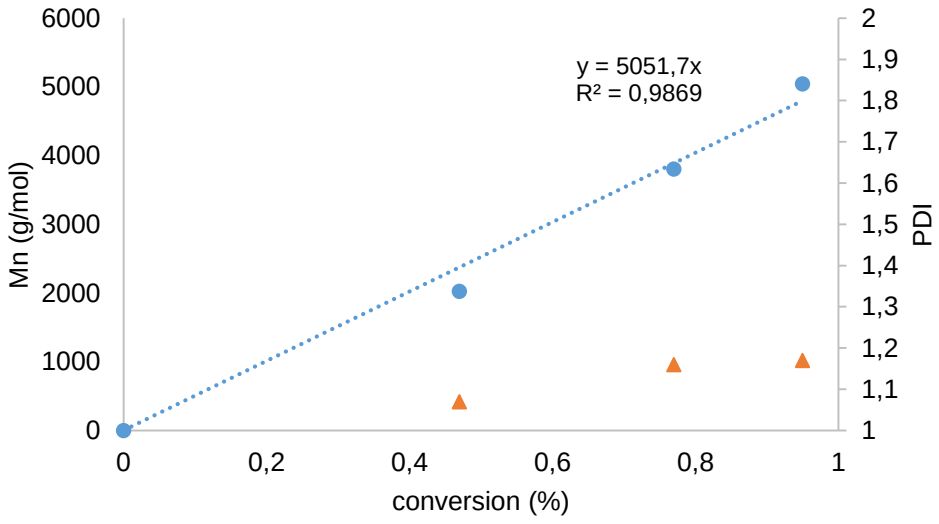

Figure 55 - Plot of Mn and PDI versus lactide conversion using V2 in toluene at 90ºC – runs 49,52 and 54.

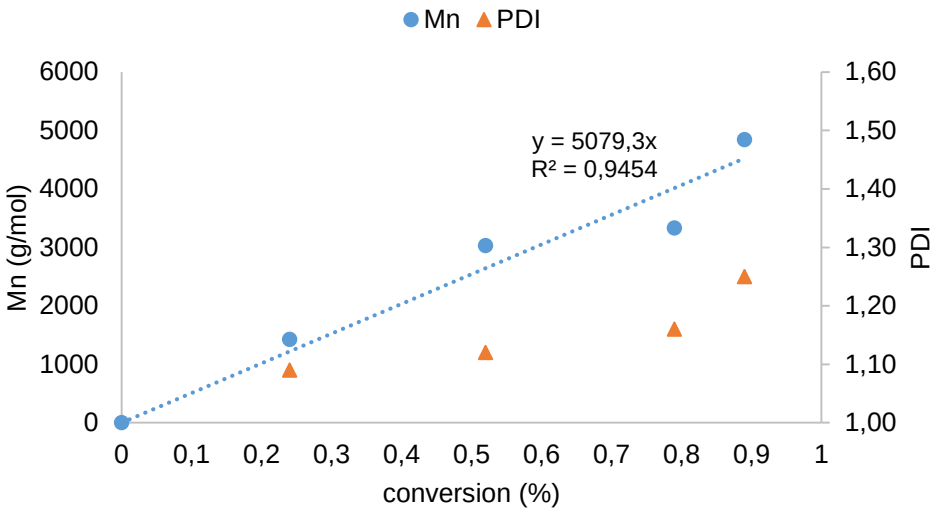

Figure 56 - Plot of Mn and PDI versus lactide conversion using V2 in bulk at 130ºC - runs 60, 62, 63 and 64.

❖ **Catalyst V3**

The polymerization results for the ROP of *rac*-lactide using catalyst V3 in toluene solution and in bulk are shown in Table 18. The catalyst proved to be very active, reaching full conversion after 18h hours in toluene at 90ºC. M_n values attained 5809 g/mol after 8h of reaction and good control of polymerization corresponding to PDI values ranging between 1.1 and 1.3 were observed. Comparing samples **72** and **84**, shows that the system is more active in bulk conditions. It took only 2 hours to reach half of the LA conversion while in solution 6 hours are required. However, a lower M_n value was obtained in bulk conditions. Additionally, sample **84** showed the formation of *meso*-lactide that will be discussed later in this chapter.

Table 18 - Polymerization of *rac*-LA using V3 and LA/catalyst=100:1.

Run	Solvent	T (ºC)	t (h)	Conversion[a] (%)	$M_{n(corrected)}$[b] (g/mol)	$M_{n(theoretical)}$[c] (g/mol)	PDI[d]
69	toluene	90	2	8	-	-	-
70	toluene	90	4	20	1766	961	1,07
71	toluene	90	4	36	3598	1730	1,18
72	toluene	90	6	51	4732	2450	1,14
73	toluene	90	6	37	4602	1778	1,15
74	toluene	90	6	42	4706	2018	1,26
75	toluene	90	6	44	3920	2114	1,17
76	toluene	90	8	76	6809	3651	1,13
77	toluene	90	8	73	6672	3507	1,14
78	toluene	90	8	70	5896	3363	1,11
79	toluene	90	12	63	5394	3027	1,14
80	toluene	90	12	60	5526	2883	1,12
81	toluene	90	16	79	5446	3795	1,12
82	toluene	90	16	65	6013	3123	1,15
83	toluene	90	18	89	4043	4276	1,23
84	bulk	130	2	51	3116	2450	1,14

[a]Determined by ^{1}H NMR analysis

[b]Determined from GPC analysis by using polystyrene standards

[c]Calculated according to the conversion (MW_{LA}=144.13g/mol) using equation (1)

[d]Determined from GPC analysis

Plots of $\ln([LA]_0/[LA]_t)$ *versus* time and a plot of the $M_{n(corrected)}$ and PDI *versus* LA conversion are presented in Figures 57 and 58.

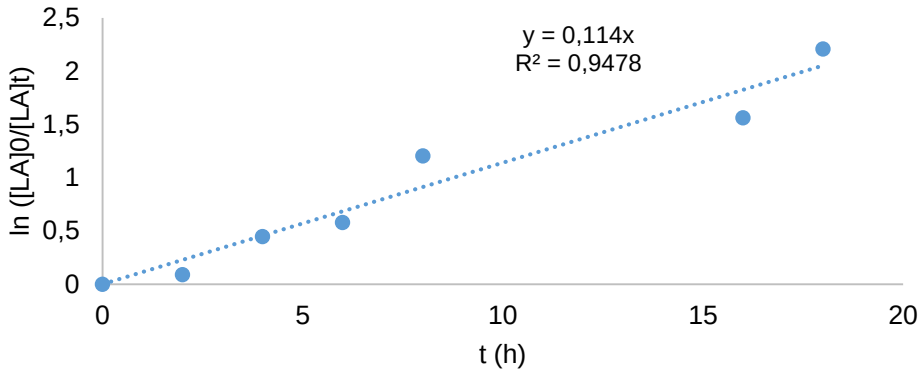

Figure 57 - Plot of $\ln([LA]_0/[LA]_t)$ versus time using V3 in toluene at 90ºC - runs 69, 71, 75, 78, 81 and 83.

The graphical representation of $M_{n(corrected)}$ *versus* LA conversion for samples **70**, **75** and **76** describe a linear relation (Figure 58).

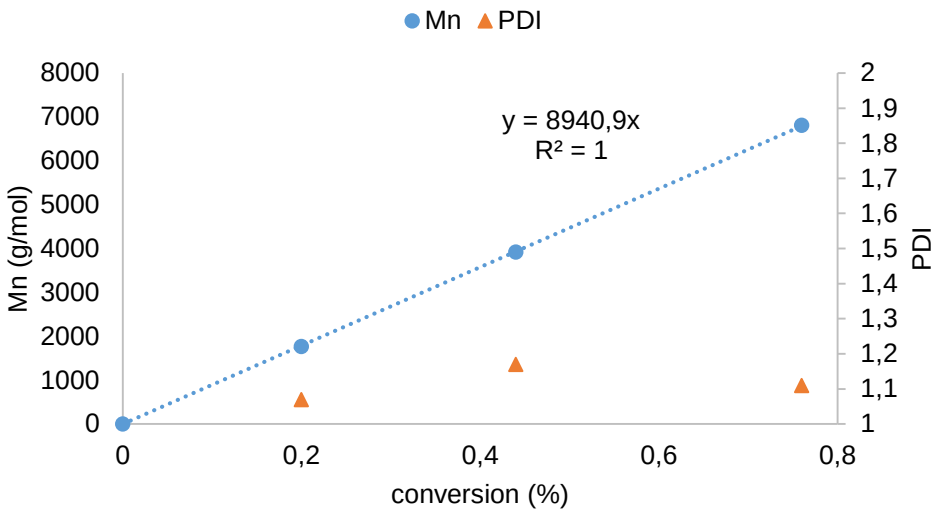

Figure 58 - Plot of Mn and PDI versus lactide conversion using V3 in toluene at 90ºC – runs 70, 75 and 76.

Comparing the performances of catalysts V3 and V2 in toluene at 90ºC, one concludes that V2 is more active, although the polymers obtained with both catalysts display similar molecular weights and PDI values are also very close. In V2, the vanadium is a more acidic metal center than in V3, favoring the activation of the substrate. In spite of the stability of V=N group in vanadium(V) complexes, probably V=O group contribute to a more stable catalyst due to the robustness of oxo-vanadium complexes.

Despite the good polymerization results presented above, vanadium catalysts V2 and V3 give rise to racemization and originate the formation of *meso*-lactide. The presence of *meso*-lactide was identified by ^{1}H NMR, one doublet at 1.70-1.75 ppm corresponding to the methyl groups of *meso*-LA. As llustrated in Figure 59, this resonance appears very close to the doublet assigned to the methyl groups of lactide, which appear around 1.65-1.68 ppm [3].

Other examples of ^{1}H NMR spectra illustrating the formation of *meso*-lactide during polymerization of PLA using catalysts V2 and V3 (in solution conditions) are presented in Annex 2 – Figures 79 to 81. In general, it may be concluded that the formation of meso-LA increases with the increasing of reaction time.

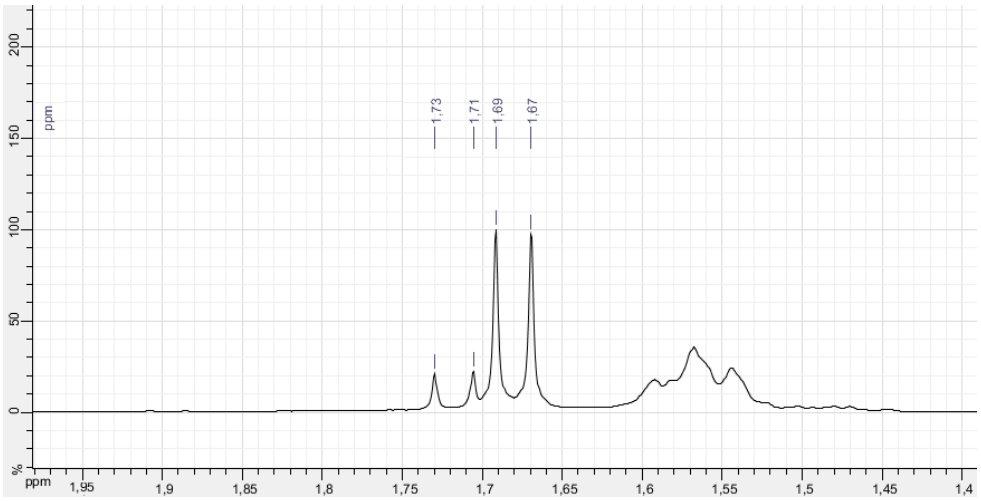

Figure 59 - ^{1}H NMR sprectrum: formation of meso-LA during polimerization of LA using V3 in bulk - run 84.

Nishida et al. investigated the thermal racemization of L-lactide because its formation has important implications in the recovery of L-lactide after depolymerization of PLLA, which is an important issue in feedstock recycling [3]. Based on this, a preliminary study of the ROP of L-lactide made using catalysts V2 and V3 and the same experimental conditions used in the ROP of *rac*-LA. The polymerization results, which are presented in Table 19, show that L-lactide reacts slower than *rac*-LA. For reaction **85**, the monomer conversion is nearly the half of the value obtained in the same conditions for reaction **54** (95%). A similar conclusion comes from the comparison of reactions **87** and **83** (89% conversion). However, using V2 as a catalyst in bulk conditions (reactions **64** and **86**) the same yield (*ca.* 90%) after 15 min, independently of the stereochemistry of the monomer. This points out the extremely high activity of V2 when used in bulk.

Table 19 - Polymerization of L-LA using LA/catalyst=100:1.

Run	Catalyst	Solvent	T (ºC)	t	Conversion[b] (%)	$M_{n(corrected)}$[c] (g/mol)	$M_{n(theoretical)}$[d] (g/mol)	PDI[e]
85	V2	toluene	90	8h	55	3232	2738	1,08
86	V2	bulk	130	15min	91	6044	4372	1,21
87	V3	toluene	90	18h	57	8186	2642	1,14
88[a]	V2	bulk	130	2h	68	15699	16335	1,08

[a]This experiment was performed with LA/catalyst=500:1.

[b]Determined by ^{1}H NMR analysis

[c]Determined from GPC analysis by using polystyrene standards

[d]Calculated according to the conversion (MW_{LA}=144.13g/mol) using equation (1)

[e]Determined from GPC analysis

The formation of *meso*-LA was not observed when the LA/catalyst ratio was increased to 500:1 in bulk conditions (reaction **88**). A conversion of 68% and a low PDI value were otained with catalyst V3. The ^{1}H NMR spectrum of a stereoregular polymer, with L-lactide and PLLA characteristic peaks well defined close to 5.0 ppm and 5.1 ppm, respectively, is depicted in Figure 60.

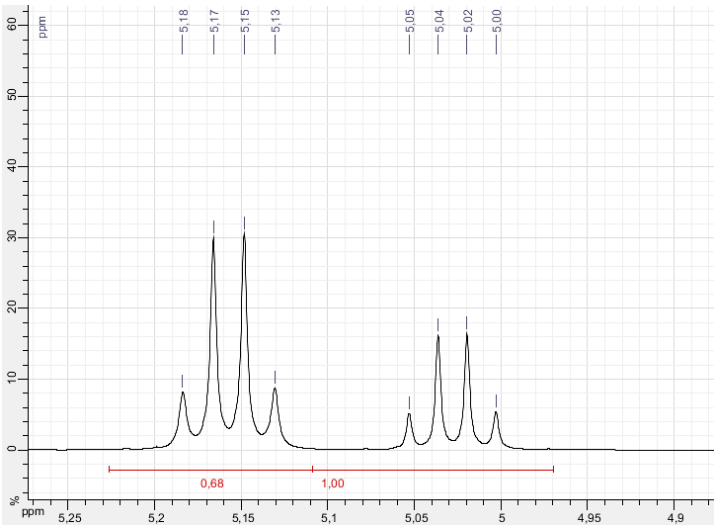

Figure 60 - ^{1}H NMR sprectrum: Polimerization of L-LA using V3 in bulk at 130ºC for 2h and LA/catalyst=500:1 - run 88.

III.2 Conclusions and Perspectives

Polymerization of *rac*-lactide was performed using three different vanadium compounds: VO(O^iPr)[ONNO], VO(O^iPr)$_3$ and V(NAda)(O^iPr)$_3$. The reactions were performed in bulk and in toluene solutions using different sets of experimental conditions (solvent, time and temperature). The resulting polymers were characterized by GPC.

VO(O^iPr)[ONNO] did not proved to be active in the ring-opening polymerization of lactide, maybe due to stereochemical reasons. In bulk, at 130ºC, the system only attained 38% of monomer conversion after 2h.

VO(O^iPr)$_3$ revealed to be very active in the ROP of lactide in solution, displaying total monomer conversion after 8 hours. The higher molecular weight value observed was 7726 g/mol. In bulk conditions, V2 is much more active and the ROP is equally well-controlled. In fact, the reaction is completed after 15 minutes, with 89% monomer conversion. In both cases, the similarity between corrected and theoretical molecular weights of the samples indicates that there are three PLA chains initiated by the three isopropoxido groups of the catalyst. The PDI values between 1.1 and 1.3 indicated a good control of polymerization. Representation of ln ($[LA]_0/[LA]_t$) versus time in solution and bulk conditions reveal first order reactions. In both conditions, PLA samples presented M_n values up to 5000 g/mol and PDI values remain between 1.0-1.2.

V(NAda)(O^iPr)$_3$ is active in the ROP of lactide, but less than the analogous oxo-complex. The system showed to be more active in bulk conditions (it took only 2 hours to reach half of the LA conversion while in solution it took 6 hours), but lower M_n values were obtained. A good control of polymerization is observed concerning the low PDI values ranging 1.1 and 1.3. This difference in activity is probably caused by the higher acidity of vanadium metal center in V2 and the robustness of oxo-vanadium complexes.

Despite interesting results were obtained, vanadium catalysts V2 and V3 originate *meso*-LA. The results showed that the polymerization of L-lactide is slower than that of *rac*-LA and also that formation of *meso*-LA may be avoid if the LA/catalyst ratio was increased to 500:1 in bulk conditions, leading to a stereoregular polymer with higher molecular weight and lower PDI.

It would be interesting to support these vanadium catalysts and compare their performance with the respective homogeneous systems.

III.3 References

[1] (a) Chemicool Periodic Table. *Vanadium*. Chemicool.com. Available: http://www.chemicool.com/elements/vanadium.html. [Accessed: 8/12/2014] (b) B.V. Venkataraman, S.Sudha, *Asian J. Exp. Sci.*, **2005**,*19*,127; (c) *Air Quality Guidelines*, World Health Organization Regional Office for Europe, Copenhagen, **2000**.

[2] A. Kowalsaki, A.Duda, S. Penczek, *macromolecules,* **1998**, *31*, 2114; M.Save, M. Schappacher, A. Soum, *Macromol. Chem. Phys.,* **2002**, *203*, 889.

[3] T. Tsukegi, T. Motoyama, Y. Shirai, H. Nishida, T. Endo, *Polymer Degradation and Stability*, **2007**, *92*, 552.

Chapter IV

EXPERIMENTAL SECTION

IV.1 Chapter II

IV.1.1 General considerations

Unless stated otherwise, all manipulations were performed under an atmosphere of dry oxygen-free nitrogen by means of standard schlenk and glovebox techniques. Solvents were pre-dried using 4 Å molecular sieves and refluxed under an atmosphere of N_2, and collected by distillation. Deuterated solvents were dried with 4 Å molecular sieves and freeze-pump-thaw degassed prior to use. L-lactide (98%) was purchased from Sigma Aldrich and was purificated by recrystallization from toluene and sublimation. Titanium(IV) tetraisopropoxido (Ti(O-*i*-Pr)$_4$) (97%) was purchased from Sigma Aldrich and was used in toluene solution (0,05M). Titanium(IV) chloride triisopropoxido (TiCl(O-*i*-Pr)$_3$) (95%) was purchased from Alfa Aesar and used as received. SBA-15 was synthesized by the Catalysis and Reaction Engineering Research Group of Técnico Lisboa, and was dried prior to use. All other reagents were commercial grade and used without further purification.

IV.1.2 General heterogeneous catalytic procedures for lactide polymerization

Drying of the support

SBA-15 was synthesized following a procedure described in [1] by the Catalysis and Reaction Engineering Research Group of Técnico Lisboa and was dried under the following conditions: heat rate 5°C/min until 400°C under a stream of nitrogen of 80 ml/min, kept at 400°C for 2 hours in air and 1 hour under nitrogen.

Impregnation of the catalyst into the support

Impregnation procedure was carried out under nitrogen using schlenk techniques.

Mesoporous silica (86.6 or 61.2 mg), Ti(O^{i}Pr)$_4$ (1 mL) and toluene (10 mL) were charged in a schlenk tube under a nitrogen atmosphere. Different amounts of titanium were applied in order to obtain different Ti/SBA-15 ratios (0.54 or 0.76 mmol/g). These reactions were stirred along different times (1.5 and 3h) at different temperatures (50ºC and room temperature).

Using Ti(O^{i}Pr)$_3$Cl, mesoporous silica (60.9 mg), Ti(O^{i}Pr)$_3$Cl (12.08 mg) and toluene (10 mL) were charged in a schlenk tube under a nitrogen atmosphere. These reactions were carried out along different time (1.5h and 3h) at different temperatures (50ºC and room temperature). After impregnation, the heterogeneous catalyst were used right away in polymerization reactions.

In an alternative impregnation procedure, mesoporous silica (250 mg), Ti(O^{i}Pr)$_4$ (2,89 or 4,09 mL) and toluene (10 mL) were charged into a schlenk tube under a nitrogen atmosphere. Different amounts of titanium were applied in order to obtain different Ti/SBA-15 ratios (0.54 or 0.76 mmol/g). These reactions were stirred for 3 hours at 50ºC. The catalyst was isolated by filtering off the solvent and the solid was washed three times with toluene and in the end the catalyst was dried under vacuum overnight and stored in the glove box.

To verify the amount of metal effectively grafted onto the support, for each different amount of titanium used, impregnation reactions were performed again. After the impregnation, the catalyst solutions were filtered and the remaining toluene solutions were evaporated to dryness and analyzed by ^{1}H-NMR.

Polimerization of lactide

Polymerization of L-lactide was carried out using a schlenk tube with magnetic stirring.

After immobilization, purified L-lactide (100 eq., 0.67 g) was added to the same schenk tube where was performed the impregnation, under nitrogen. The reactions were carried out in different conditions of temperature (70ºC, 90ºC and 110ºC), time (4h and 24h) and molar ratio L-lactide /Ti (100 eq. and 200 eq.).

For the alternative procedure of preparation of the catalysts, purified L-lactide (100 eq., 0.67g), dried toluene (10 mL) and the Ti(O^{i}Pr)$_4$/SBA-15 (61,1 mg) were charged into a schlenk tube under nitrogen. The polymerization tests were carried out for 24h at 70°C.

In both cases, the reactions were terminated by addition of 2 ml of water and the polymers were fully precipitated out of solution in an excess of methanol. The suspension was filtered under vacuum and the obtained composite was dried at 40°C under vacuum overnight.

The yields of the reactions were calculated using the following equation:

$$yield = \frac{m_{LA}}{m_{PLA}} \cdot 100\% \qquad \text{equation (4),}$$

where, m_{LA} is the mass of L-lactide and m_{PLA} is the mass of dried polylactide obtained by weight.

Soxhlet extraction in THF was used to separate the polymer from the catalyst.

Selected polylactide samples were characterized by Thermogravimetric Analysis, Differential Scanning Calorimetry and Gel Permeation Chromatography.

IV.1.3 General homogeneous catalytic procedures for lactide polymerization

Polymerization of L-lactide was carried out using schlenk techniques. Predetermined amounts of purified L-lactide (100 eq., 0.67 g), toluene (1M, 4 mL) and Ti(O-*i*-Pr)$_4$ in toluene solution (1 eq., 0,0463 mmol,1 mL) were charged into a schlenk tube under a nitrogen atmosphere. The resulting solution was vigorously stirred along different times (2, 4, 6 and 24h) at different temperatures (RT and 70ºC). In the case of Ti(O^{i}Pr)$_3$Cl, predetermined amounts of

purified L-lactide (100 eq., 0.67g), toluene (10mL) and Ti(O-*i*-Pr)$_4$ in toluene solution (1 eq., 0,0463 mmol,12.08 mg) were charged into a schlenk tube under a nitrogen atmosphere. The resulting solution was vigorously stirred along different times (2 and 24h) at 70ºC.

The reactions were terminated by addition of 2 mL of water and the polymers were completely precipitated out of solution by addition of an excess of methanol. The solutions were separated by filtration and the polymers obtained were dried at 40°C under vacuum for 12 h.

The yields of reactions were calculated by equation (4) – see section IV.1.2.

IV.1.4 Characterization techniques of the support

- **Nitrogen adsorption – BET method**

This technique was used to determine the specific surface area of the support. Nitrogen adsorption isotherms were measured with an ASAP 2010 Micromeritics equipment at -196ºC. Prior to the experiment, the sample was degassed at 300 ºC for 3 h. The analyses were performed by researchers of the Catalysis and Reaction Engineering Research Group of Instituto Superior Técnico, Lisboa.

- **Scanning Electron Microscopy**

Scanning electron microscopy (SEM) was used to reveal information about the SBA-15 sample including external morphology (texture), chemical composition, and crystalline structure and orientation of constituents of the sample, by using a beam of high-energy electrons to generate a variety of signals derived from the electron-sample interactions at the surface of the solid. The analyses were performed by researchers of the Catalysis and Reaction Engineering Research Group of Instituto Superior Técnico, Lisboa.

- **Transmission Electron Microscopy**

Transmission Electron Microscopy (TEM) was used for the production and visualization of images from a sample of SBA-15 by illuminating the sample with electrons (i.e. the electron beam) within a high vacuum, and detecting the electrons that are transmitted through the sample. The analyses were performed by researchers of the Catalysis and Reaction Engineering Research Group of Instituto Superior Técnico, Lisboa.

IV.1.5 Characterization techniques of the polymer

- **Nuclear Magnetic Resonance**

NMR spectra were recorded a Bruker AVANCE II 300 MHz or Bruker AVANCE 400 MHz spectrometers, in deuterated toluene solution at 296K temperature, unless stated otherwise, referenced internally to residual proton-solvent resonances, and reported relative to tetramethylsilane (0 ppm).

^{1}H NMR was used to determine the monomer to polymer conversion based on the relative integration of the lactide and polylactide corresponding signals.

- **Thermogravimetric analysis**

Thermogravimetric analysis (TGA) is a thermal analysis technique and was used to measure the amount and rate of weight variation of a material as a function of temperature and time in a controlled atmosphere.

Thermogravimetric analyses of selected samples of polymers were performed using a TGA 92 SETARAM equipment under air atmosphere-at a heating rate of 10ºC/min.

- **Differential Scanning Calorimetry**

Differential scanning calorimetry (DSC) can be used to predict glass transitions, melting and boiling points, crystallization time and temperature, relative stability of different crystalline forms, changes in heat capacity. Polymer thermal analysis was performed with a TA Instruments DSC2980 with MDSC option. The sample weights ranged from 4 to 5 mg and they were corrected for SBA-15 content. A temperature interval from 25 to 210ºC was studied at a heating rate of 10 ºC/min.

The DSC analysis were performed using the following method:

1) Equilibrate at 25.00°C
2) Ramp 10.00°C/min to 210.00°C
3) Mark end of cycle 1
4) Isothermal for 1.00 min
5) Ramp 10.00°C/min to 25.00°C
6) Mark end of cycle 2
7) Isothermal for 1.00 min
8) Ramp 10.00°C/min to 210.00°C
9) End of method.

- **Gel Permeation Chromatography**

The number-average, weight-average molar masses and molar mass distribution of the polylactide samples were determined by Gel Permeation Chromatography/Size Exclusion Chromatography (GPC/SEC) by researchers of the Organometallic Chemistry and Homogeneous Catalysis Research Group of Centro de Química Estrutural of Instituto Superior Técnico, Lisboa. The analyses were performed in a HPLC Waters chromatograph, containing an isocratic pump Waters 1515 and a refractive index detector Waters 2414. In this apparatus both the oven and detector were stabilized at 40ºC and two 50 Å PLgel and two 100 Å PLgel (Polymer labs) columns were used. The software Empower2 was used for the acquisition and data processing.

THF was used as eluent and the flow rate was set up at 1.0 mL/min. Before use, the solvent was filtrated through 0.45 µm PTFE membranes Fluoropore (Millipore) and degassed in an ultrasound bath for 45 min. The polymer samples were also filtered through 0.20 µm PTFE filters Durapore (Millipore).

Molecular weights were calibrated relative to polystyrene standards (TSK Tosoh Co.). The obtained $M_{n(SEC)}$values were corrected using the next correction factor as reported in the literature [2]:

$$M_{n(corrected)} = 0{,}58 \cdot M_{n(SEC)} \qquad \text{equation (5)}$$

IV.2 Chapter III

IV.1 General considerations

All experiments were carried out under N_2 using standard schlenk techniques or in a nitrogen-filled MBraun Unilab glovebox. THF, dichloromethane, pentane and toluene were first dried through a solvent purification system (MBraun SPS) and stored at least a couple of days over activated molecular sieves (4 Å) in a glovebox prior to use. *Rac*-lactide [3,6-dimethyl-1,4-dioxane-2,5-dione] and L-lactide [(3S)-cis-3,6-dimethyl-1,4-dioxane-2,5-dione] were purchased from Sigma-Aldrich and recrystallized from cold toluene and sublimed prior to use. Vanadium complexes were synthesized by Coordination Chemistry Laboratory in University of Toulouse and placed under Argon in sealed ampules. Once opened, they were kept in closed vials in glovebox. All other chemicals were purchased from Sigma-Aldrich and were used as received unless indicated otherwise.

IV.2 Polymerization representative procedure

Solution polymerization conditions

In a glovebox, the desired vanadium initiator (1 eq., 5 mg), *rac*-lactide (100 eq.) and solvent ($[M]_0$=1M, THF, dichloromethane or toluene) added via syringe all at once were charge in a vial equipped with Teflon-tight screw cap. The solution was vigorously stirred according the considered time and at chosen temperature conditions. When the appropriate time was reached, aliquots were taken and analyzed by 1H NMR sprectroscopy to estimate the conversion. The reaction mixture was finished by quenching with dichloromethane. The polymer samples were dried in vacuum and subsequently analyzed by SEC.

Bulk polymerization conditions

In a glovebox, the desired initiator (1 eq., 5 mg) and the appropriate *rac*-lactide (100 eq.) were charged in a small vial equipped with a Teflon-tight screw cap. The reaction mixtures were heated at 130ºC until complete melt of the mixture and kept at this temperature for different times.

IV.3 Characterization techniques of the polymer

❖ Nuclear Magnetic Resonance

Deuterated solvents were purchased from Euroisotope (CEA, Saclay, France), desgassed under a N_2 flow and stored over activated molecular sieves (4Å) in a glove box prior to use. NMR spectra were recorded on Bruker AC300 MHz and 400 MHz NMR spectrometers, in Teflon-valved J-Young NMR tubes at room temperature. ^{1}H chemical shifts are reported vs. $SiMe_4$ and were determined by reference to the residual ^{1}H solvent peaks.

The monomer to polymer conversion was calculated by ^{1}H NMR spectroscopy based on the relative integration of the corresponding signals – Table 20.

Table 20 - ^{1}H NMR signals used to estimate monomer conversion to polymer.

Polymer δ (ppm)[a]	**Monomer δ (ppm)[a]**	**^{1}H NMR spectrum**
PLA δ=5.20-5.30	*rac*-LA δ=5.02	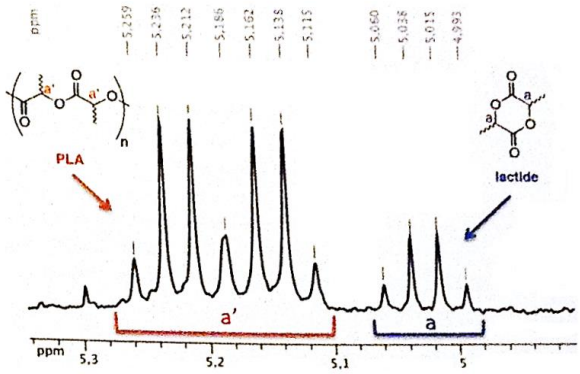

[a] $CDCl_3$, 25ºC.

❖ Size-exclusion chromatography

The number-average, weight-average molar masses (M_n and M_w, respectively) and molar mass distribution (M_w/M_n) of the PLA samples were determined by size exclusion chromatography (SEC) at 30ºC or 40ºC with Shimadzu LC20AD ultra-fast liquid chromatography equipped with a Shimadzu RID10A refractometer detector. THF was used as the eluent and the flow rate was set up at 1.0 mL/min. A Varian PLGel pre-column and a Variam PLGel 5 µm were used. Calibrations were performed using polystyrene standards (400-100000 g/mol) and raw values of $M_{n(SEC)}$ were thus obtained. These values were corrected using the equation (5) presented in the previous section IV.1.5.

IV.3 References

[1] Artur Bento, PhD Thesis, *Development of high performance polyethylene nanocomposites, via in-situ polymerization in mesoporous materials*, Instituto Superior Técnico, Lisboa, 2014.

[2] A. Kowalsaki, A.Duda, S. Penczek, *macromolecules,* **1998**, *31*, 2114; M.Save, M. Schappacher, A. Soum, *Macromol. Chem. Phys.,* **2002**, *203*, 889.

Annexes

Annex 1 – DSC results

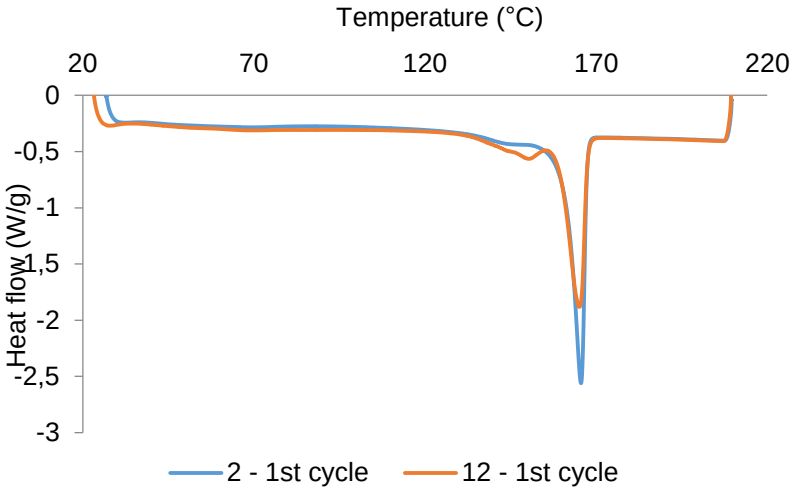

Figure 61 - DSC curve: Plot of 1st cycle for samples 2 and 12.

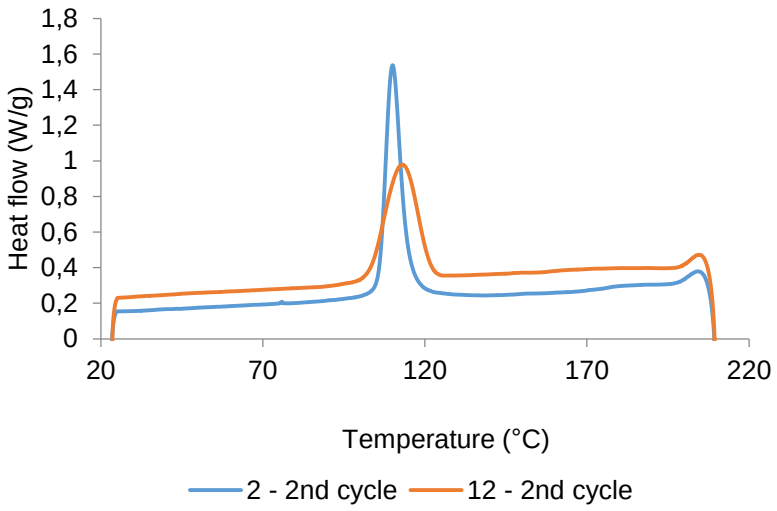

Figure 62 - DSC curve: Plot of 2nd cycle for samples 2 and 12.

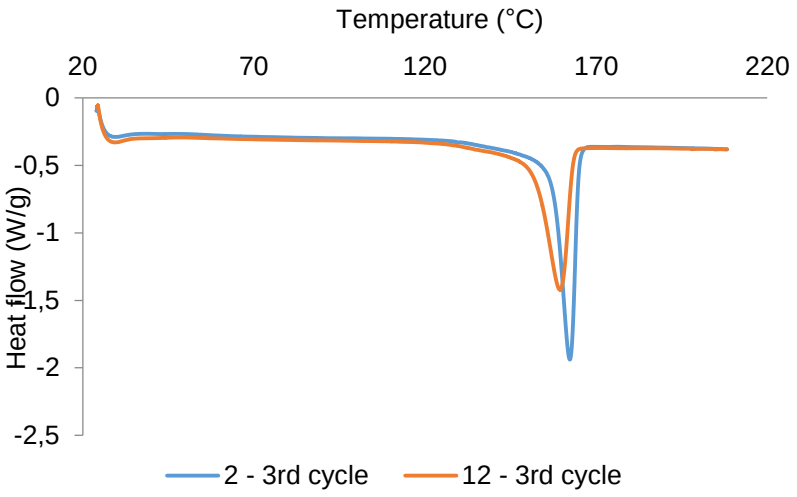

Figure 63 - DSC curve: Plot of 3rd cycle for samples 2 and 12.

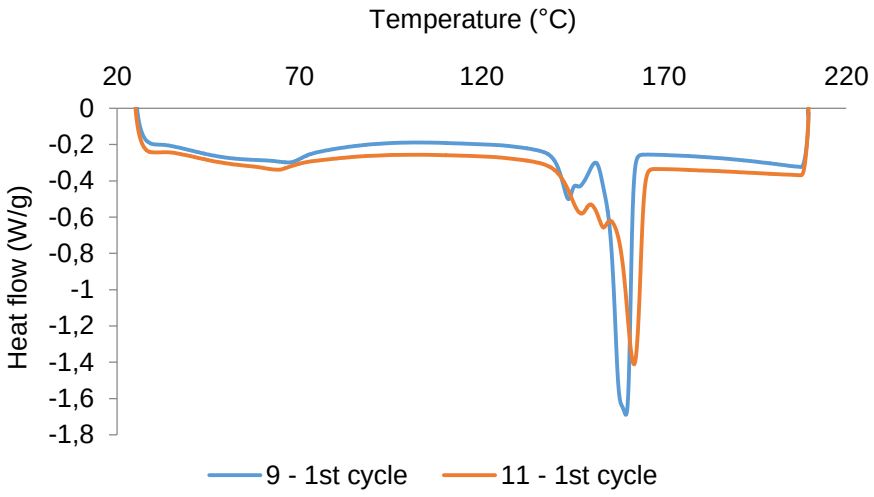

Figure 64 - DSC curve: Plot of 1st cycle for samples 9 and 11.

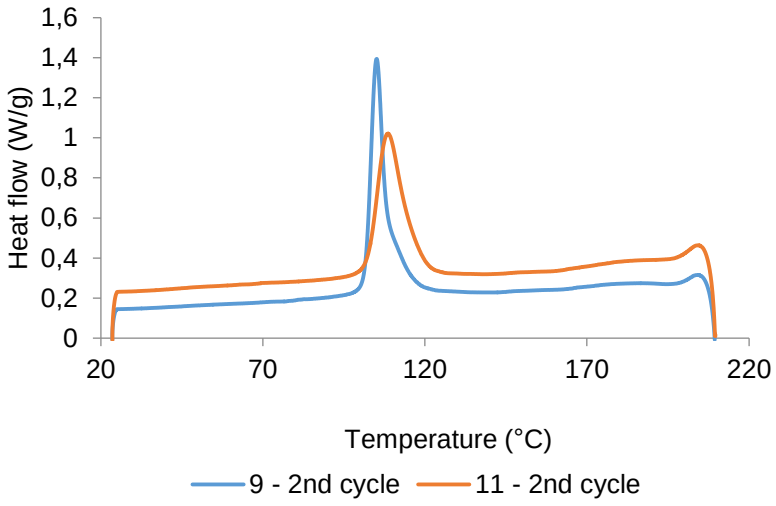

Figure 65 - DSC curve: Plot of 2nd cycle for samples 9 and 11.

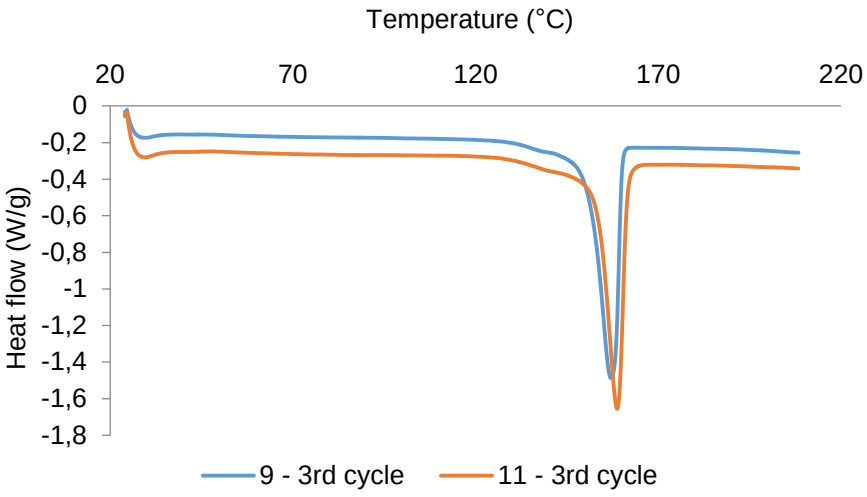

Figure 66 - DSC curve: Plot of 3rd cycle for samples 9 and 11.

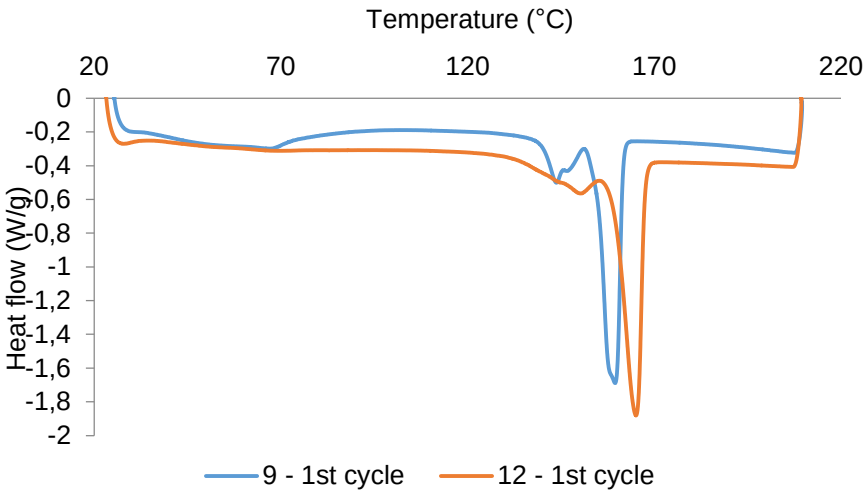

Figure 67 - DSC curve: Plot of 1st cycle for samples 9 and 12.

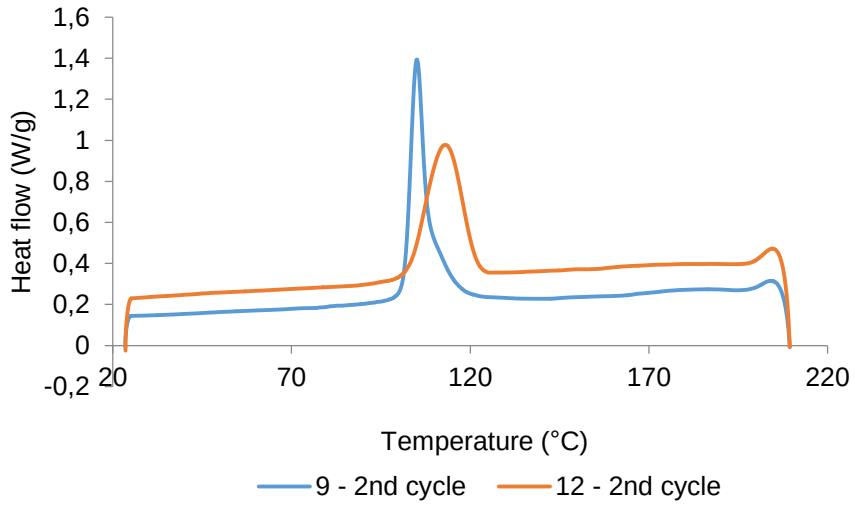

Figure 68 - DSC curve: Plot of 2nd cycle for samples 9 and 12.

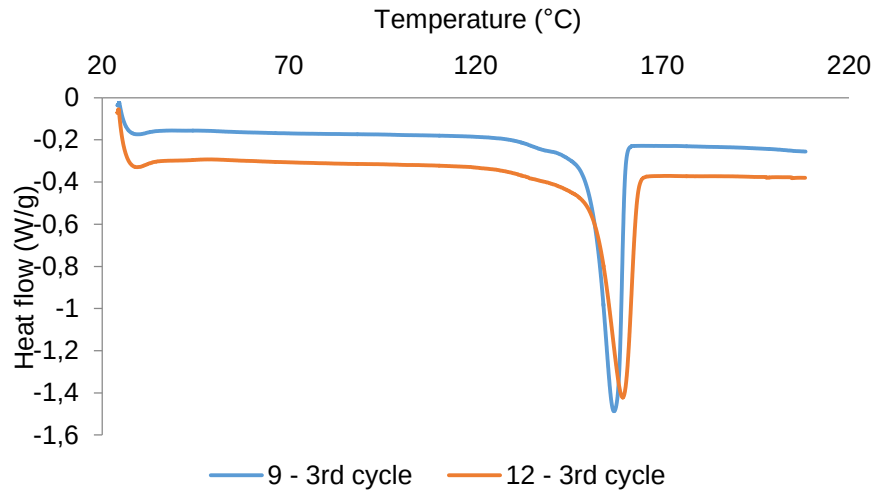

Figure 69 - DSC curve: Plot of 3rd cycle for samples 9 and 12.

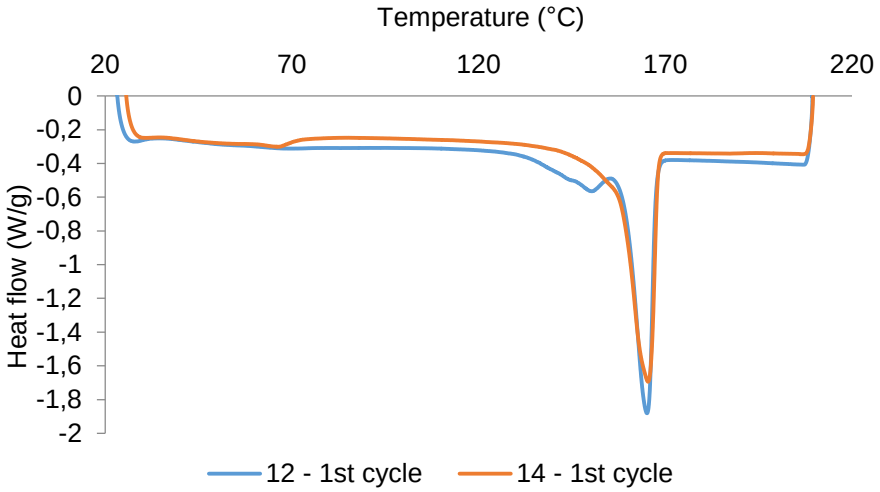

Figure 70 - DSC curve: Plot of 1st cycle for samples 12 and 14.

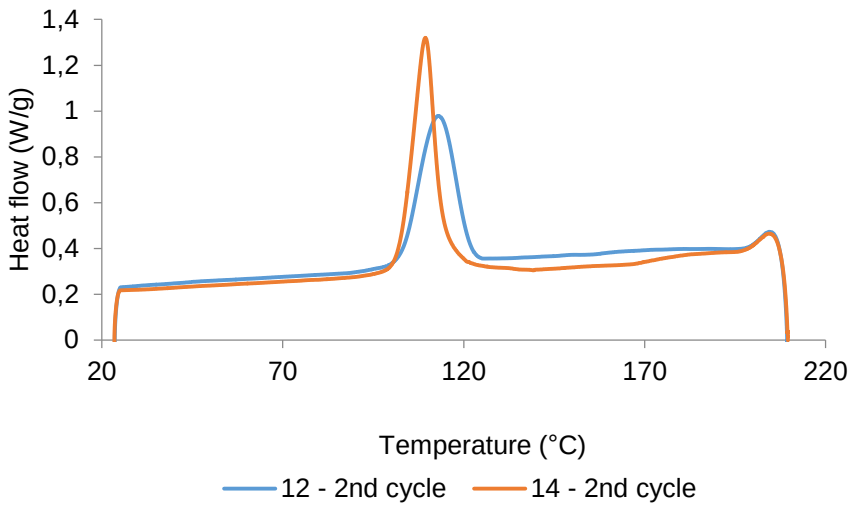

Figure 71 - DSC curve: Plot of 2nd cycle for samples 12 and 14.

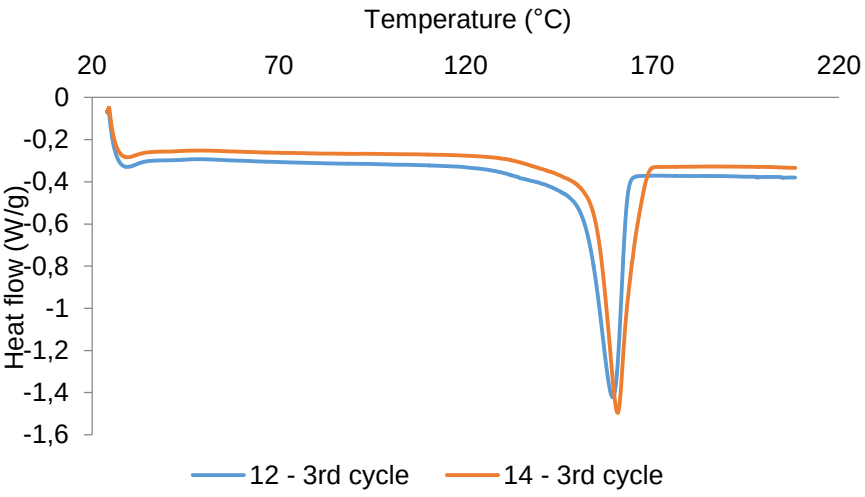

Figure 72 - DSC curve: Plot of 3rd cycle for samples 12 and 14.

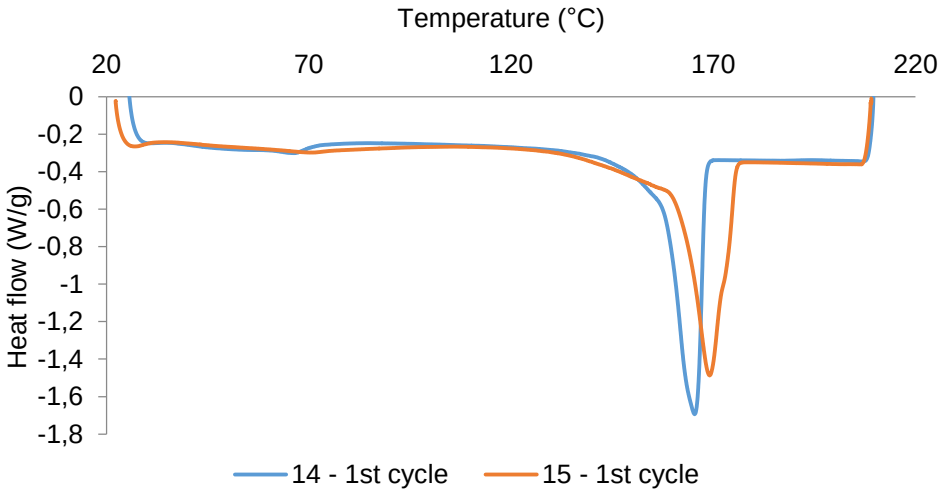

Figure 73 - DSC curve: Plot of 1st cycle for samples 14 and 15.

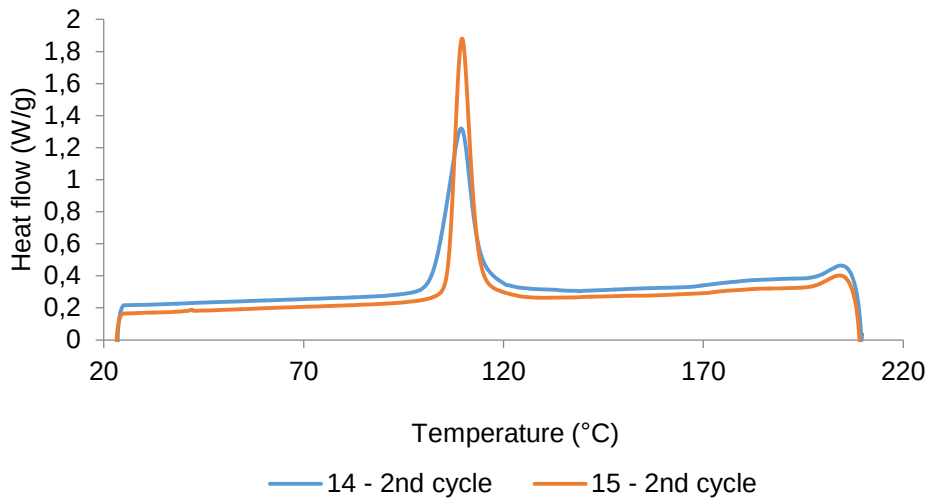

Figure 74 - DSC curve: Plot of 2nd cycle for samples 14 and 15.

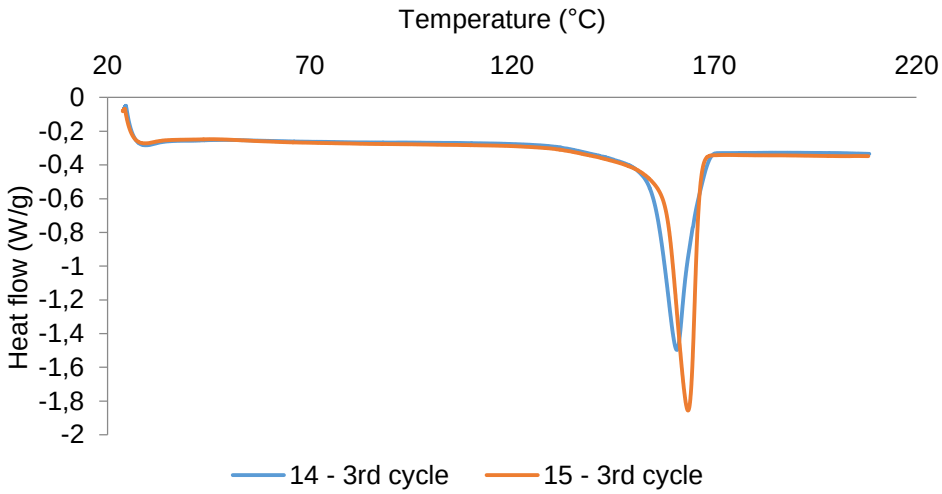

Figure 75 - DSC curve: Plot of 3rd cycle for samples 14 and 15.

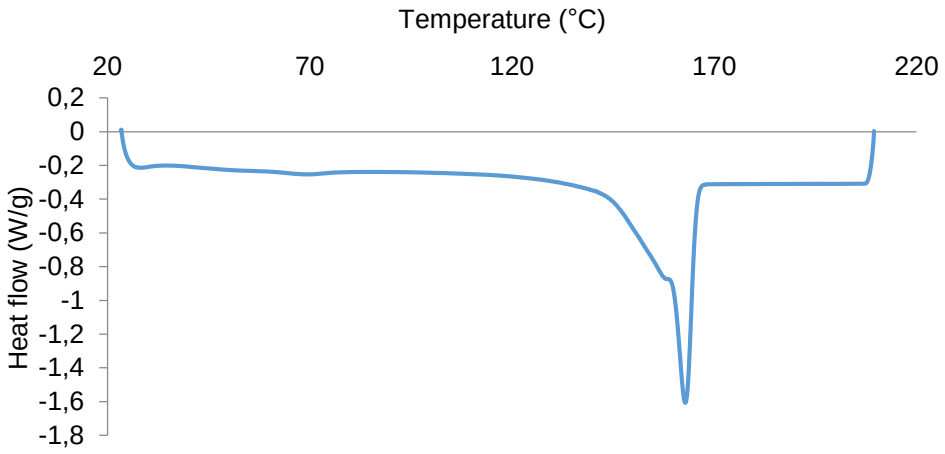

Figure 76 - DSC curve: Plot of 1st cycle for sample 35.

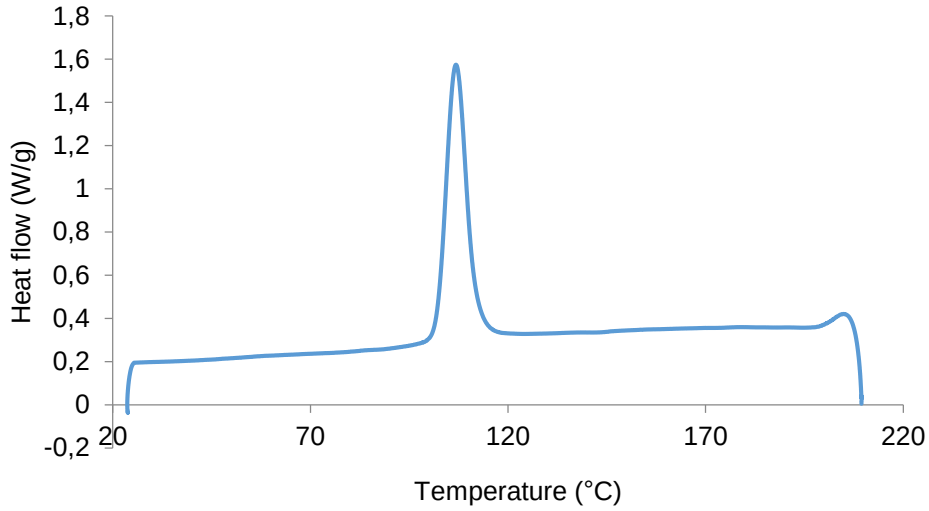

Figure 77 - DSC curve: Plot of 2nd cycle for sample 35.

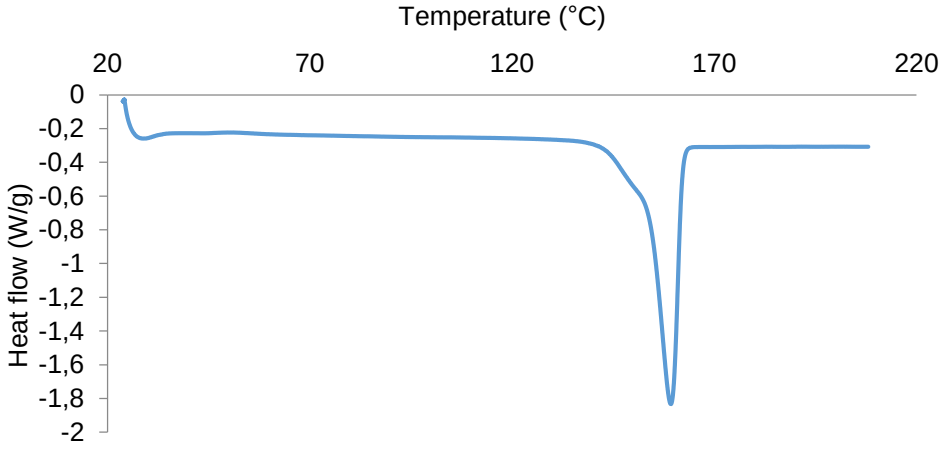

Figure 78 - DSC curve: Plot of 3rd cycle for sample 35.

Annex 2 – Formation of *meso*-lactide

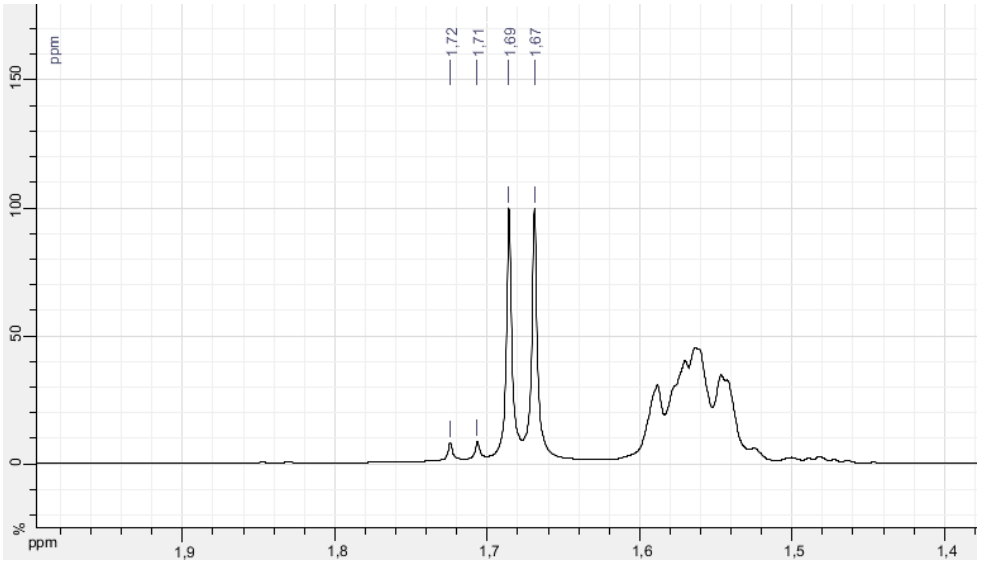

Figure 79 - ^{1}H NMR sprectrum: formation of meso-LA during polimerization of LA using V2 in solution- run 55.

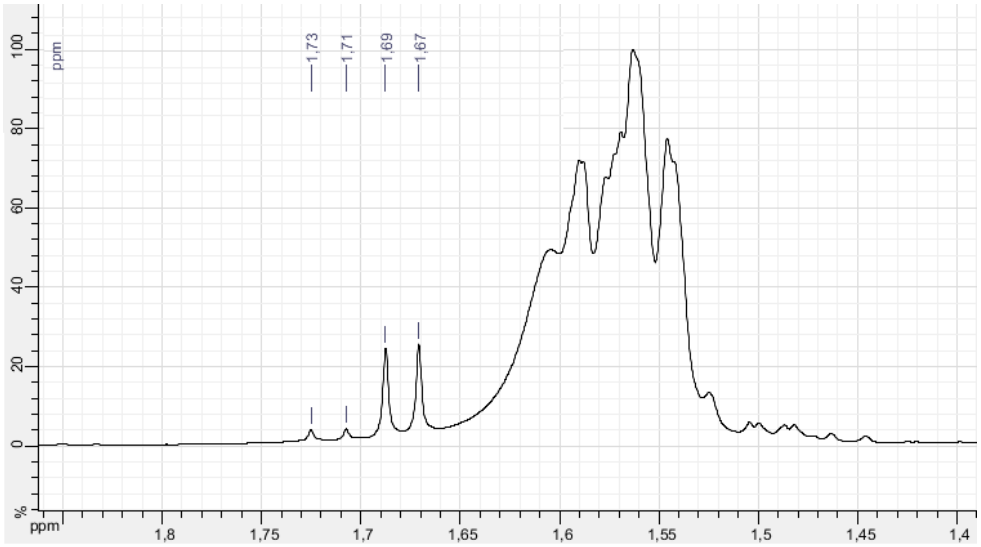

Figure 80 - ^{1}H NMR sprectrum: formation of meso-LA during polimerization of LA using V2 in bulk - run 68.

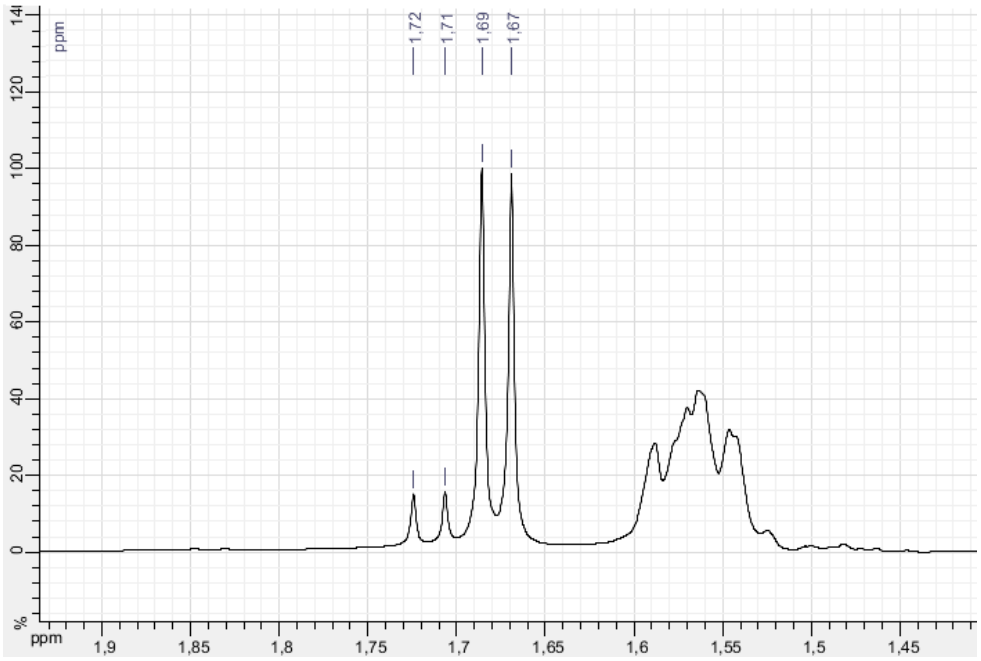

Figure 81 - ^{1}H NMR sprectrum: formation of meso-LA during polimerization of LA using V3 in solution - run 82.